Development of highly sensitive tools to investigate the *Salmonella* Type III Secretion System

Dissertation

der Mathematisch-Naturwissenschaftlichen Fakultät

der Eberhard Karls Universität Tübingen

zur Erlangung des Grades eines

Doktors der Naturwissenschaften

(Dr. rer. nat.)

vorgelegt von

Sibel Westerhausen, geb. Şeker

aus Uşak/Türkei

Tübingen

2020

Gedruckt mit Genehmigung der Mathematisch-Naturwissenschaftlichen Fakultät der Eberhard Karls Universität Tübingen.

Tag der mündlichen Qualifikation:	28.01.2021
Stellvertretender Dekan:	Prof. Dr. József Fortágh
1. Berichterstatter:	Prof. Ph.D. Samuel Wagner
2. Berichterstatter:	Prof. Dr. Ana J. Garcia-Saéz

Table of Contents

List of abbreviations

aa amino acid

Δ delta symbol for gene deletion

SPI Salmonella Pathogenicity Island

ATP Adenosine triphospahte

SRP Single recognition particle

GTP Guanosine triphosphate

PMF Proton motive force

SCV Salmonella containing vacuole

Inv Invasion protein

Org oxygen regulated protein

Spa Surface presented antigen protein

Prg PhoP repressed gene protein

ΔΨ delta psi symbol for membrane potential

ΔpH delta pH symbol for proton concentration gradient

CBD Chperone binding domain

ABD Actin binding domain

GEF Guanosine exchange factor

DEVD one letter amino acid code for caspase cleavage site

FRET Förster resonance energy transfer

cAMP cyclic adenosine monophosphate

GFP Green fluorescent protein

FlAsH Fluorescein arsenical hairpin

LOV Light oxygen voltage

YFP Yellow fluorescent protein

SDS-PAGE Sodium deodecylsulfate Polyacrylamide gel electrophoresis

CCCP Carbonylcyanid-m-chlorphenylhydrazon

NLuc Nanoluc

NanoBiT Nanoluc Binary Technology

LgBiT LargeBiT

SmBiT SmallBiT

HiBiT HighBiT

MBP Maltose binding protein

RLU Relative luminescence unit

MOI Multiplicity of infection

kDa kilodalton

MW Molecular weight

LB Lennox broth

T3SS Type III Secretion System

Deutsche Zusammenfassung

Bakterien besitzen Pathogenitätsmechanismen, um ihr eigenes Überleben zu sichern. Ein solches Pathogenitätsmechanismus ist das nadelähnliche Type III Sekretionsystem (T3SS). In den letzten Jahren wurden viele Methoden entwickelt, um T3SS sezernierte oder injizierte Proteine zu detektieren. Jedoch ist keine dieser Methoden einfach, schnell und unkompliziert, um ausreichend direkte Aussagen über die Quantität der Proteine zu treffen oder Kinetiken messen zu können. Dabei würde ein solcher Assay helfen, viele relevante biologische Fragen über das T3SS zu beantworten und auch hilfreich bei der Entdeckung von Inhibitoren gegen das T3SS sein. In dieser Arbeit präsentiere ich Methoden, die es uns erlauben, Proteine des T3SS i.) in der extracellulären Umgebung, ii.) in der Wirtszelle und iii) im Periplasma quantitativ und schnell zu detektieren. Dafür nutzte ich das von Promega neu entwickelte Reporterprotein NanoLuc (NLuc). Im ersten und zweiten Teil dieser Arbeit wurde NLuc an das sezernierte Effektorprotein SipA fusioniert, welches durch das T3SS in die extrazelluläre Umgebung und in die Wirtszelle transportiert wird. Der auf NLuc basierende Sekretions- und Injektionsassay bewies sich für das T3SS als sehr sensitiv und ermöglichte die Quantifizierung von SipA in verschiedenen Mutanten. Dieser neu etablierte Assay funktionierte bei Hochdurchsatzmessungen für die Entwicklung und Entdeckung von Inhibitoren als auch für Messungen der Kinetik, um die zeitliche Sekretion und Injektion zu beobachten.

Die Assemblierung des T3SS erfolgt schrittweise. Wenn der substratspezifische Wechsel durch das selbstgespaltene Schaltprotein SpaS induziert wird, wird der Aufbau des T3SS mit der Sekretion von Zwischensubstraten fortgesetzt. Die Regulation dieses Mechanismus ist unbekannt. Die Ausführung der Nadellängenkontrolle wird oft mit diesem Wechsel verbunden. Genetische Daten stellen dieses Modell jedoch in Frage und legen nahe, dass diese beiden Ereignisse unabhängig voneinander sind. Wir fragten uns, ob der Wechsel zu intermediären Substraten und späten Substraten unbedingt die vorherige Sezernierung der frühen Substrate erfordert. Um diese Frage zu klären, versuchten wir, einen Assay zu entwickeln, der die periplasmatische Sekretion in nadeldefizienten Mutanten detektiert. Dazu verwendeten wir die Split-Variante von NLuc. Das große Fragment von splitNLuc, LgBiT wurde als Komplementationspartner für die mit dem kleinen Fragment, HiBiT fusionierte T3SS Substrate ins Periplasma transloziert. Wir wurden mit verschiedenen Herausforderungen konfrontiert. Letztendlich haben wir alle Probleme überwunden und konnten den Assay erfolgreich in Proof-of-Concept-Experimenten einsetzen. Wir generierten auch die am besten geeigneten nadeldefekten Mutanten: Mit dem Assay und den Stämmen, die wir etabliert haben, wird es schließlich möglich sein, unser Verständnis des Prozesses vom substratspezifischen Wechsel zu vertiefen.

Abstract

Bacteria have evolved different pathogenicity mechanisms to ensure their survival. One of them is the Type III Secretion System (T3SS). *Salmonella* employs the T3SS to secrete and inject effector proteins into the extracellular milieu and the host cell. Many methods have been established in the last few years to investigate the T3SS. However, none of these assays is sufficiently simple, quick or quantitative. Here, I present easy and rapid tools that allow detection of T3SS secreted proteins into the i.) extracellular environment; ii.) host cell and iii.) bacterial periplasm. The assays are based on the newly engineered luciferase NanoLuc (NLuc). NLuc proved to be a perfect reporter protein for T3SS proteins because of its high sensitivity and small size. In the first and second part of this thesis, the T3SS effector protein SipA served as fusion partner for NLuc to detect and quantify protein secretion in the extracellular environment and host cells. Thereafter, I could successfully extend the use of this system for high throughput screening to identify new T3SS inhibitors as well as to monitor real-time injection into host cells.

The assembly of the T3SS occurs in a stepwise manner. Once the basal body and cytoplasmic components are assembled, the secretion of early substrates starts. When substrate specificity switching is induced by the autocleaved switching protein SpaS, the assembly of T3SS proceeds with the secretion of intermediate substrates. The regulation of this switching mechanism is unknown. The execution of needle length control is often connected to the substrate specificity switching and is believed to regulate the switching. However, genetic data challenge this model and suggest that these two events are independent of each other. Therefore, we wondered whether switching to the intermediate substrates and late substrates strictly requires the prior secretion of early substrates. In order to address this question, we sought to develop an assay to monitor periplasmic secretion in needle deficient mutants. For this, we utilized the split variant of NLuc and targeted the large fragment of splitNLuc, LgBiT, to the periplasm as a complementation partner of T3SS substrates tagged with the small fragment of splitNLuc, HiBiT. Optimization of the assay required longer than expected as we faced different biological and technical challenges, e.g. in targeting LgBiT exclusively and stably to the periplasm and in detecting a specific luminescence signal in the periplasmic compartment. Eventually, we overcame all issues and were able to successfully use the assay in proof-of-concept experiments. We also generated the most suitable needle deficient mutants: With the tool and strains we established, it will finally be possible to deepen our understanding of the process of substrate specificity switching.

1 Introduction

Transport of proteins is one of the most important functions in all living organisms. Protein transport into other compartments or organelles of a single cell, into the extracellular environment as well as into other adjacent cells, all these forms of transport are regarded as protein secretion. Nature has created a variety of signal sequences to target different pathways to specific compartments or organelles, so that all proteins find the way to their destination (Stathopoulous, 2008).

Gram-negative and Gram-positive bacteria secrete proteins through different types of secretion systems to obtain nutrients from their environment, communicate with other bacteria and interact with host cells. Different bacteria have evolved several protein secretion systems to cope with different environmental situations. These secretion systems are composed of a variety of components and secrete different substrates to achieve their functions (Green and Mecsas, 2016).

Here, I will provide a short overview about the general secretion pathways that are mainly used to transport proteins through the inner membrane. The Type III secretion system (T3SS) will be extensively discussed afterwards.

1.1 General protein transport pathways through the inner membrane

The universally conserved general secretion (Sec) pathway is one of the most important routes for proteins exported out of the cytoplasm (Fig.1). These proteins possess a particular signal sequence: A positively charged N-terminus and a hydrophobic central part (h-region) followed by a polar region. While the physicochemical properties of this signal peptide are conserved among Sec-translocated proteins, the amino acid sequence can be different thus resulting in either post-translational or co-translational targeting to the translocon (Tsirigotaki *et al.*, 2017). Interestingly, some integral membrane proteins completely lack the signal peptide: Their very hydrophobic, transmembrane domain is recognized as a signal instead (Tsirigotaki *et al.*, 2017).

The Sec translocon, consisting of the three subunits, SecY, SecE and SecG, mainly differs from other translocation conduits by having two opening sites (Natale, Brüser and Driessen, 2008). The transversal opening is for proteins which are post-translationally targeted to the Sec translocon. The ATPase SecA and also the ribosome associated chaperone trigger factor (TF) bind to the ribosomal exit site while the protein is being translated after the nascent chain has reached a particular length. Alternatively, SecB recognizes the signal sequence of some proteins

and binds to the nascent chain, stabilizing the unfolded pre-protein (Huber *et al.*, 2017). SecB transfers its substrate to the SecYEG-bound SecA, which energises the protein translocation by using ATP in a stepwise manner, while a membrane embedded peptidase cleaves the signal sequence of the pre-protein during this step (Driessen and Nouwen, 2008). However, it has to be mentioned that the trigger factor and SecB are not essential. It still needs to be investigated to which extent they are involved in the Sec-dependent protein export pathway (Tsirigotaki *et al.*, 2017).

Two proteins Skp and PpiD act as periplasmic chaperones for the newly translocated proteins by interacting with the SecYEG channel (Harms *et al.*, 2001; Antonoaea *et al.*, 2008; Sachelaru *et al.*, 2014). Proteins destined for the periplasm might subsequently get secreted to the outside through of the secretion machineries (T2SS and T5SS) or integrated into the outer membrane (Crane and Randall, 2017).

Very hydrophobic proteins that must be integrated into the inner membrane are too unstable to be maintained in the cytoplasm. Therefore, these proteins are translocated to the SecYEG channel in a co-translational manner with the signal recognition particle (SRP), a small 4.5S RNA bound to the protein Ffh (Steinberg *et al.*, 2018). Like SecA and TF, SRP binds to the exit tunnel of the ribosome and recognizes the very hydrophobic signal sequence of the nascent chain early during translation (Zhang *et al.*, 2010). This complex (SRP-ribosome associated nascent chain, SRP-RNC) is targeted to the membrane bound SRP receptor FtsY. Thus, FtsY can transfer the complex to the SecYEG channel and release SRP while using GTP, allowing the exit tunnel of the ribosome to interact with the Sec translocon and slowly elongate the protein within the channel. The lateral opening of the channel allows then the insertion of the protein into the membrane with co-insertase/chaperone YidC (Denks *et al.*, 2014; Freudl, 2018).

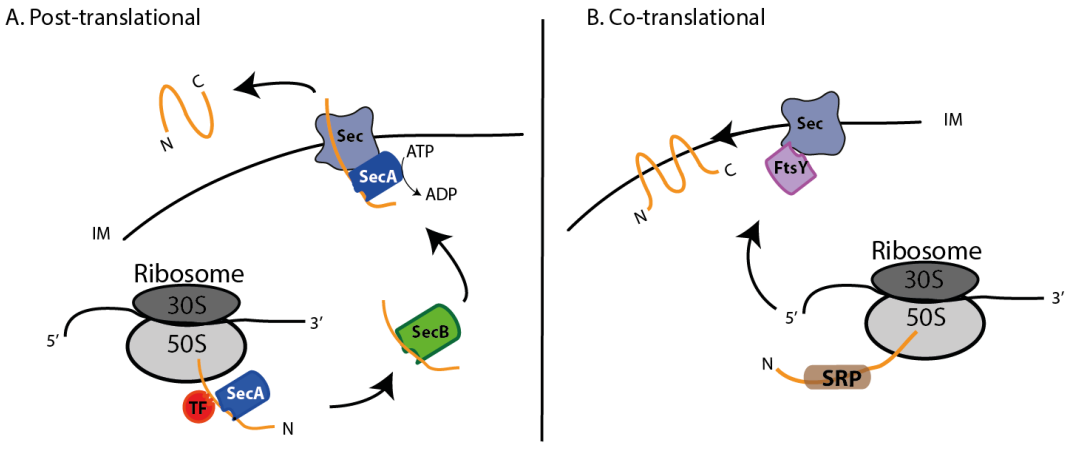

Fig. 1: The two Sec pathways. **A.** In the post-translational pathway, SecA and transcription factor TF are bound to the nascent protein during translation. SecB transports the protein to the SecYEG-bound SecA, which energizes the transport through the translocon. **B.** Very hydrophobic proteins are recognized by the SRP-complex during translation and are targeted to the FtsY receptor which aids the ribosome to elongate the protein into the channel. **Abbreviations:** IM: inner membrane, TF: Trigger factor, SRP: Signal recognition particle.

1.1.1 Protein degradation system

The maintenance of protein function is a balancing act between a functional cooperation of molecular chaperones and proteases (Voos and Pollecker, 2020). Translocated proteins that have reached their destination can start to maturate, fold, and assemble into their active conformation supported by chaperones. Failure to do so leads to misfolded and aggregated proteins, which are functionally impaired. Although, chaperones can recognize misfolded and aggregated proteins, thus stabilizing those as well, misfolded proteins do tend to accumulate. This accumulation decreases the amount of fully functional proteins and limits the amount of available chaperones. The consequences are additional non-productive folding and increased protein aggregation (Dill *et al.*, 2008; Amm, Sommer and Wolf, 2013). The bacterial cell has developed strategies to overcome this issue. One of them is to activate the heat shock and protein stress response networks. These pathways include several proteases like the ATPase dependent machinery part of the AAA+ (ATPases associated with diverse cellular activities) superfamily (Truscott, Bezawork-Geleta and Dougan, 2011). Among them are ClpXP, ClpAP and Lon. Lon possesses an unfoldase and peptidase activity in one polypeptide chain, while in the two component systems these activities are distributed on two proteins (Olivares, Baker and Sauer, 2016). These systems are ClpXP and ClpAP. ClpP takes the role of the serine peptidase component while ClpA and ClpX have unfoldase activity (Farrell, Grossman and Sauer, 2005).

Over 450 proteins are known to be translocated to the periplasm via the Sec and Tat pathway (Merdanovic *et al.*, 2011). Considering the amount of proteins, it is not unlikely that protein

aggregation will also occur in the periplasm. Therefore, the cell has established protein degradation mechanisms outside the cytoplasm (Fig. 2). DegP and Tsp are the most prominent periplasmic proteases. In these proteases the so called PDZ domain mediates interaction with other proteins or displays protease activity (Spiers *et al.*, 2002). DegP contains multiple PDZ domains and serves not only as protease, but also plays an important role as chaperone (Iwanczyk *et al.*, 2007). The tail specific protease Tsp is a conserved serine protease harbouring one PDZ domain with protease function. Tsp preferentially degrades unfolded substrates with hydrophobic C-terminus (Silber, Keiler and Sauer, 1992). Proteins with stalled or interrupted translations are marked with a short peptide tag for degradation, the so called ssrA tag (Jentsch, 1996). The ClpAP and ClpXP systems recognize and degrade the misfolded proteins appended with a ssrA tag. However, Tsp has been shown to degrade ssrA-tagged proteins too, having overlapping function with ClpAP and ClpXP proteins (Keiler, Waller and Sauer, 1996). DegP and Tsp are also believed to play an important role in protein quality control, since it was shown that strains lacking these proteins have growth defects (Soltes *et al.*, 2017).

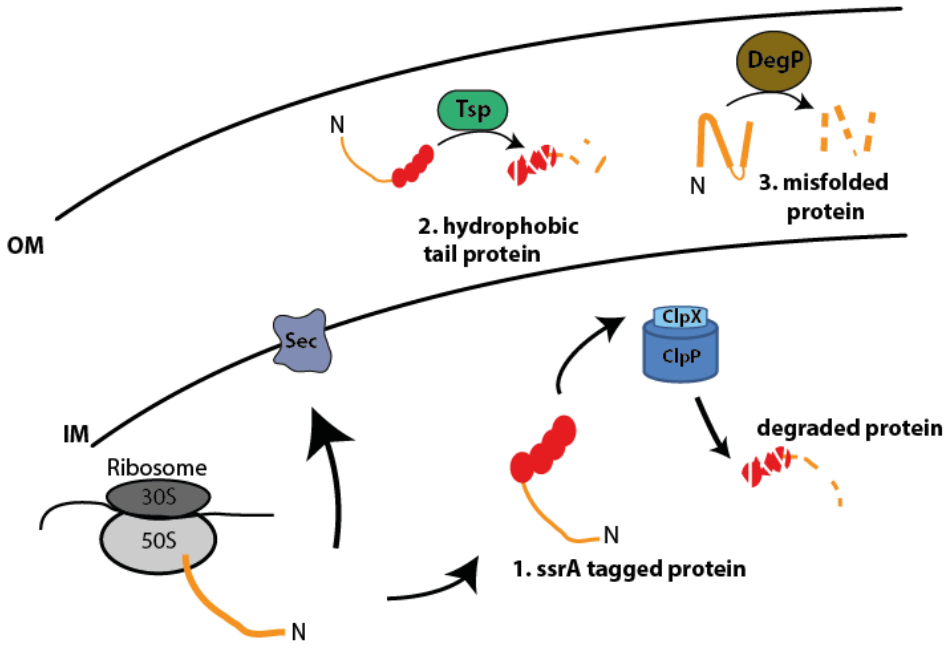

Fig. 2: A simplified overview of protein quality control within the cell. Protein defects can occur during translation or maturation. When ribosomes stall during translation, a ssrA-tag is added to C-terminus of the nascent polypeptide. **1.** ClpX and ClpP recognize and degrade the ssrA-tagged peptide. **2.** The tail specific protease Tsp has been demonstrated to degrade ssrA-tagged peptides in the periplasm. **3.** Another periplasmic protease is DegP which degrades misfolded substrates but also off-pathway substrates for the Bam maschinery. **Abbreviations:** OM: outer membrane, IM: inner membrane, Tsp: tail specific protease.

1.2 The type III secretion system

The T3SS is widespread among different pathogenic bacteria, and can be found in different *Yersinia* species, in *Shigella flexneri*, enteropathogenic *Escherichia coli* (*EPEC*), *Pseudomonas aeruginosa*, in *Chlamydia* species, *Salmonella Typhimurium*, and it is even conserved in some plant pathogens like *Erwinia* and *Xanthomonas*. While the T3SSs of these pathogens display highly similar, their secreted effectors vary in functions and effects on the host cell leading to a multitude of diseases (Hueck, 1998).

Salmonella enterica serovar Typhimurium (*S.* Typhimurium) is a Gram-negative, rod-shaped and non-sporulating bacterium that belongs to the *Enterobacteriaceae* family. Not restricted on a specific host, *S.* Typhimurium can infect a broad range of animals as well as humans. It is usually acquired through contaminated food or water leading to self-limiting gastroenteritis. *Salmonella* gastroenteritis is one of the most common food-borne diseases, and although it is not a severe threat for healthy adults (Majowicz *et al.*, 2010), immune-compromised people and children can develop systemic salmonellosis when infected with non-typhoidal *Salmonella* serovars (Gordon, 2008; Bula-Rudas, Rathore and Maraqa, 2015). Especially in developing countries lacking clean water, or with poor sanitation and hygiene, mortality rates can rapidly increase.

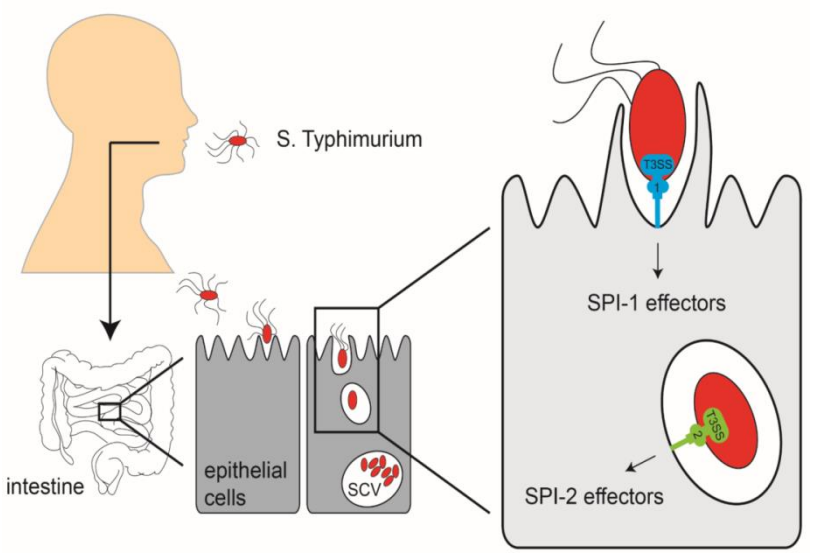

Fig. 3: Infection route of *S.*Typhimurium. Once ingested, *S.* Typhimurium reaches the intestine where it infects epithelial cells via its *Salmonella* pathogenicity islands (SPI). SPI-1 expresses the T3SS-1 required for the invasion. T3SS-1 is rapidly down-regulated in the Salmonella containing vacuole (SCV) allowing the expression of the second T3SS (T3SS-2) encoded by SPI-2. This secretion system enables the bacteria to spread and replicate itself (Lea Krampen, 2017). **Abbreviations:** SCV: *Salmonella* containing vacuole, T3SS: Type III secretion system, SPI: *Salmonella* pathogenicity island.

Salmonella employs three pathways to enter the epithelial barrier of a human host (Sansonetti, 2002). All of them require the bacteria to pass through and survive the acidic pH of the stomach to reach the small intestine wherein they need to survive host defense mechanisms like digestive enzymes, bile salts and antimicrobial peptides. From here on, *Salmonella* can 1) transmigrate through specialized epithelial cells, the Microfold cell (M-cell), 2) invade apically villous epithelial cells or 3) be captured luminally by CD18 expressing dendritic cells in order to cross the epithelial barrier (Sansonetti, 2002; Haraga, Ohlson and Miller, 2008). *Salmonella* invades preferentially M-cells, but it can also invade non-phagocytotic epithelial cells by adhering to the apical site followed by membrane ruffling reflecting cytoskeletal changes (Fig.3). While the *Salmonella* pathogenicity island-1 (SPI-1) has been shown to contribute to the invasion of epithelial cells, its importance for crossing CD18-positive cells could not been clarified (Vazquez-Torres *et al.*, 1999). After the epithelial barrier has been ruptured, *Salmonella* enters macrophages and induces apoptosis. Nonetheless, *Salmonella* can also survive and replicate inside macrophages, which leads to local and systemic dissemination throughout the reticuloendothelial system (Sansonetti, 2002; Haraga, Ohlson and Miller, 2008). However, a *Salmonella* subpopulation has been discovered in macrophages that fails to replicate. The nutrient poor vacuolar environment triggers the formation of this heterogeneous subpopulation. These so-called persisters can undermine the host immune response, survive inside macrophages and resist antibiotic treatment by reprogramming the host cell (Helaine *et al.*, 2014; Stapels *et al.*, 2018)

1.2.1 The two-virulence associated type III secretion systems of *Salmonella*

Salmonella is described as the only pathogen to possess two chromosomally encoded virulent T3SSs (T3SS-1 and T3SS-2) on two different *Salmonella* pathogenicity islands (SPI). Their usage depends on the stage of infection as they allow overcoming different defence host strategies (Hueck, 1998). The SPIs are known to be horizontally acquired genes enabling *Salmonella* to adapt to different niches during pathogenesis (Ilyas, Tsai and Coombes, 2017). The *Salmonella* pathogenicity island-1 (SPI-1) is a 40 kb region encoding the structural components of T3SS-1 as well as chaperones, effector proteins and the transcriptional regulators controlling SPI-1 expression and interaction with other SPIs (Lou *et al.*, 2019). The regulation of SPI-1 is tightly controlled by three different AraC-like transcriptional regulators, HilD, HilC and RtsA, that form a complex forward feedback loop to activate expression of *hilA*. HilA, which is the main transcriptional regulator of the structural T3SS genes, is indirectly

influenced by many environmental stimuli through HilD (De Nisco, Rivera-Cancel and Orth, 2018; Palmer, Kim and Slauch, 2019).

SPI-1 is also fine-tuned by the flagellar regulator *fliT* through the flagellar regulons flhDC and fliZ (Que, Wu and Huang, 2013). FliZ has also been shown to directly modulate HilA (Fàbrega and Vila, 2013).

Furthermore, HilD mediates the crosstalk between SPI-1 and SPI-2 (Bustamante *et al.*, 2008). The pathogenicity island-2 (SPI-2) is a 25 kb locus encoding the T3SS-2. The histone-like nucleoid structuring protein (H-NS) has been shown to play an important role in gene silencing of this region (Fass and Groisman, 2009). Additionally, three different two-component systems are involved in the transcriptional regulation of SPI-2: i.) OmpR/EnvZ; ii.) PhoP/PhoQ and iii.) SsrA/SsrB. Both, OmpR/EnvZ and PhoP/PhoQ regulate SsrA/SsrB. This regulation depends on environmental cues, such as low concentrations of Mg^{2+} and $Ca2^{+}$ or low osmolarity and pH (Fass and Groisman, 2009).

In the intestinal lumen, *Salmonella* reaches the epithelial cells by using its flagellum and by chemotaxis aided by fimbrias and adhesins. The tip protein SipD of the T3SS-1 has also been reported to mediate intimate cell contact. Once cell contact is established, the hydrophobic translocon proteins SipB and SipC are also exposed to the extracellular environment forming a pore in the host cell membrane (Lara-Tejero and Galán, 2009). This is followed by a hierarchical injection of effectors promoting the uptake of the bacterium by the host cell. In the host cell cytosol, *Salmonella* resides within the *Salmonella* cointaining vacuole (SCV). Following internalization in the vacuole, the T3SS-1 is downregulated and the T3SS-2 is upregulated (Steele-Mortimer, 2008). T3SS-2 is induced by the low pH, low magnesium and calcium concentrations as well as the oxygen limitation inside the vacuole (Deiwick *et al.*, 1998). The effectors translocated by the T3SS-2 through the SCV membrane are involved in maturation, maintenance, trafficking and stability of the SCV. Moreover, translocated effector proteins are involved in inhibiting intracellular trafficking thereby blocking the fusion of the SCV with the lysosome (Uchiya *et al.*, 1999). During maturation, the integrity of the SCV is ensured by a bacterial-induced F-actin meshwork. Subsequently, the SCV migrates close to the Golgi apparatus ensuring acquisition of nutrients, which is important for bacterial replication (Salcedo and Holden, 2003; Fàbrega and Vila, 2013).

In addition to the *Salmonella* replicating population inside the SCV, recent studies identified a subpopulation outside the SCV, which gains access to the cytoplasm of the host cell by breaching the early SCV through the T3SS-1. This cytosolic subpopulation has been shown to

replicate even faster than inside the SCV (Castanheira and García-del Portillo, 2017). While its role is not completely clear, it has been suggested that it could prolong the lifespan of the infected host cells (Finn *et al.*, 2017).

1.3 SPI-1 T3SS - The molecular syringe

The T3SS-1 referred to as injectosome is a 6 MDa complex molecular syringe consisting of more than 20 proteins (Fig. 4) (Wagner *et al.*, 2018). Phylogenomic and structural analyses indicate that the injectisome has evolved from the flagellum (Abby and Rocha, 2012). The flagellar T3SS secreted components build up the flagellar filament that ensures motility (Table 1) (Tipping *et al.*, 2013). The entire injectisome can be divided in different substructures. The part of the needle complex anchored in the bacterial inner and outer membranes is called the basal body and includes the export apparatus (Galán *et al.*, 2014; Notti and Stebbins, 2016). The hollow needle filament protrudes from the basal body and has at its distal end a specialized tip complex, composed of the sensing tip protein and two translocon proteins (Schraidt *et al.*, 2010; Lombardi *et al.*, 2019). Below, I will give a detailed description of the different substructures.

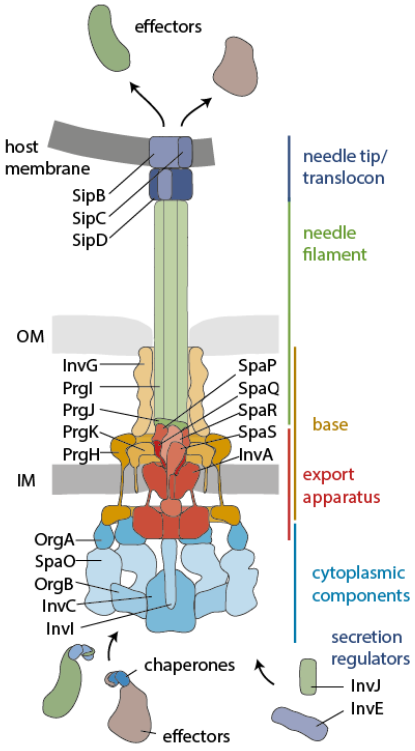

Fig. 4: The T3SS-1 and its components. The syringe like structure of the T3SS consists of different components. The cytoplasmic components are connected to the export apparatus and base, where the needle elongates capped by the tip and translocon. Different secretion regulators ensure correct assembly and secretion. Effector proteins bind to their cognate

chaperone for correct targeting to the T3SS and are released by the gate complex for secretion through the narrow conduit in an unfolded manner (Wagner *et al.*, 2018). **Abbreviations:** OM: outer membrane, IM: inner membrane, Sip: *Salmonella* invasion protein, Inv: invasion protein, Prg: PhoP repressed gene protein, Spa: Surface presentation of antigen protein, Org: oxgen regulated protein.

In the cytoplasm, the ATPase (invasion protein C, InvC), the stalk protein (invasion protein I, InvI), the two oxygen regulated proteins (OrgB and OrgA) and the surface presentation of antigen protein (SpaO) can be found. SpaO, OrgB and OrgA form the sorting platform, which, as the name suggests, ensures secretion of substrates in a hierarchical order (Lara-Tejero *et al.*, 2011; Bernal *et al.*, 2019).

Table 1: Unified nomenclature and nomenclature of the homologues T3SS proteins in *Salmonella, Flagellar, Shigella and Yersinia* (modified after Galán *et al.*, 2014).

Uni	*Salmonella*		*Flagellar*	*Shigella*	*Yersinia*
	SPI-1	**SPI-2**			
SctC	InvG	SsaC	-	MxiD	YscC
SctF	PrgI	SsaG	-	MxiH	YscF
SctI	PrgJ	SsaI	-	MxiI	YscI
SctJ	PrgK	SsaJ	FliF	MxiJ	YscJ
SctD	PrgH	SsaD	FliG	MxiG	YscD
SctK	OrgA	-	-	MxiA	YscK
SctQ	SpaO	SsaQ	FliM+FliN	Spa33 (SpaO)	YscQ
SctL	OrgB	SsaK	FliH	MxiN	YscL
SctN	InvC	SsaN	FliI	Spa47 (SpaL)	YscN
SctO	InvI	SsaO	FliJ	Spa13 (SpaM)	YscO
SctR	SpaP	SsaR	FliP	Spa24 (SpaP)	YscR
SctS	SpaQ	SsaS	FliQ	Spa9 (SpaQ)	YscS
SctT	SpaR	SsaT	FliR	Spa29 (SpaR)	YscT
SctU	SpaS	SsaU	FlhB	Spa40 (SpaS)	YscU
SctV	InvA	SsaV	FlhA	MxiA	YscV
SctE	SipB	SseC	-	IpaB	YopB
SctB	SipC	SseD	FliC	IpaC	YopD
SctA	SipD	-	-	IpaD	LcrV
SctP	InvJ	SsaP	FliK	Spa32 (SpaN)	YscP
SctW	InvE	SsaL	-	MxiC	YopN

The cytoplasmic components can exist both as free complexes in the cytoplasm and injectisome bound. In the free form they are believed to be loaded with chaperone-substrate complexes and to serve as a carrier for the injectisome (Zhang *et al.*, 2017). The ATPase is then believed to remove the chaperone, and unfold and insert the substrate into the secretion channel (Akeda and Galán, 2005).

The base is composed of three proteins with two membrane-spanning ring structures: The two PhoP-repressed gene proteins PrgH and PrgK as well as InvG. InvG forms a concentric 15meric ring at the outer membrane (outer membrane ring, OR), reminiscent of the secretin of the T2SS (Natarajan *et al.*, 2020). InvG possesses three N-terminal domains that expand into the

periplasm connecting directly to PrgH (Worrall *et al.*, 2016). The membrane and supramembrane (MS) rings in the inner membrane are formed by two inner concentric rings consisting of 24 subunits of the lipid anchored protein PrgK (inner MS) and the single transmembrane protein PrgH (outer MS) (Spreter *et al.*, 2009).

Five highly conserved proteins can be found in the inner membrane constituting the export apparatus (Wagner *et al.*, 2010). These five proteins are essential for secretion and are highly hydrophobic with up to 8 transmembrane domains (Galán *et al.*, 2014). One of them, the so-called major export protein invasion protein A (InvA), is a nonameric ring, present at the central patch of the base, which may form the entrance of the translocation channel (Worrall, Vuckovic and Strynadka, 2010). The export apparatus protein SpaS is also called switch protein, since it plays a crucial role in substrate specificity switch (Zarivach *et al.*, 2008). The minor export protein complex SpaPQR forms a translocation channel, which is constricted at several points. It is believed that SpaS interacts with SpaR to open the translocation channel (Kuhlen *et al.*, 2018).

More than 100 copies of the needle filament protein PrgI assemble with their helical hairpin structure into a right-handed hollow needle with an average length of 35 nm (Broz *et al.*, 2007). While the termini of the needle filament face inwards and the termini of the export apparatus face outwards, the components are only loosely connected (Marlovits *et al.*, 2006; Dietsche *et al.*, 2016). The inner rod protein PrgJ is responsible for the tight connection of the needle filament to the export apparatus by serving as an adaptor (Torres-Vargas *et al.*, 2019). At the distal end of almost each needle, the hydrophilic tip protein SipD (*Salmonella* invasion protein D) forms a pentameric scaffold for the two hydrophobic translocation pore proteins SipB and SipC (Mueller *et al.*, 2005; Epler *et al.*, 2012).

1.3.1 Assembly of the injectisome

Due to the presence of so many substructures, the correct assembly of each component has to happen in a highly coordinated manner. The first components are embedded in the membrane in a Sec-dependent pathway. This is followed by Sec-independent assembly once the machinery becomes secretion competent (Diepold and Wagner, 2014). The starting point, as well as different steps of the assembly of the T3SS, are still controversial and may be different in various bacterial species.

Two different assembling models have been proposed. An outside-in assembly model (Fig.5) derived from observations in *Yersinia* suggested that the subunits of the secretin assemble independently into a pre-pore at the outer membrane with the aid of the pilotin protein invH

(Diepold *et al.*, 2010). This pre-pore formation is facilitated by peptidoglycan (PG) lytic enzymes (García-Gómez *et al.*, 2011). Upon its assembly into the outer membrane, secretin recruits the outer inner ring protein PrgH. At the inner membrane, the export apparatus proteins SpaPQR are assembled prior to the recruitment of SpaS and InvA in a Sec-dependent manner (Sukhan *et al.*, 2001; Dietsche *et al.*, 2016). Subsequently, PrgK is recruited to the export apparatus. The secretin InvG is afterwards connected through the inner membrane rings with the export apparatus (Diepold *et al.*, 2010). Once the cytoplasmic components are recruited to the assembled base, the system becomes secretion competent.

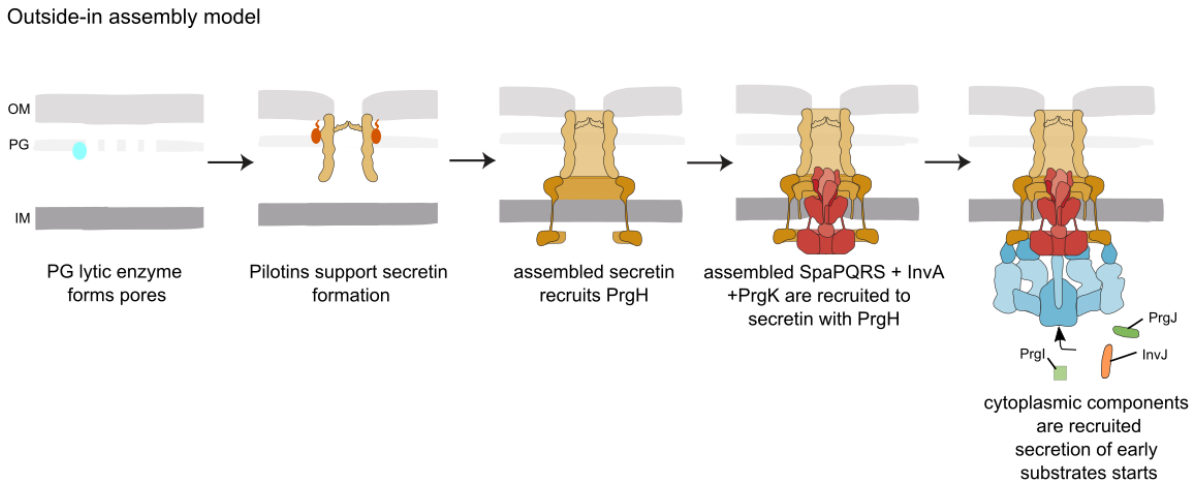

Fig. 5: Outside-in assembly model. The completion of the T3SS is initiated by the secretin assembly. The PG lytic enzyme forms pores in the PG layer for secretin formation aided by pilotins. Subsequently, PrgH attaches to InvG and the assembled export apparatus follows. Upon completion of the membrane rings, the cytoplasmic components with the ATPase assemble allowing the secretion of the early substrates (modified after Wagner *et al*., 2018). **Abbreviations:** OM: outer membrane, PG: Peptidoglycan, IM: inner membrane, Prg: PhoP repressed gene protein, Spa: Surface presentation of antigen protein, Inv: Invasion protein.

Opposing this, is the inside-out assembling model (Fig.6), which proposes the inner membrane as the starting point for the assembly of the export apparatus (Wagner *et al.*, 2010). In this model, the assembled SpaPQRS complex with InvA recruits the two inner membrane ring proteins PrgH and PrgK. This is followed by the assembly of the cytoplasmic components thus allowing the secretion of early substrates (Wagner *et al.*, 2018). The early substrate PrgJ activates the PG lytic enzyme above the assembled complex and the secretin is formed with the support of pilotins into the pre-pore (Burkinshaw *et al.*, 2015). Subsequently, InvG is coupled to the IM components (Worrall *et al.*, 2016). The needle polymerizes and completes the assembly of the secretion system.

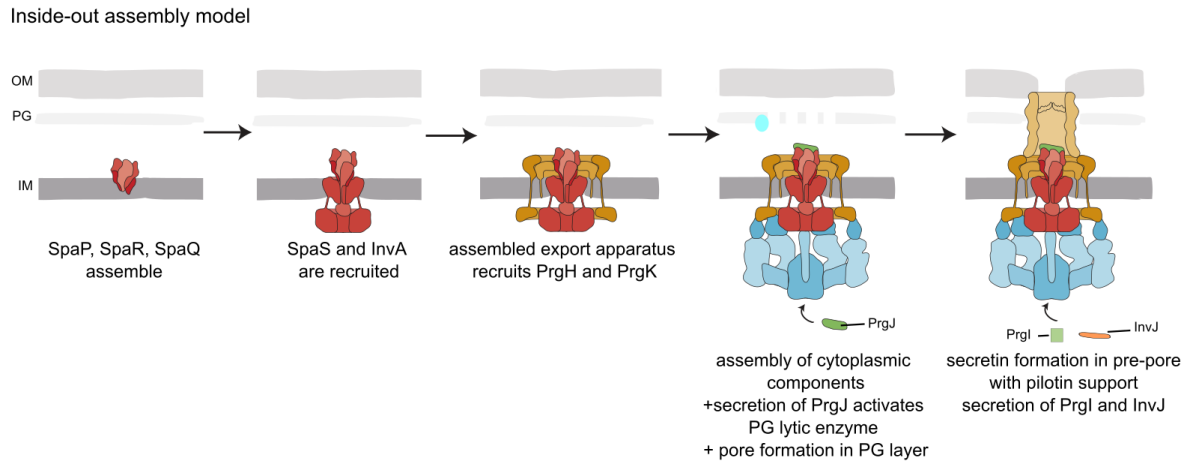

Fig. 6: Inside-out assembly model. The T3SS assembly is initiated by the export apparatus components SpaP, SpaR and SpaQ at the inner membrane. This is followed by the incorporation of SpaS and InvA. The inner membrane ring proteins PrgH and PrgK oligomerize around the completed export apparatus. The cytoplasmic components assemble allowing the secretion of PrgJ which activates the PG lytic enzyme. The secretin can then assemble in the pre-pores supported by pilotins. PrgI and InvJ are secreted and needle polymerization starts opening the periplasmic gate (modified after Wagner *et al*., 2018). **Abbreviations:** OM: outer membrane, PG: Peptidoglycan, IM: inner membrane, Prg: PhoP repressed gene protein, Spa: Surface presentation of antigen protein, Inv: Invasion protein.

The interaction of PrgH with PrgK and InvG (Burkinshaw *et al.*, 2015; Worrall *et al.*, 2016) as well as the enhanced enzymatic activity of the PG lytic enzyme in the presence of PrgJ (Burkinshaw *et al.*, 2015) support the inside-out assembling pathway for the T3SS of *Salmonella* (Wagner *et al.*, 2018; Hu, Worrall and Strynadka, 2020).

1.3.2 Energy source of the injectisome

The energy source for the export of substrates has been a controversial issue for a long time. The ATPase was primarily considered to be the fuel for the secretion process because T3SS effector proteins were shown to bind to it (Akeda and Galán, 2005; Galán, 2008). Additionally, the structure of the T3SS ATPase shares similar features to other ATP driven unfoldase- and translocase enzymes, leading to the assumption that it could facilitate effector secretion (Kato, Lefebre and Galán, 2015). But unlike other ATPases, the hexameric channel of InvC is blocked by the stalk protein InvI, challenging the theory that the substrates could be threaded through the central pore (Hu *et al.*, 2015).

The importance of the proton motive force (PMF) was discovered very early and independently by Paul *et al.* and Minamino *et al.* in flagella. The authors reported that the ATPase complex is not essential for protein export and that the export is intrinsically driven by the PMF (Minamino and Namba, 2008; Paul *et al.*, 2008). A system solely dependent on PMF dependent could even be shown by increasing the available PMF and overexpressing flagellar substrates in ATPase

mutants (Erhardt *et al.*, 2014). Mutations in the ATPase were also used to prove that infrequent ATP hydrolysis is sufficient for export of the flagellar proteins (Minamino *et al.*, 2014).

The PMF itself consists of two components: The ΔpH, i.e. the proton concentration gradient, and the ΔΨ, which is the electric potential difference between the periplasm and cytoplasm (Lee and Rietsch, 2015; Shen and Blocker, 2016). These two forces can be uncoupled and analysed separately with specific inhibitors. Investigations of these two separate components in flagellar T3SS (fT3SS) revealed that they are differently utilized (Paul *et al.*, 2008). The ΔpH was shown to be dispensable for the export of substrates in wild type strains and the ΔΨ proposed to be the main component. However, in strains lacking the ATPase the ΔpH becomes essential. Additionally, like flagellar motors, the fT3SS can shift to utilize sodium ions in ATPase complex deficient strains to drive secretion (Minamino *et al.*, 2016).

Although, fT3S and virulence-associated T3S systems lacking the ATPase were capable of substrate export, it needs to be mentioned that these were inefficient in secretion (Erhardt *et al.*, 2014). Nevertheless, it is believed that the ATPase is not involved in unfolding and that the InvA homolog FlhA is capable of stripping chaperones to unfold the substrates (Bange *et al.*, 2010; Kinoshita *et al.*, 2013). However, FlhA requires an activation step, which is performed by the ATPase and the stalk protein, suggesting that the stalk protein rotates within the hexameric ring during the ATP conversion thereby interacting with FlhA (Minamino *et al.*, 2016). One subunit of FliI is also proposed to form a free complex with two OrgB homologs (FliH), in order to bind cytosolic chaperone-substrate complexes and to recruit them to FlhA (Fig. 8) (Imada *et al.*, 2016; Gao *et al.*, 2018; Xing *et al.*, 2018).

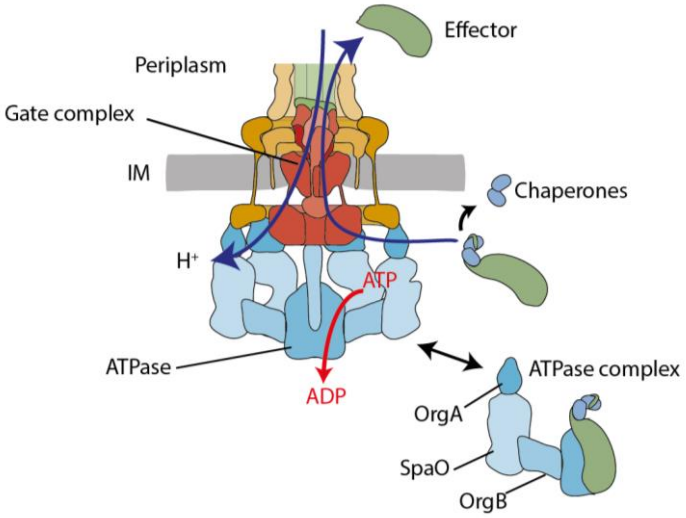

Fig. 8: PMF and ATP harnessed by the gate complex for secretion. The ATPase complex, consisting of ATPase (InvC), OrgA, SpaO and OrgB, hands over effector proteins to the gate complex, which utilizes the PMF for secretion of the effector proteins. ATP hydrolysis facilitates this process (Adapted from Wagner *et al.*, 2018). **Abbreviations:** IM: inner membrane, Org: oxygen regulated gene protein, SpaO: Surface presentation of antigen protein O.

The utilisation of the PMF seems to vary from bacteria to bacteria. The injectisome in *Pseudomonas aeruginosa* requires both PMF components, the ΔΨ and the ΔpH, while in *Shigella flexneri*, similar to the fT3SS, only the ΔΨ fuels the secretion (Lee *et al.*, 2014; Shen and Blocker, 2016). Additionally, the role of the ATPase could also vary between fTSS and injectisomes. Although the PMF is the main driving force for secretion in all systems, it is still not clear whether the ATPase acts only as ignition key for activating the gate complex or whether it also dechaperones and unfolds substrates (Galán, 2008; Lee and Rietsch, 2015; Terashima *et al.*, 2018).

The common notion among all these systems is that the InvA homologous and the ATPase/stalk protein play an important role in the PMF conversion.

1.3.3 Needle length regulation and substrate specificity switch

Once the basal body associates with the cytoplasmic components, the system becomes secretion competent and starts to export three different early substrates, the so-called inner rod protein or rather adaptor protein PrgJ, the needle filament protein PrgI and the needle-length control protein InvJ (Kimbrough and Miller, 2000; Kubori *et al.*, 2000) (Fig. 9). As described above, the needle filament proteins assemble on the needle adaptor, which anchors to the distal end of the minor export apparatus by closely interacting with the N-termini of SpaP and SpaR (Dietsche *et al.*, 2016; Kuhlen *et al.*, 2018). For elongation, the needle subunits travel through the already built up needle to the growing tip, where they get inserted. It was recently shown that the needle filament elongation is supported by OrgC, having similarities to the flagellar

capping protein (Kato *et al.*, 2018). The opening of the secretin gate at the outer membrane is then induced in two steps (allosteric and steric) via the assembling and continuously polymerizing needle (Hu *et al.*, 2019).

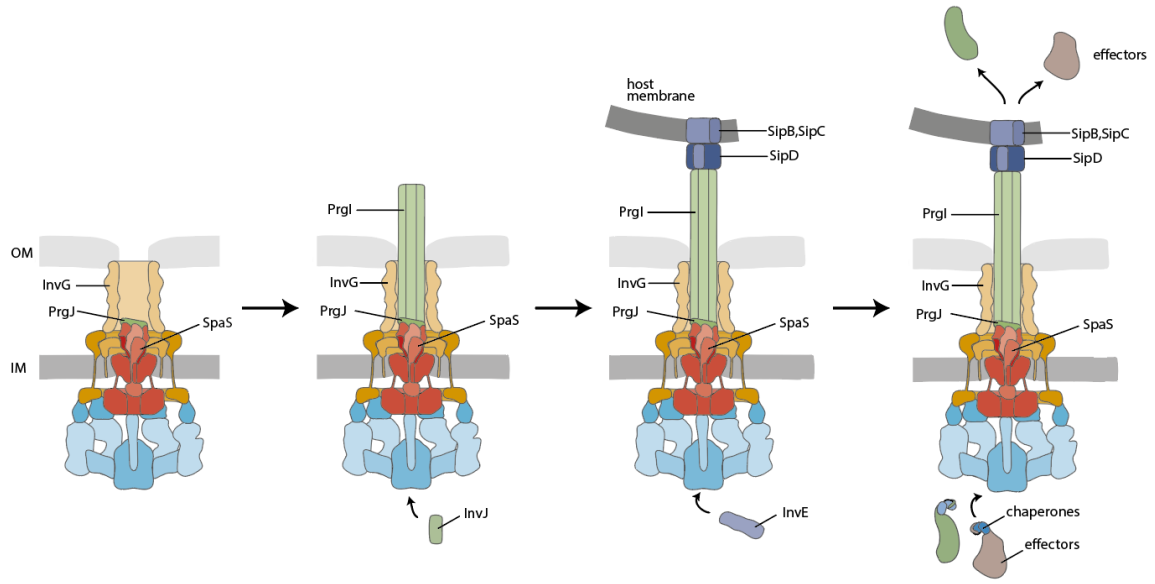

Fig. 9: Two substrate switches occur in the injectisomes. The secretion of early substrates starts upon assembly of the basal body. PrgJ is secreted first as one of the early substrates, followed by InvJ and PrgI. The first switch, also called substrate specificity switch, enables secretion of intermediate substrates: The tip and translocon proteins SipBCD. Once the system is secretion competent a second switch leads to injection of effectors (late substrates) e.g. SipA, SopE or SptP. **Abbreviation:** OM: outer membrane, IM: inner membrane, Inv: invasion protein, Prg: PhoP repressed gene protein, Sip: Salmonella invasion protein, SpaS: Surface presentation of antigen protein S.

The secreted early substrate InvJ is believed to control needle length. This notion is based on the observation that lack of InvJ leads to uncontrolled needle elongation (Sukhan *et al.*, 2001). Several models were proposed for explaining the mechanism of needle length regulation. In one of them, the so-called timer model, it was speculated that the needle elongates until the adaptor protein PrgJ is fully assembled and connection of the needle with the base is established. This would lead to termination of needle subunit secretion and to a conformational change within the base inducing secretion of intermediate substrates (Marlovits *et al.*, 2006). However, this model is based on experiments that were performed by overexpressing PrgJ, and was quickly questioned when the same experiments were performed under native conditions (Lefebre and Gálan, 2014; Wee and Hughes, 2015). Furthermore, it was shown that the needle length correlates directly with the length of the ruler protein InvJ (Journet *et al.*, 2003). Additionally, very recent data suggest that inner rod assembly precedes assembly of the needle filament (Torres-Vargas *et al.*, 2019).

The C-terminal core domain of the ruler protein is largely conserved among different species (Agrain *et al.*, 2005; Bergeron *et al.*, 2016; Kinoshita *et al.*, 2020). The best studied ruler protein

is flagellar FliK which consists of two domains $FliK_N$ and $FliK_C$ connected by a flexible linker $FliK_L$ (Kinoshita *et al.*, 2017) (Fig. 10, shown for *Salmonella* homolog InvJ). It has been proposed that the N-terminal $FliK_N$ determines the hook length while the C-terminal compactly folded $FliK_C$ with its intrinsically disordered C-terminal tail ($FliK_{CT}$) suppresses switching during hook assembly. However, $FliK_C$ induces the substrate specificity switching by interacting with the autocleavage protein once the hook has reached the preset length (Minamino and Macnab, 2000; Minamino *et al.*, 2004; Ferris and Minamino, 2006; Erhardt *et al.*, 2011; Kinoshita *et al.*, 2020)

After gaining more insights into the structure of FliK, new models have been put forward to explain how the needle or hook length sensing mechanism is regulated independently of the inner rod. One hypothesis proposes that the secreted N-terminus of FliK folds into a ball shape when it reaches the tip. This ball shape moves away from the tip by Brownian motion, thereby pulling the rest of the protein. Meanwhile its C-terminal domain gets unfolded and has a chance to interact with the cytoplasmic domain of FlhB (Minamino and Macnab, 2000; Aizawa, 2019).

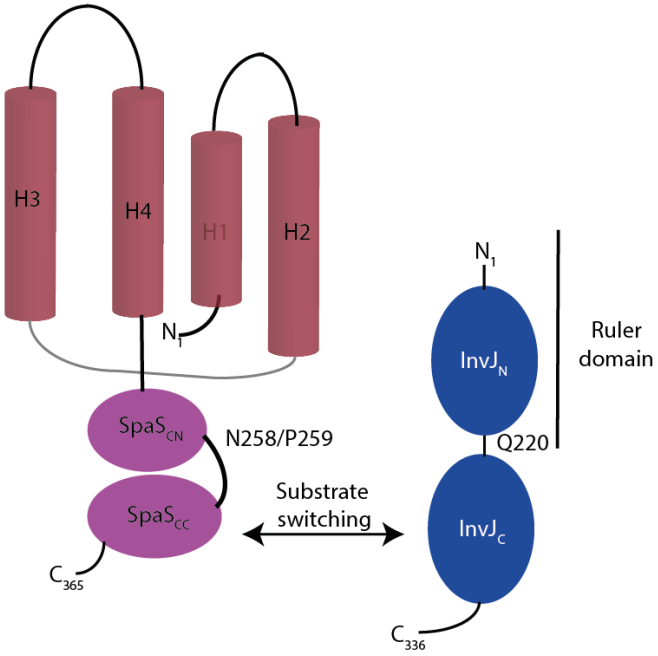

Fig. 10: Proposed SpaS- InvJ interaction. SpaS consists of 4 N-terminal helices and two C-terminal cytoplasmic domains $SpaS_{CN}$ and $SpaS_{CC}$. The helices are believed to be part of the export apparatus (not shown). The autocleavage occurs in between the two cytoplasmic domains. The $SpaS_{CC}$ domain is believed to interact with the C-terminal domain of InvJ inducing the substrate specificity switch. While the N-terminal domain of InvJ (here shown in a compact form) acts as ruler determining the needle length of the T3SS (adapted from Ferris and Minamino, 2006; Kuhlen *et al.*, 2020).

Autocleavage protein SpaS and its homologues were predicted to consist of a N-terminal region with four transmembrane domains (TM) embedded in the inner membrane and a C-terminal cytoplasmic domain (Ferris and Minamino, 2006) . However, Kuhlen *et al.* have recently solved the structure of the putative N-terminal transmembrane domain of FlhB, the SpaS homolog in flagella, and have shown that this is part of the export apparatus rather than being an accessory factor. This finding suggests a role for FlhB in gate opening (Kuhlen *et al.*, 2020). The structure of the hydrophobic FlhB domain revealed the presence of four α-helices with a long loop ($FlhB_L$) in between the helix two and three (Kuhlen *et al.*, 2020). A flexible linker of 30 amino acids connects the N-terminal domain with the cytoplasmic C-terminal domain. This cytoplasmic domain is composed of five ß-sheets and three α-helices arranged in a canonical fold. The NPTH motif, which is highly conserved among species, lies in an exposed loop between strands ß1 and ß2 (Fig. 10). The intrinsically induced cleavage of SpaS occurs within this motif between Asp258 and Pro259 residues (Lavander *et al.*, 2002; Deane *et al.*, 2008; Zarivach *et al.*, 2008). The resulting fragments of the cleavage $SpaS_{CN}$ and $SpaS_{CC}$ are believed to retain interaction with each other, but some existing data point out that the C-terminal fragment might be secreted in some T3SS (Ferris *et al.*, 2005; Frost *et al.*, 2012).

Mutations in the NPTH motif of SpaS and its homologs lead to an autocleavage defective protein ($SpaS_{N258A}$) impairing secretion of intermediate and some late substrates (Ferris and Minamino, 2006; Sorg *et al.*, 2007; Zarivach *et al.*, 2008). Based on this observation, autocleavage of SpaS was suggested to be the regulatory signal for the secretion switch from early to intermediate substrates (Riordan and Schneewind, 2008; Erhardt *et al.*, 2010). Deane *et al.*, by looking at the crystal structure of the C-terminal domain of Spa40, the homolog of SpaS in *Shigella flexneri*, observed a minor structural rearrangement upon cleavage involving the surface exposure of a loop. Hence, they concluded that the gained altered surface features rather than cleavage *per se* are critical for the regulation of secretion substrates (Deane *et al.*, 2008).

On the contrary, recent findings by Monjarás Feria *et al.* revealed that autocleavage of SpaS occurs after its folding process and that the autocleaved SpaS is incorporated into the base of the assembling T3SS. These data demonstrated that the gained conformational flexibility rather than the changed surface properties plays a role in the substrate specificity switch after cleavage (Monjarás Feria *et al.*, 2015).

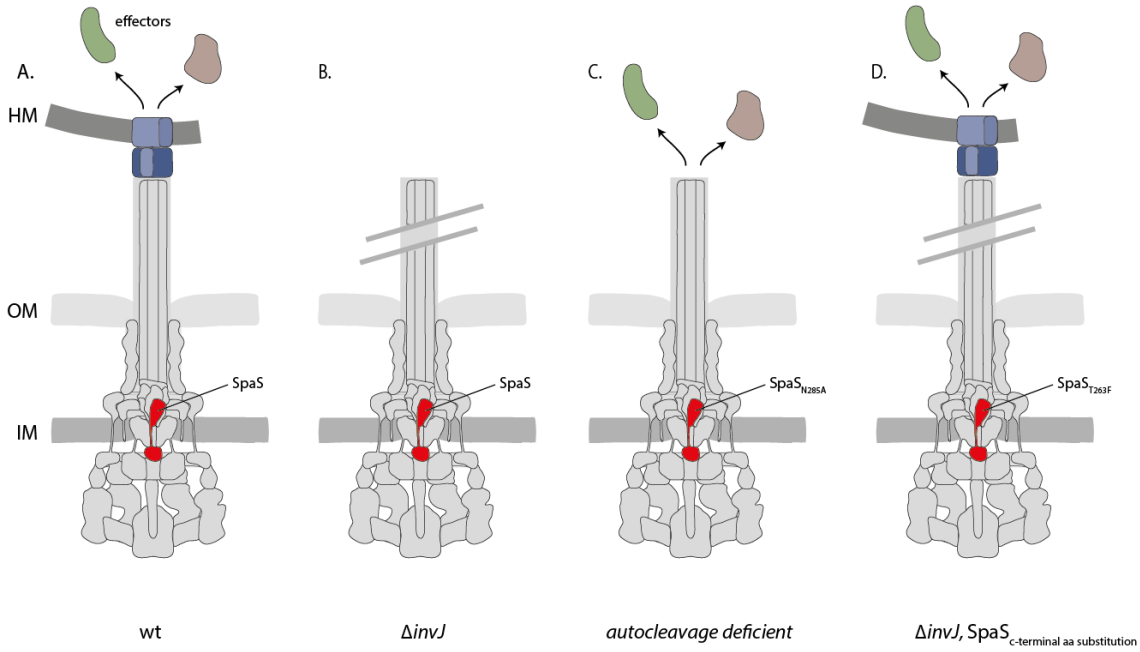

Fig. 11: Different phenotypes of *invJ* and *spaS* mutants. **A.** InvJ and SpaS regulate the secretion of intermediate substrates upon needle elongation in wt. **B.** *invJ* deficient mutants are locked in secretion of early substrates. They are incapable to regulate the needle length and can not secrete intermediate substrate. **C.** Autocleavage deficient mutants have normal needle length, but cannot switch and thus are not able to secrete intermediate substrate. **D.** The suppressor mutation T263F within SpaS can partly bypass the Δ*invJ* phenotype by autonomous switching enabling the secretion of intermediate substrates, but can not restore needle length. **Abbreviations:** HM: host membrane, OM: outer membrane, IM: inner membrane, wt: wild type

Needle length control and substrate specificity switching are often seen as one mechanism. By looking at different *spaS* mutants it becomes clear that they are two distinct processes. Autocleavage mutants are not capable to switch and thus cannot secrete intermediate substrates, but the needle length is indistinguishable from that of wild type strains (Hirano *et al.*, 1994; Sorg *et al.*, 2007; Wiesand *et al.*, 2009; Monjarás Feria *et al.*, 2015) (Fig. 11 C). The assumption that needle elongation stops after secretion of the tip has been challenged by this observation in the autoceavage mutants. Another yet unknown mechanism independent of switching must be involved in either actively stopping further secretion of early substrates, or prohibiting further assembly at its distal end, possibly as a consequence of conformational changes in needle filaments (Wagner *et al.*, 2018). Interestingly, appendage of the signal sequence of late substrates to the tip protein could completely restore the secretion of the needle tip protein in the autocleavage mutant. This led to the presumption that the prevention of the autocleavage simply prohibits secretion of intermediate substrates due to their signal sequence (Sorg *et al.*, 2007).

However, the interplay between the ruler protein and the autocleavage protein has been shown *in vitro* in several species (Minamino and Macnab, 2000; Edqvist *et al.*, 2003). Mutants lacking the ruler protein were impaired in the secretion of intermediate substrates and had very long needles (Fig. 11 B). Amino acids substitutions in the C-terminal cytosolic domain of the SpaS homologues FlhB and YscU partially restored the phenotype caused by the lack of the ruler protein in the corresponding species (Fig. 11 D) (Kutsukake, Minamino and Yokoseki, 1994; Edqvist *et al.*, 2003). These data led to the assumption that the ruler and the autocleavage protein coordinately regulate the secretion of intermediate substrates (Edqvist *et al.*, 2003). This interplay between the two proteins still needs to be proven *in vivo*.

Upon the substrate specificity switch, the sorting platform gets loaded with the hydrophobic translocator proteins and secretes them (Lara-Tejero *et al.*, 2011). At this stage, when the needle is completely assembled, the secretion of the T3SS effectors is triggered by external factors. *In vivo*, host cell contact is sensed by the needle tip, which undergoes a conformational change. This conformational change is transmitted as a signal to the export apparatus triggering secretion (Armentrout and Rietsch, 2016). *In vitro* the host cell contact can be mimicked by the addition of Congo red in *Shigella* or calcium depletion thereby triggering the secretion in *Yersinia* and *EPEC* (Straley *et al.*, 1993; Bahrani, Sansonetti and Parsot, 1997; Ide *et al.*, 2003). However, in *Salmonella* neither Congo red nor calcium depletion leads to induction of effector secretion. It has been suggested that the needle tip senses cholesterol/sphingomyelin of the host membrane and initiates afterwards the completion of the translocation pore (Lafont *et al.*, 2002; Hayward *et al.*, 2005). The bound translocator proteins might affect the structure of the needle transmitting a signal to the cytoplasmic side and initiating the second switch for secretion of late substrates. This was the case when bacteria were preincubated with deoxycholate (DOC), which can be found in the small intestine as bile acid. Although, the *Shigella* and *Salmonella* tip protein are highly homologous, SipD was shown not to bind DOC and DOC to inhibit SPI-1 expression (Stensrud *et al.*, 2008; McShan *et al.*, 2017).

Secretion of effector proteins is believed to be controlled by the tip and translocon proteins SipD, SipC and SipB and by the gatekeeper protein InvE (Kubori and Galán, 2002; Cherradi *et al.*, 2013; Lee *et al.*, 2014; Deng *et al.*, 2015; Shen and Blocker, 2016). Deletion of *invE* was shown to lead to a similar phenotype as that of the knockout mutant of *sipD*. InvE deficient mutants downregulate the secretion of intermediate substrates and upregulate the secretion of late substrates. This indicates that InvE positively regulates the secretion of intermediate substrates, but negatively influences that of late substrates (Kubori and Galán, 2002). Strains deficient for SipD were additionally shown to upregulate the secretion of the translocon

proteins, SipB and SipC (Kaniga, Trollinger and Galan, 1995). Whether SipD interacts with InvE is not clear, but recent data suggest that the N-terminus of InvE affects the stability of SipD without a direct interaction (Kim *et al.*, 2013).

Another protein appearing to be involved in switching from intermediate to late substrates is InvA. The InvA homolog EscV was shown to bind the gatekeeper protein and the substrate-chaperone complexes with its cytosolic C-terminus (Portaliou *et al.*, 2017). But how such an interaction leads to hierarchical secretion of substrates in association with SipD and SpaS remains to be investigated.

1.3.4 Effectors of the T3SS-1

The main biological function of the T3SS is to inject effector proteins across the host cell membrane. About 100 different effector proteins are believed to be secreted by the different T3SSs (Rüter and Schmidt, 2016). Some with redundant properties cooperate with each other to orchestrate the modulation of the host cell pathways (Ramos-Morales, 2012; Galán and Waksman, 2018)(Fig. 12), thus enabling host cell invasion, induction of inflammation, intracellular bacterial survival and replication. To achieve this, the injected T3SS effectors target different pathways like immune signalling pathways, endo-and exocytotic processes, barrier function, protein transport pathways, cell proliferation and migration as well as pathways leading to apoptosis (Fàbrega and Vila, 2013). Biochemical activities of the host cell like ubiquitination, phosphorylation or ligation are also exploited to fulfil the effector functions. Some effectors can by themselves carry out biochemical functions like proteolysis, ribolysis or mimic ubiquitination, and many other biochemical activities (Dean, 2011).

Most of the T3 secreted effector proteins possess a N-terminal signal sequence in the first 15-25 amino acids, and a chaperone binding domain of about 100 amino acids located downstream (Boyd, Lambermont and Cornelis, 2000; Lee and Galán, 2004). The secretion signal is not conserved, but contains some specific features as being inherently unstructured and enriched in amino acids like serine, threonine, isoleucine and proline (Lloyd *et al.*, 2001). Additionally, the amino acid frequence and the physicochemical properties seem to be very important (Arnold *et al.*, 2009). Interestingly, some effector proteins like the effector protein SipB have an additional C-terminal signal sequence, requiring both the N- and C-terminal region to be secreted through the T3SS. In absence of its C-terminal secretion signal, SipB is secreted through the fT3SS instead (Kim *et al.*, 2007).

Salmonella injects a cocktail of effectors for invasion. While some of these effector proteins are very well known, some still need to be investigated. The best studied effectors are SopE, SopE2 and SopB (in literature often referred as SigD), SipA and SopD (Galán, 2001; Raffatellu *et al.*, 2004). With their redundant functions, these effectors drive the uptake into the host cell.

SopE and SopE2 are known as guanine nucleotide exchange factors (GEFs). Both, SopE and SopE2 can directly bind to the small Rho GTPases CDC42 and Rac1, which are involved in the regulation of the actin cytoskeleton: The binding of the effectors to these proteins leads to actin polymerization (Hardt *et al.*, 1998; Stender *et al.*, 2000).

The effector protein SipA has been shown to form small foci at the host cell-bacteria contact site, anchoring the bacteria to the host cell. Although not essential for invasion, SipA is responsible for the spatial restriction of the cytoskeletal rearrangements induced by the other effectors to make invasion more efficient (Zhou, Mooseker and Galán, 1999). SipA mechanically stabilizes actin filaments (F-actin) by direct binding and displacement of the host actin binding proteins ADF/cofilin, which are involved in the depolymerization of F-actin. Additionally, SipA acts as an inhibitor of F-actin disassembly of actin filaments by blocking the severing activity of the host actin binding protein gelsolin. As a result, F-actin fragments, which are already capped, are reannealed reducing the numbers of free ends (McGhie, Hayward and Koronakis, 2001, 2004). Besides this actin binding function at the C-terminus, SipA harbours one more functional domain at the N-terminus partly overlapping with its chaperone binding site (Schlumberger *et al.*, 2007). This domain was proposed to play a role in the perinuclear positioning of the SCV by interacting with the SPI-2 effector SifA, as well as in the transmigration of polymorphonuclear leukocytes (Brawn, Hayward and Koronakis, 2007; McIntosh *et al.*, 2017).

Interestingly, these two functional domains are separated by a caspase cleavage motif. The DEVD motif is believed to release the N-terminal domain from the actin binding C-terminus for independent activation of inflammations depending on the cell type (Srikanth *et al.*, 2010).

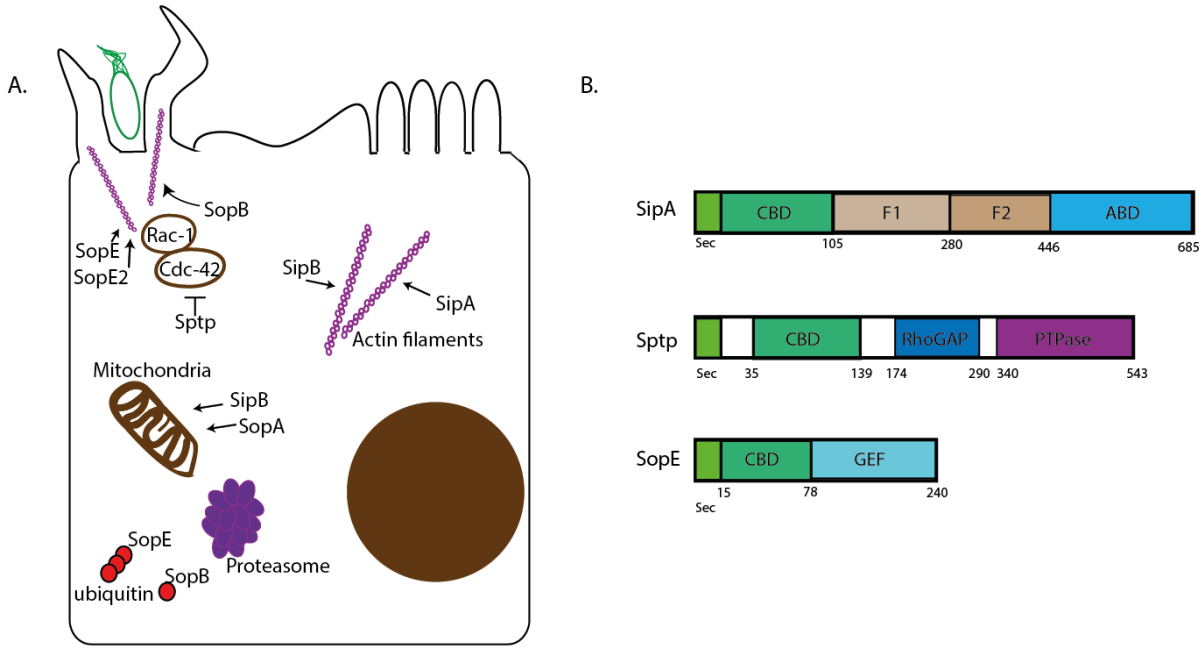

Fig. 12: Effector functions inside the host cell and their functional protein domains. **A.** T3SS effector proteins possess a specific secretion signal at their N-terminus mostly followed by the chaperone binding domain (CBD). SipA comprises two functional domains (F1, F2) which are believed to affect the foci formation and SipA-SipA interaction. SopE consists of a Sec signal, CBD and a guanine nucleotide exchange (GEF) domain. **B.** The actin binding domain (ABD) of SipA binds directly to F-actin. SptP reverses the function of earlier injected effectors with its Rho GTPase-activating protein (GAP) activity towards Cdc42. The GEF domain of SopE is known to rearrange the cell cytoskeleton. Besides these effectors, SipB and SopE play a major role in interfering with host cell functions. SopE and SopB also carry ubiquitination sites ensuring rapid degradation inside the host cell. **Abbreviation:** Sop: *Salmonella* outer protein, Sip: *Salmonella* invasion protein, Rac-1: Rho GTPase, Cdc-42: Rho family GTPase, CBD: chaperone binding domain, ABD: actin binding domain, RhoGAP: Rho GTPase activating protein domain, PTPase: protein tyrosine phosphatase domain, GEF: Guanine nucleotide exchange factor domain.

SopB dynamically modulates the phosphoinositide cycles at the site of invasion, acting as a lipid phosphatase: By targeting phosphatidylinositol in the membrane and removing the phosphate at 4' and 5' position SopB promotes the increase of different phosphatidylinositol 3-phosphate species (Terebiznik *et al.*, 2002). This in turn allows SCV fission from the membrane and the recruitment of the GTPase Rab5 and the kinase Vps34 involved in the maturation of the SCV (Mallo *et al.*, 2008). New data also suggest that SopB recruits a member of the nexin family, SNX9, through the generation of PtdIns(2,3)P_2, to promote actin polymerization and, indirectly, ruffle formation (Piscatelli, Li and Zhou, 2016).

The effector protein SopD has been shown to be recruited by SopB. Although the mechanism is not known, SopD acts cooperatively with SopB to contribute to the internalization process that leads partly to a pro-inflammatory responses (Bakowski *et al.*, 2007). The overreaction to this signal might alterate the homoeostasis of the host cell, impacting the bacterial survival, replication and dissemination inside the host (Stecher *et al.*, 2007).

SptP is an effector that reverses the above-mentioned effects on the actin cytoskeleton and possesses a N-terminal GTPase activitation (GAP) domain and protein tyrosine phosphatase activity. It was shown that the GAP domain of SptP binds to the active GTP-bound form of Rac1 and Cdc42 and promotes disruption of the actin cytoskeleton thus opposing the effects of SopE. Thus, the infected host cells can regain their normal cytoskeletal architecture (Fu and Galán, 1999).

It has been suggested that there might be a kind of hierarchical regulation in the injection of these effectors or in their molecular amount in order to avoid functional interference. It was previously shown that SopE and SptP were delivered simultaneously in equivalent amounts into host cells, but that a temporal regulation occurs inside the host cell due to different degradation patterns of the effectors. SopE possesses polyubiquitination sites resulting in a shorter half-life than SptP. Thus, SptP can fulfill its function once SopE is degraded. However, a recent publication challenged these previous findings and demonstrated that effectors are expressed in different molecular amounts and that they are hierarchically injected into the host cell with SipA and SopE being injected first followed by SptP (Schlumberger *et al.*, 2005; Winnen *et al.*, 2008; Van Engelenburg and Palmer, 2010).

How exactly hierarchical injection is regulated and whether there is a difference in the affinity of the effectors for the translocation channel of the injectisome is still not clear.

1.4 Tools for investigating T3SS secretion and injection

Effector proteins mediate different functions like obtaining nutrients from their environment, communicating with other bacteria and interacting with host cells. Therefore, investigating effector proteins is a necessary approach to reveal how bacteria interacts with their environment.

A couple of methods have been established in the last decades to investigate the secretion and translocation of the T3SS effectors. One of the traditional methods is the Western blot based fractionation assay which was established very early, even before having much knowledge about the structure of the secretion system (Collazo and Galán, 1997).

In the new digital era, different bioinformatic tools can predict many properties of effectors, such as the ability to be secreted, based on the secretion signal or secondary structures. However, these digital tools are still error-prone and the prediction outcomes need to be experimentally proven (Maffei, Francetic and Subtil, 2017).

I will only provide a short overview of some methods for the Western blot-based fractionation assay and will discuss the assays based on enzymatic and fluorescent readouts. Furthermore, I will discuss luciferases in detail as this is important for this thesis.

1.4.1 Fractionation based assays

Assays based on fractionation are simple, since they allow the separate detection of proteins inside bacteria, in the supernatant or in host cells. Reporter proteins are not required when antibodies against the protein of interest are available. The most commonly used bacterial secretion assay based on Western blotting and immunodetection provides information about the proteins that are expressed and remain cell associated (whole cell fraction) and those secreted in the supernatant. A second commonly used fractionation based assay is the so-called translocation assay based on Western blot and immunodetection, whereby, besides the bacterial fraction, two additional fractions from the host cell can be distinguished: One containing the translocated bacteria and the other containing translocated effectors (Collazo and Galán, 1997).

Spheroplasting can also be considered as a fractionation-based assay for the localization of T3SS components. This method was first described to investigate the lipid composition of the bacterial membrane of *Bacillus stearothermophilus* (Bodman and Welker, 1969). The treatment of bacteria with a Ca^{2+}-Chelator EDTA and lyzozyme under osmotic conditions, releases the bacterial outer membrane with the digested peptidoglycan layer, and thus spheroplasts are generated. In the best case, cells are not lysed by the harsh treatment conditions and the fractions are not cross-contaminated (Kuo *et al.*, 2007).

Although, these assays are easy to perform, they are tedious and only semi-quantitative. Additionally, as end-point measurements, these assays do not deliver any information about secretion kinetics.

1.4.2 Enzymatic assays

Reporter-based assays may use as a readout the enzymatic activity of the tag fused to the bacterial proteins. Mostly restricted to a particular space of activity, these assays provide information about translocation of effectors.

The TEM-1 ß-lactamase assay for analysing protein translocation was firstly described in enteropathogenic/ enterohemorrhagic *Escherichia coli* (EPEC/EHEC). By preloading the host cells with the membrane-permeable substrate coumarin cephalosporin (CCF2 or CCF4), the injected effector- ß- lactamase fusion protein is capable to cleave the lactam ring in CCF2,

disturbing the Förster resonance energy transfer (FRET) signal of CCF2 and leading to a change in the fluorescence from green to blue emission (Charpentier and Oswald, 2004). Years later, Mills and colleagues could show the applicability of the TEM assay to analyse real-time translocation of EPEC/EHEC effectors in the host cell (Mills *et al.*, 2008). However, the CCF2 preloaded in the host cell is depleted after about 40 min, impeding a precise and correct measurement of effector translocation (Mills *et al.*, 2008). Harmon *et al*. used the TEM assay for discovering compounds that inhibited effector translocation in *Yersinia* (Harmon *et al.*, 2010).

A further approach to analyse effector translocation in the host cell is based on the use of the adenylate cyclase, which needs calmodulin for its activation to convert ATP to cAMP (Fig. 13). Sory et al. took advantage of the fact that calmodulin is a eukaryotic specific protein and thereby not present in the bacterial cell. The adenylate cyclase was fused to *Yersinia* effector proteins and the translocated effector fusion proteins were detected by an increase of cAMP production inside the host cell (Sory *et al.*, 1995).

Type IV and Type III secretion dependent translocation was also monitored by employing the Cre/loxP recombinase system (Schulein *et al.*, 2005; Briones, Hofreuter and Galán, 2006). The T3SS effector protein SopE was fused to the P1 Cre recombinase and the host cells were transfected with a plasmid containing a reporter firefly luciferase or GFP flanked by loxP. Upon injection, the transcription of the fused firefly luciferase or GFP was activated due to the recombinase event on the flanking loxP sites. Although it worked well *in vitro*, the efficiency of the system *in vivo* was not sufficient and did not allow quantitative measurements (Briones, Hofreuter and Galán, 2006; Ehsani, Rodrigues and Enninga, 2009).

The carboxypeptidase G2 (CPG2) was applied as read-out for a host-cell independent screening assay (Yount *et al.*, 2010). In this very simple approach, the 43 kDa large metalloprotease CPG2 is fused to the *Salmonella* T3SS effector SopE2. Since CPG2 selectively hydrolyses glutamate from diverse substrates, Yount et al used the the fluoregenic dye 2-dicyanomethylene-3-cyano-2,5-dihydrofuran (CyFur) and synthetized the derivative Glu-CyFur, as substrate for CPG2 (Yount *et al.*, 2010). The resulting fluorescence upon cleavge was used as readout for the secretion of SopE2. With this assay, Tsou and colleagues could explore the inhibitory activity of flavonoids against the T3SS (Tsou *et al.*, 2016).

A recent approach used as enzymatic read-out the increased activity of the transcription factor NF-kB in the host cell. It has already been shown that bacterial T3SS activates the NF-kB pathway (Hobbie *et al.*, 1997). Duncan and colleagues utilized a luminescence-based NF-κB reporter system to screen compounds inhibiting the *Yersinia* T3SS (Duncan *et al.*, 2013).

However, similar to the cAMP production assay, this assay is also not useful for *in vitro* assays, i.e. in the absence of a host cell.

1.4.3 Fluorescence protein-based assays

The 26.9 kDa large GFP is the most-known fluorescent protein and has been used as a tag for bacterial T3SS effectors in *Shigella*. However, type III substrates fused to the GFP were no longer secreted, but rather blocked the system with their bulky green fluorescent tag (Enninga *et al.*, 2005). It is believed that the T3SS is unable to unfold the compact ß-barrel structure of GFP and thus effector fusion proteins are not able to pass through the hollow needle (Jaumouillé *et al.*, 2008). However, Jaumouillé and colleagues took advantage of this system and, by fusing GFP to the translocon pore protein IpaC variants, they showed that secretion occured at one bacterial pole in *Shigella flexneri* (Jaumouillé *et al.*, 2008).

Schlumberger and colleagues also employed GFP, but with a different strategy (Schlumberger *et al.*, 2005). Instead of tagging an effector protein of the T3SS, they appended GFP to InvB, the cognate chaperone of the *Salmonella* T3SS effector protein SipA. The InvB-GFP fusion construct was expressed inside the host cell and upon bacterial injection of SipA, InvB-GFP was recruited to SipA foci at the site of bacterial-host cell contact (Schlumberger *et al.*, 2005).

Another GFP-based approach was developed by Van Engelenburg and Palmer by utilizing a split GFP variant. The large GFP1-10 fragment was expressed *in trans* in the host cell, while the last ß strand GFP11 was coupled to the *Salmonella* SPI-2 effector proteins PipB2, SteA and SteC. In this way, the complementation of GFP occurred inside the host cell and the small GFP11 fragment as a tag did not affect the secretion of effector proteins as previously observed for the full length GFP. Nonetheless, the complementation has a slow maturation time, therefore the split GFP lacks the dynamic behavior required to study effector proteins with quick and short mode of action (VanEngelenburg and Palmer, 2008).

The tetracysteine tag that binds to the biarsenic dye FlAsH allowed Enninga *et al.* to monitor effector translocation in the host cell (Fig.13). The *Shigella* effector proteins IpaC and IpaB were appended with a tetracysteine and, similarly to the TEM ß-lactamase assay, host cells or bacterial cells were labeled with the dye prior to injection. In comparison to the CCF2 dye that is used in the ß-lactamase assay, the FlAsH dye is a biarsenic, organometallic reagent and

therefore toxic in a way that long exposure times to the dye would induce the death of eukaryotic cells (Enninga *et al.*, 2005).

The Light, Oxygen and Voltage (LOV) sensing domain of the plant blue light receptor, phototropin, was recently developed for use as a reporter protein for investigating T3SS based translocation of effectors (Gawthorne *et al.*, 2012; McIntosh *et al.*, 2017). In comparison to other fluorescent proteins, the LOV protein is very small (~10 kDa), active under anaerobic conditions and capable to recover after photobleaching (Chapman *et al.*, 2008). Different variants, improved LOV (iLOV) and phiLOV, have been engineered to increase photostability and fluorescence (Chapman *et al.*, 2008; Christie *et al.*, 2012). However, phiLOV appended to the effector protein Tir displayed decreased fluorescence in comparison to GFP fusion proteins, making it impossible to detect less abundant proteins (Gawthorne *et al.*, 2016). Moreover, some proteins that were known to be targeted to the periplasm, when tagged with LOV, did not show any fluorescence after being translocated by the Sec translocon (Gawthorne *et al.*, 2012). The fluorescent properties of LOV rely on the binding to the chromophore flavin mononucleotide. Since the transport through the Sec-translocon occurs in an unfolded state, Gawthorne *et al.* proposed that the reason for the lack of the fluorescence signal might be the release of flavin during the unfolding of LOV. Alternatively, the loss of the fluorescence may be the result of LOV interfering with the function of the tagged proteins, despite its small size (Gawthorne *et al.*, 2012).

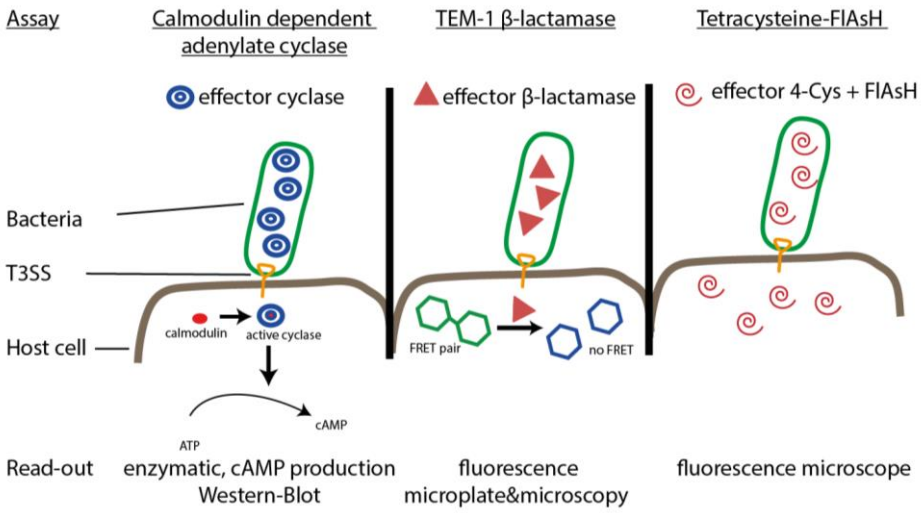

Fig. 13: Overview of the effector translocation assays. Effector proteins are tagged with calmodulin dependent adenylate cyclase, TEM-1 ß-lactamase or a tetra cysteine motif. Upon effector translocation adenylate cyclase can bind calmodulin and produce cAMP. Effectors tagged with the ß-lactamase are able to cleave the FRET substrate inside the host cell allowing detection of the altered fluorescence signal. Bacterial strains with the tetracysteine motif in their effector proteins are stained with the organometallic FlAsH dye enabling to monitor effector translocation. The readouts of the different assays can be

obtained via western blot, fluorescence microscopy and microplate measurement. **Abbreviations:** T3SS: Type III secretion system, ATP: Adenosine triphosphate, cAMP: cyclic adenosine monophosphate, FRET: Förster (Fluorescence) energy transfer, Cys: Cysteine, FLAsH: Fluorescein arsenical hairpin binder, a fluorescein based biarsenical dye

1.4.4 Bioluminescence and bioluminescence-based assays

Bioluminescence can be found in many living organisms and is based on an exothermic reaction that is enzymatically catalysed leading to an excited state of the orbitals and photons, which are subsequently emitted (Fereja, Hymete and Gunasekaran, 2013). Although luminescence had already been observed in ancient times, the first experiments with bioluminescence just started at the end of the 19th century. During these times, the substrate got named "luciferin" and the enzyme that catalyses the reaction was called "luciferase" (Fan and Wood, 2007; England, Ehlerding and Cai, 2016).

In the early 20th century, E. Harvey studied bacterial luciferases and found out that they require oxygen for their light reactions (Goodkind and Harvey, 1952). The first luciferase was extracted in 1940s by McElroy, even prior to the discovery of the fluorescent protein GFP (McElroy and Ballentine, 1944). This allowed the molecular manipulation of the first luciferase enzyme in the following years. Throughout the years, several more luciferases have been discovered and utilised in different applications (England, 2016; Fan and Wood, 2007).

The most widely used luciferases are the Red firefly, Renilla, and the Gaussia luciferases (Fig.14). The monomeric firefly luciferase (RFLuc, 62 kDa) was first isolated from *Photinus pyralis* in 1956 (Green and McElroy, 1956). It belongs to the ATP-dependent luciferases and requires Mg^{2+}, O_2 and luciferin as substrate to produce light with a peak emission of 560 nm (de Wet *et al.*, 1987). Since the RFLuc needs ATP to generate light, several companies use this property of the RFLuc to develop assays that measure ATP levels (Leach and Webster, 1986).

The Renilla luciferase (RLuc), isolated from the sea pansy *Renilla reniformis* is a 36 kDa enzyme. As a monomeric luciferase, it converts coelenterazine to coelenteramide in an ATP independent manner and emits light with a spectral maximum of 480 nm (Lorenz *et al.*, 1991).

Besides the Renilla luciferase, the marine copepod *Gaussia princeps* luciferase (GLuc) utilizes coelenterazine as its substrate in an ATP-independent manner and emits light at the same peak wavelength (480 nm), but is smaller with a molecular weight of only 19.9 kDa (Tannous *et al.*, 2004). The Gaussia Dura luciferase (GDLuc) is a mutated variant of the original Gaussia Luciferase and was developed to stabilize the luminescence signal (Ho *et al.*, 2013).

Two different Cypridinia luciferases are also well studied. Both are derived from the marine ostracods *Vargula hilgendorfii* and from the *Cypridinia noctiluca*, respectively. They share sequence similarity of about 80% and use the same substrate, vargulin, leading to a peak emission of 460 nm (Nakajima *et al.*, 2004). The *Cypridinia noctiluca* luciferase (CLuc) is commercially available from NEB and Thermo Fisher Scientific. It is about 62 kDa and highly stable under physiological conditions (Wu *et al.*, 2009).

Not only the mass and the substrates are different among the luciferases, but also the enzymatic turnover and quantum yield resulting in fold differences in luminescence. While the RFLuc has a high enzymatic turnover and quantum yield of almost 90%, the enzymatic turnover and quantum yield for the RLuc is quite low with only 6% (Tannous *et al.*, 2004; Michelini *et al.*, 2008). CLuc has been reported to have a quantum yield of about 30% (Shimomura and Johnson, 1970). Although, RLuc has a low quantum yield, it is often used as a donor for bioluminescence resonance energy transfer (BRET) based assays, since its emission wavelength is compatible with GFP or YFP (Sapsford, Berti and Medintz, 2006).

Both, CLuc and Gluc are naturally secreted. This specific property makes them very good reporters for investigating secretory pathways in mammalian cells (Tannous *et al.*, 2004).

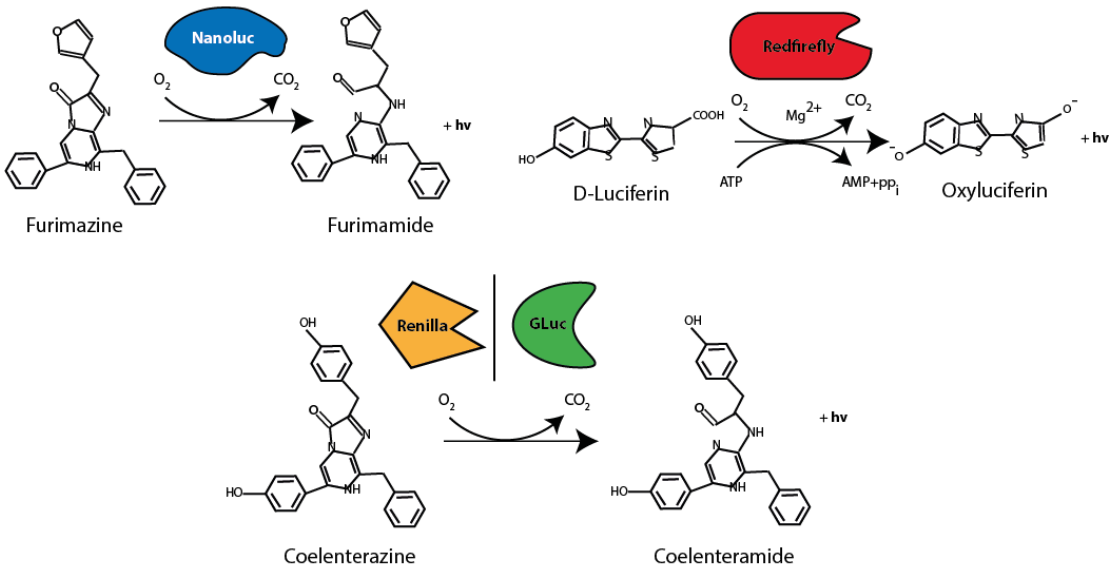

Fig. 14: Luciferases and their substrates. The engineered luciferase Nanoluc converts Furimazine to Furimamide by consuming O_2. The commonly used luciferase Firefly requires ATP to convert D-Luciferin to Oxyluciferin. The Luciferases Renilla and GLuc use coelenterazine as substrate. **Abbreviation:** GLuc: Gaussia luciferases

1.5 The development of the engineered luciferase Nanoluc

The luciferase from the deep-sea shrimp *Oplophorus gracilorostris* was firstly isolated and described in 1975 reacting with Cypridinia luciferin (Yamaguchi, 1975). Although it was difficult to isolate the luciferin of the *Oplophorus gracilorostris* luciferase due to its instability in 1975, three years later in 1978, Shimomura and colleagues found out that this luciferase can also utilize coelenterazine as substrate with an emission maximum at 462 nm (Shimomura *et al.*, 1978). Additionally, it was found that the *Oplophorus gracilorostris* luciferase exists as a heterotetrametric protein of 106 kDa and is resistant to heat up to 50 °C, which is very unusual for a luciferase. The optimum pH of the luminescence reaction was pH 9 (Shimomura *et al.*, 1978; Inouye *et al.*, 2000).

By denaturing the heterotetrametric protein with SDS-PAGE, Inouye and colleagues discovered that the *Oplophorus gracilorostris* luciferase consists of two larger subunits of 35 kDa and two smaller subunits of 19 kDa (Inouye *et al.*, 2000). The activities of both subunits were tested but only the smaller subunit showed a catalytic activity in presence of coelenterazine. Interestingly by co-expressing both subunits, no enhancement in activity was detected. Although the 35 kDa subunit have a rather stabilizing effect on the 19 kDa subunit, interaction between the two subunits could not be definitively proven (Inouye *et al.*, 2000).

The 19 kDa subunit shows an overall sequence similarity to the *E.coli* amine oxidase, but its amino terminal domain is homologous to a fatty acid binding protein (Inouye *et al.*, 2000). Hall and colleagues used this remote sequence similarity and exchanged the amino acids in the 19 kDa protein with the corresponding amino acids of the fatty acid binding protein, which appeared to play a role in stabilizing the protein (Hall *et al.*, 2012). By doing so, they could improve the stability of the small 19 kDa subunit, but in order to increase the luminescence they carried out three optimization steps. The first step included a round of random mutagenesis, which identified eight beneficial mutations. In the second step, they improved the substrate by using coelenterazine analogues. In the last step they exploited the superior coelenterazine analogue furimazine to identify additional mutations in the small subunit for increasing the luminescence. This led to the final protein Nanoluc (NLuc) (Fig. 15). Nanoluc with fumirazine exhibited a 2.5-million-fold brighter luminescence in comparison to the native 19 kDa protein with coelenterazine. NLuc showed higher signal intensity than RFLuc and RLuc. The reason for that cannot be explained by the quantum yield, since this is high for RFLuc. Rather, the increased catalytic turnover is presumed to play a role in the increased intensity (Hall *et al.*, 2012).

Independently, Inouye *et al.* compared different coelenterazine analogues as substrate for the same optimized small subunit of the *Oplophorus gracilorostris* luciferase, which they referred

to as Nanokaz instead of NanoLuc (Inouye *et al.*, 2013). The structure of Nanokaz was resolved in 2016 (Tomabechi *et al.*, 2016). This revealed that the structural similarity between Nanokaz and the fatty acid binding protein, with 11 ß-strands and 4 a-helices forming a ß-barrel, was higher than that based on comparison of the primary amino acid sequences. The ß-barrel structure of Nanokaz displays a central cavity, which probably serves as the binding pocket for the substrate (Tomabechi *et al.*, 2016).

While the structure was going to be resolved, Zhou and colleagues used NLuc for a complementation-based assay to unravel the mechanism of protein aggregation. Their idea was to split NLuc in two protein fragments and append one of them to the protein of interest. If protein aggregation occurs, the appended fragment would not be able to complement with the other fragment. In absence of protein aggregation, they would be able to detect a luminescence signal. By computational modelling, they identified several possible sites for fragmentation of NLuc, but one fragmentation in particular, which generated N65 (aa 1-65) and C66 (aa 66-171), led to the maximum luminescence signal in comparison to the other fragmentations. With this approach, they could not only show that the luminescence signal increases with the solubility of the appended protein, but they also showed how fast NLuc could reassemble and how insensitive to folding/unfolding cycles this reassembly was (Zhao *et al.*, 2016).

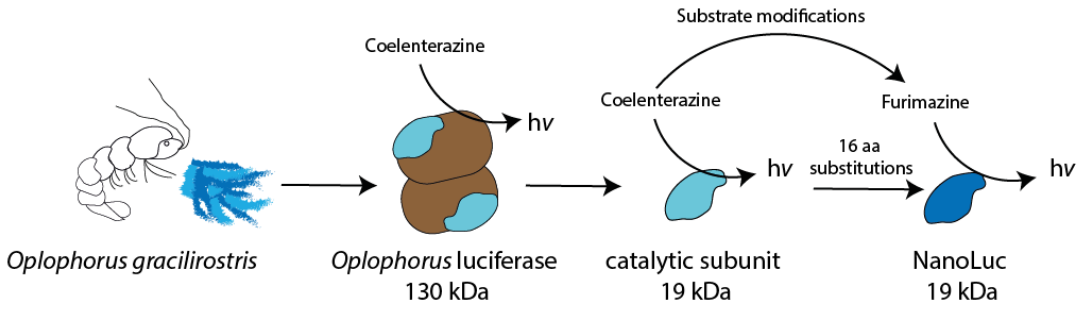

Fig. 15: The development of NLuc. The *Oplophorus* luciferase derived from the deep-sea shrimp *Oplophorus gracillirostis* consists of two larger and two smaller subunits. The smaller subunit with about 19 kDa comprises the catalytic activity but is not intrinsically stable. Substitution of 16 aa and modification of its native substrate coelenterazine enable NLuc to convert Furimazine and produce a high intensity light signal (Hall *et al.*, 2012; Tomabechi *et al.*, 2016). **Abbreviations:** aa: amino acid, kDa: kilodalton

Just some months later, Dixon and colleagues presented a split variant of NLuc, but in contrast to Zhou and his collegues, they used the known structural model and fragmented NLuc between position 156 and 157 to obtain one large fragment of 156 aa and a smaller one of only 13 aa, which only includes one ß-strand. To stabilize the larger fragment, random mutations were introduced. For the smaller fragment, the dissociation constant K_D was adjusted. Since a too strong intrinsic affinity of the larger fragment could have affected the interaction characteristics of the tagged protein of interest, specific deletions or additions of amino acids on the smaller fragment were carried out. The final protein complementation system (Nanoluc binary Technology, NanoBiT) consists of one larger stable fragment of 18 kDa (LargeBit, LgBiT) and a smaller fragment of only 1.3 kDa (smallBiT, smBiT) with a K_D value of 190 µM (Dixon *et al.*, 2016).

While a semirandom library was generated to reduce the intrinsic affinity of the smaller fragment, a peptide with an interestingly high affinity for LgBiT was identified. This peptide was referred to as HighBiT (HiBiT) and was used as a tag to monitor the regulated expression and post-translational modifications of endogenous proteins (Schwinn *et al.*, 2018).

Due to its sensitivity and stability, NLuc has been used in many applications ever since it was published. The range of applications is very broad from investigating gene regulation, signalling pathways and protein-protein interactions to bioluminescence imaging (England, Ehlerding and Cai, 2016).

However, despite the advantages that NLuc and the other luciferases offer, they did not receive much attention in the field of microbiological techniques. Except for the GLuc luciferase and the indirect exploitation of RFLuc, none of them have been considered as reporter system for the T3SS. Rather, fluorescent proteins or enzymatic assays are more commonly used, even though they are not optimal and have limitations (Maffei, Francetic and Subtil, 2017).

2 Aim of this thesis

The fundamental function of the T3SS is to secrete and inject effector proteins into the host cell. These secreted virulence factors are known to play important roles in the modulation of host cell activities. Although many assays have been established for the evaluation of protein secretion, they are quite limited in their application spectrum. Different biochemical, genetical, cell biological and microscopic techniques have been used to elucidate the function of bacterial secreted effectors. Also, computational approaches are very helpful in analysing the sequences and structure of effectors thus providing crucial information about their functional domains. The traditional Western blot analysis is broadly used to characterize effector proteins that are either only secreted to the extracellular environment or injected into the host cell. Antibodies usually neither provide the sensitivity to detect low abundant proteins nor are they useful in a high throughput scale. Instead, fluorescent or enzymatic reporter assay provide a better sensitivity and allow monitoring the kinetics of secretion and injection. However, the enzymatic or fluorescent reporter proteins are bulky (GFP), toxic (biarsenic FlaSH), not quantitative (β-lactamase) or insensitive and not amenable to High-Throughput (HTP) screens (Cya with cAMP read-out). Moreover, the readouts are usually complicated and require specific equipment.

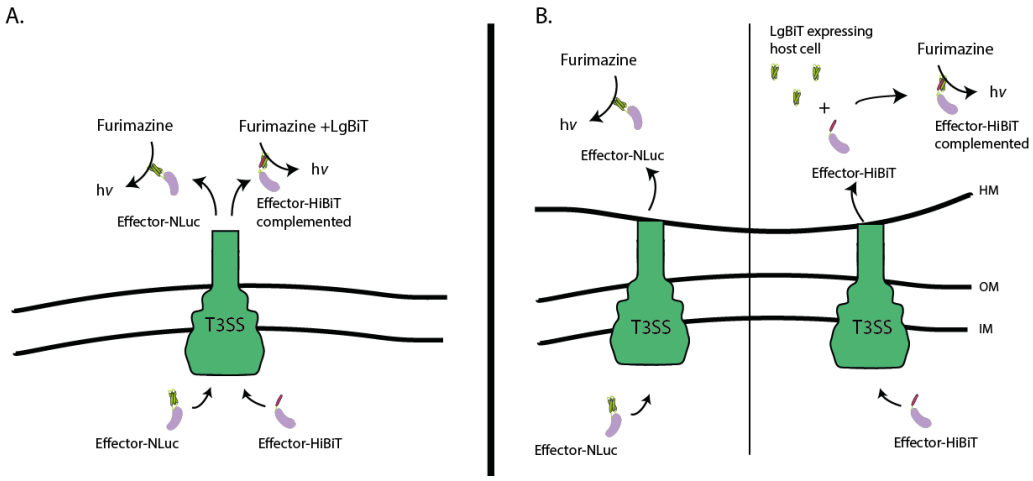

Fig. 16: NLuc based secretion and injection assay. **A.** Effectors tagged either with NLuc or HiBiT are secreted by the T3SS enabling quick detection upon substrate addition. **B.** Injection can be determined by monitoring the presence of effector fusion proteins inside the host cell: LgBiT is constitutively expressed inside the host cell and leads to complementation uponinjection of effector-HiBiT fusion proteins. **Abbreviations:** NLuc: NanoLuc, LgBiT: large subunit (LargeBiT) of NLuc, HiBiT: high affinity binding small subunit of NLuc (HighBiT), HM: host membrane, OM: bacterial outer membrane, IM: bacterial inner membrane

The main objective of my thesis was to develop a versatile tool that can differently be utilized depending on the specific scientific question. At first, we focussed on developing assays that would provide a simple, quick and quantitative assessment of secretion into the extracellular environment (Fig. 16 A) and into the host cell (injection, Fig. 16 B). This could be achieved by using NLuc and its split variant to overcome the limitations of the previously established assays.

Substrate specificity switching is one of the essential mechanisms of the T3SS, but it is poorly understood. Upon switching, the intermediate substrates, the tip and translocon subunits, are secreted to ensure the translocation competency. Based on the phenotype of *spaS* and *invJ* mutants, it is believed that these two proteins coordinately regulate the switching. SpaS itself was believed for a long time to control the switching by ongoing autocleavage. However, recent work revealed that SpaS is autocleaved before the incorporation into the base and that its autocleavage is *per se* not the inducer. The involvement of InvJ in switch regulation was based on the observation that *invJ* mutants display uncontrolled needle length and are incapable to secrete intermediate substrate. Strikingly, autocleavage deficient mutants have normal needle length, but are not capable to secrete intermediate substrates. Furthermore, specific *spaS* mutants were discovered that could switch autonomously independently of the needle length regulator InvJ. Based on these findings we sought to know whether it is possible to create an artificial T3SS lacking the needle, but still capable to secrete intermediate substrates into the periplasm. Such a system could facilitate investigating how substrate specificity switching is induced, whether switching can occur upon SpaS maturation independently of needle length regulation, and what type of mechanism ensures the hierarchical secretion of substrates. For this, we needed a very sensitive and quantifiable method to detect proteins in the periplasm and determine whether switching occurs independently of needle length regulation. In the best case, this tool could enable us to monitor the timing of switching and the altered secretion of early and intermediate substrates. Since previous experiments with NanoLuc and its split variant proved to be very sensitive, we decided to develop a periplasmic secretion assay based on NanoLuc (Fig.17).

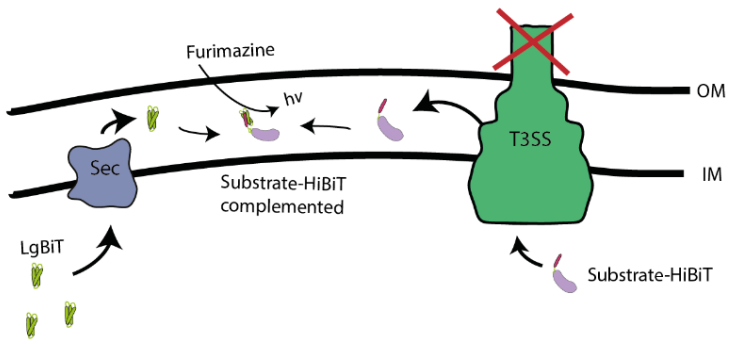

Fig. 17: Overview of the periplasmic secretion assay setup. LgBiT is translocated to the periplasm via the Sec-translocon. Substrates coupled to HiBiT are delivered to the periplasm by the T3SS. Upon complementation in the periplasm, NanoBiTs substrate is converted and light detectable. **Abbreviations:** LgBiT: large subunit of NLuc, HiBiT: small subunit of NLuc, OM: outer membrane, IM: inner membrane

3 Material and Methods

3.1 Chemical and Materials

Chemicals and Materials were from Sigma-Aldrich, Eppendorf and Thermo Fisher unless otherwise specified. Media and buffers used in this study are listed in Table 2.

3.2 Bacterial strains and growth conditions

Bacterial strains used in this study are listed in Table 3 and Table 4. All *Salmonella* strains were derived from *Salmonella enterica* serovar Typhimurium strain SL1344 (Hoiseth and Stocker, 1981) and created by allelic exchange (Kaniga, Bossio and Galán, 1994). The *Escherichia coli* strains NEB5α and λpir116 were used for molecular cloning. *S.* Typhimurium strains and *E. coli* strains were grown in either liquid Lennox broth (LB) medium at 37 °C, 180 rpm or on LB agar medium at 37 °C. *Salmonella* strains were cultured with low aeration at 37°C in Lennox broth supplemented with 0.3 M NaCl to induce expression of *S*PI-1. Whenever required, bacterial cultures were supplemented with ampicillin (100 µg/ml), chloramphenicol (50 µg/ml), tetracycline (12.5 µg/ml), streptomycin (50 µg/ml), or kanamycin (25 µg/ml). The *E. coli* β2163 strain used for allelic exchange was additionally supplemented with 100 µg/ ml diaminopimelic acid (DAP) for growth.

3.3 Molecular cloning and plasmid construction

Plasmids were generated by Gibson cloning (Gibson *et al.*, 2009) and DNA modifications were introduced by QuikChange using KOD (Novagen) or Q5 polymerase (NEB). Taq polymerase (NEB) was used for colony PCR. Oligonucleotides used for plasmid constructions were synthetized by Eurofins and Integrated DNA Technologies and are listed in Table 5. PCR or plasmid purifications were conducted using Qiagen kits according to the manufacturer's instructions. Plasmids were transformed either in heat shock competent *E. coli* or electro competent *Salmonella* strains. The used plasmids can be found in Table 6. Expression of pT10-based plasmids was induced by the addition of 100 µM rhamnose to the culture medium.

3.4 Allelic exchange

Gene insertion and deletion in *Salmonella* chromosome was performed by allelic exchange (Babic, Guérout and Mazel, 2008). The gene modifications were carried out on a suicide plasmid pSB890 that encodes the tetracyline resistance gene and the target gene plus 1,000 bp up- and downstream of the flanking regions that are homologous to the chromosomal

destination locus. The cloning and propagation of the suicide plasmid was performed in the *E. coli* pir116 strain. This strain expresses the Π protein that initiates the replication of plasmids containing the R6K origin of replication. Afterwards, the suicide plasmid was electroporated in to the *E. coli* β2163 strain, which is able to mate with *Salmonella* strains, allowing the suicide plasmid to integrate into the Salmonella chromosome and create merodiploids. The suicide plasmid carries the *sacB* gene encoding the enzyme levansucrase, which converts sucrose to the cytotoxic product levan. *Salmonella* colonies were counterselected on sucrose plates for loss of the suicide plasmid. The resulting colonies were identified for insertion or deletion by colony PCR and confirmed by sequencing analysis (Eurofins).

3.5 Protein biochemical and immunological methods

3.5.1 Western blot-based secretion assay[1]

Salmonella was cultured at 37 °C for 5 h. For separation of whole cells and cell culture supernatant, the bacterial suspensions were centrifuged at 10,000 × *g* for 2 min at 4 °C. Whole cells were directly resuspended in 1x SDS loading buffer (Table 2). The supernatant was filtered through a 0.22 µm pore size filter, sodium deoxycholate was added to a final concentration of 0.1 % (w/v), and proteins were precipitated by addition of 10% trichloroacetic acid (w/v) for 30 min at 4°C. After pelleting by centrifugation at 20,000 × *g* for 20 min at 4 °C, precipitated proteins were washed with acetone and subsequently resuspended in SDS loading buffer.

3.5.2 Spheroplasting

The bacterial overnight cultures were backdiluted to A_{600} = 0.1 and grown until A_{600} = 1 at 37 °C. 0.5 ODU were harvested and resuspended in 500 µl 0.8 M sucrose. Subsequently, 60 mM Tris (pH 8.0), 20 µg/mL lysozyme, 50 µg/mL DNase, 1.3 mM EDTA were sequentially added to disrupt the outer membrane with inversion steps in between. The suspension was incubated for 20 min at RT. Finally, 4 mM $MgCl_2$ was added to stop the reaction. The spheroplasts and periplasmic fraction were separated by 10 min centrifugation at 6000 x *g*, 4 °C. The periplasmic fraction was supplemented with sodium deoxycholate to a final concentration of 0.1 % (w/v), and proteins were precipitated by addition of 10 % trichloroacetic acid (w /v) for 30 min at 4°C. After pelleting by centrifugation at 20,000 × *g* for 20 min at 4 °C, precipitated proteins were washed with acetone and subsequently resuspended in SDS loading buffer. Spheroplasts and periplasmic fraction were resuspended in solubilization buffer and separated by SDS PAGE.

[1] The chapter 3.5.1 has previously been published in Molecular Microbiology by (Westerhausen *et al.*, 2020)

3.5.3 SDS PAGE, Western blotting and immunodetection[2]

For protein detection, samples were separated by SDS PAGE using SERVAGel™ TG Prime™ 8-16% precast gels and transferred to a PVDF membrane (Bio-Rad) using standard protocols. Membranes were probed with antibodies listed in table 7. Detection was performed using the Odyssey imaging system (Li-Cor Biosystems). The scanned membranes were analysed with the software Image Studio (Li-Cor Biosystems).

3.5.4 MBP-NLuc and MBP-HiBiT purification[3]

NLuc and HiBiT respectively, were cloned into a pMal-c5X vector to yield a C-terminal translational fusion with maltose-binding protein (MBP). *E. coli* BL21 was transformed with the plasmids. Bacterial cultures were grown overnight at 37°C in LB broth and backdiluted in Terrific Broth (TB) the next day to an A_{600} = 0.1. They were grown to an A_{600} = 0.6-0.8 at 37°C. Subsequently, expression of MBP-NLuc/HiBiT was induced by addition of IPTG to a final concentration of 0.5 mM. Then, bacteria were further grown at 37 °C for 4 h. Bacterial cells were harvested by centrifugation (6,000 × *g*, 15 min, 4°C) and resuspended in column binding buffer (CB) containing 200 mM NaCl, 20 mM Tris-HCl (pH 7.4), 1 mM EDTA, Protease inhibitor (Sigma-Aldrich, P8849, 1:100), DNAse 10 µg/ml, 1 mM $MgSO_4$ and lysozyme (10 µg/ml) and lysed with a French press. The obtained solution containing cell lysate and cell debris was two times centrifuged at 15,000 × *g* for 20 min at 4 °C. MBP-NLuc/HiBiT in the clear lysate was bound to an amylose resin (NEB), washed with CB and eluted with 10 mM maltose in the same buffer. Buffer was exchanged to 1xPBS (Table 2) by using the Amicon Ultra system (Merck).

3.6 Luciferase based assays

3.6.1 Luciferase secretion assays[4]

To measure NLuc, RFLuc, Gluc, GDLuc, Rluc and Cluc activity of secreted translational fusions, bacteria were grown under *S*PI-1-inducing conditions for 5 h. Culture supernatants were separated from whole bacterial cells by centrifugation at 10,000 × *g* for 2 min. The following buffers were prepared with their substrates according to the manufacturers' protocols: For NLuc, 25 µl of Nano-Glo Assay Buffer containing furimazine (NLuc working solution, Promega) was added to 25 µl of the culture supernatant; for RFLuc, 30 µl of reconstituted One-

[2,3] The chapters 3.5.3 and 3.5.4 have previously been published in Molecular Microbiology by Westerhausen *et al.,* 2020 and slightly modified for this thesis.

[4]The chapter 3.6.1 has previously been published in Molecular Microbiology by Westerhausen *et al*., 2020.

glo assay buffer containing luciferin (Promega) was added to 30 µl of the culture supernatant; for Gluc and GDLuc, 50 µl of the assay buffer containing coelenterazine (Thermo Fisher) was added to 20 µl of culture supernatant; for Rluc, 25 µl of the reconstituted assay buffer (Promega), in which the substrate was 1:100 diluted, was added to 25 µl of the culture supernatant; for Cluc, a working solution was prepared containing assay buffer and 1:100 of the substrate vargulin (Thermo Fisher). 30 µl of the working solution was added to 10 µl of the supernatant. The luciferase activities were measured in white 384-well plates (MaxiSorp, Nunc), with acquisition settings as recommended by the manufacturers.

3.6.2 NLuc assay for wall-bound protein[5]

In order to measure wall-bound protein, overnight cultures of *S.* Typhimurium were back-diluted to an A_{600} = 0.1 and 50 µl of the bacterial suspension was transferred to a 384-well micro-plate (MaxiSorp, Nunc) and grown at 37 °C for 5 h. The plate was washed with water using a microplate washer (Tecan Hydrospeed). The NLuc working solution was diluted in 1x PBS (30 µl 1x PBS + 10 µl NLuc working solution) and added to each well to measure luminescence using the Tecan Spark reader with following settings: attenuation: auto, settle time: 0 ms, integration time: 100 ms.

For the inhibitor screen, 0.5 µl of each compound (Table S1) was added to 50 µl bacterial culture prior to incubation at 37 °C for 5 h, and the plate was processed as described above.

3.6.3 Test of NLuc stability[6]

40 µl recombinant MBP-NLuc was added (2 µg, final concentration) to 1 ml LB/ 0.3 M NaCl and to 1 ml culture supernatant of wild type *S.* Typhimurium. Samples were kept at 37 °C, at room temperature, or on ice for up to 4 h. Aliquots were removed over time and transferred to a 384-well plate. Subsequently, 25 µl of the NLuc working solution was added and luminescence was directly measured in a microplate reader (Tecan Spark) with settings as described above.

3.6.4 Kinetic measurements[7]

SipA-NLuc was introduced by allelic exchange into the chromosome of a *S.* Typhimurium strain expressing the master regulator of SPI-1, *hilA* under the control of an arabinose inducible

[5,6] The chapters 3.6.2 and 3.6.3 have previously been published in Molecular Microbiology byWesterhausen *et al*., 2020.
[7]The chapter 3.6.4 has previously been published in Molecular Microbiology by Westerhausen *et al*., 2020

promotor (P_{ara}-*hilA*). The resulting strain was grown overnight at 37 °C in LB/0.3 M NaCl, and was back-diluted the following day to an A_{600} = 0.1. Bacterial cultures were grown to an A_{600} = 0.9 in an Erlenmeyer flask in a 37°C water bath with stirring. Expression of *S*PI-1 was induced by addition of arabinose to a final concentration of 0.02% (v/v), and thereafter samples were taken at different time points for assessment of the luminescence of secreted SipA-NLuc or for immunodetection of PrgK. For testing the role of the PMF inhibitors, bacterial cells were washed twice after reaching an A_{600} = 0.9 in LB/0.3 M NaCl containing either 120 mM Tris-HCl, pH 7.0 for CCCP (Sigma) or 120 mM Tris-HCl, pH 7.0 and 150 mM KCl for valinomycin (Sigma). For potassium benzoate, cells at the same growth stage (A_{600} = 0.9) were harvested and then washed twice with LB/0.3 M NaCl containing 80 mM MES buffer, pH 6.8. The cultures in the different media (without inhibitor, with 0.02% (v/v) arabinose) were kept in the water bath at 37°C and 200 µl of samples were taken at different time points and kept on ice. The inhibitors were added to the bacterial culture 60 min after *hilA*-induction. Cultures were kept in the water bath and samples were taken every 10 min. Samples were centrifuged at 10,000xg for 2 min to separate whole cells and supernatant. 25 µl of the supernatant was transferred to a white 384-well plate and luminescence was measured upon addition of the NLuc working solution in a luminometer.

3.6.5 Luminescence detection of whole cells

The bacterial overnight cultures were backdiluted to A_{600} = 0.1 and grown until A_{600} = 1 at 37 °C. 0.5 ODU were harvested and resuspended in 500 µl 1x PBS (Table 2) supplemented with 1 mM EDTA. Samples were kept on ice for 30 min. 25 µl of each sample was transferred to a 384-well plate in duplicates. For the NLuc containing samples, the Nano-Glo luciferase assay buffer was reconstituted by addition of 1:50 luciferase assay substrate (indicated in experiments as lytic). The cell impermeable substrate was diluted 1:50 in HiBiT Extracellular Detection system buffer. For the LgBiT containing samples, the HiBiT Extracellular Detection system substrate and the cell impermeable substrate were reconstituted 1:50 in the HiBiT Extracellular Detection system buffer and the HiBiT Lytic Detection system substrate in the HiBiT Lytic Detection system buffer. The HiBiT buffer working solutions were additionally mixed with 1:100 purified MBP-HiBiT or 1:100 LgBiT. The different Nano-Glo buffer components can be found in Table 8. The luminescence was measured in Tecan Spark either directly, for Nanoluc containing samples or after 10 min, for LgBiT/HiBiT containing samples.

3.7 Cell culture

The human immortalized cervical cell line HeLa and the HeLa cell line stably expressing LgBiT were grown in Dulbecco's modified Eagle's Medium (DMEM, Gibco) supplemented with 10 % (v/v) fetal calf serum (FCS, Gibco), 1 % (v/v) penicillin/ streptomycin (Gibco) and 1 % (v/v) L-glutamine (Gibco). Cells were cultured at 37°C with 5 % CO_2 and 95 % humidified atmosphere and passaged further at confluency. Thereafter, cells were washed with 1x Phosphate Buffered Saline solution (PBS, Gibco) and incubated with 0.05 % (v/v) Trypsine-EDTA for 5 min at 37 °C. Detached cells were resuspended in culture medium and subsequently counted in a hemocytometer. Cells were seeded 24-48 h before the experiments.

3.7.1 Injection assay and injection kinetics with host cells

1×10^4 HeLa cells and LgBiT expressing HeLa cells were seeded in white 96 well plates with glass bottom 24 h before infection in 100 µl DMEM with 10 % (v/v) FCS (Gibco). *S.* Typhimurium was washed and resuspended in Hank´s Buffered Salt Solution (HBSS) to infect the cells at a multiplicity of infection (MOI) of 50 for 60 min. After infection, cells were gently washed with a microplate washer (Tecan Hydrospeed, 5 cycles dispensing and aspirating (speed: 70 µl/sec)) using 1 × PBS (Gibco). A final wash volume of 100 µl was used together with 25 µl of Nanoglo live cell assay buffer (Promega) containing the substrate for luminescence measurements in a Tecan Spark reader with the following settings: attenuation: auto, settle time: 0 ms, integration time: 1,000 ms. For monitoring the injection kinetics, HeLa LgBiT cells were seeded and *S.* Typhimurium bacteria in HBSS were added to the cells as described above. Directly upon addition of the bacteria, 25 µl of the reconstituted Nanoglo live cell buffer was added to the infection culture and luminescence reading was carried out for 90 min with a 2 min reading interval in the Tecan Spark with the same settings as for the injection assay.

Table 2: Media, Buffer and Solutions used in this study.

Name	Component
LB	85.56 mM NaCl, 1 % (w/v) tryptone and 0.5 % (w/v) yeast extract were dissolved in 1 l H2O and autoclaved
LB- broth supplemented with 0.3 M NaCl	300 mM NaCl, 1 % (w/v) tryptone and 0.5 % (w/v) yeast extract were dissolved in 1 l H2O and autoclaved
LB agar plates	2 % (w/v) LB Lennox and 1.5 % (w/v) agar were dissolved in 300 ml H2O
Sucrose agar plates	1 % (w/v) g tryptone, 0.5 % yeast extract and 1.5 % (w/v) agar were dissolved in 400 ml H_2O and autoclaved. Afterwards, 10 % (w/v) sterile filtered (0.22µm) 50% (w/v) sucrose were added
SOB	2 % (w/v) tryptone, 0.5 % (w/v) yeast extract, 8.56 mM NaCl and 2.5 mM KCl were dissolved in 2 l H2O and autoclaved. Then, sterile filtered (0.22 µm) 1M $MgCl_2$ and 1M $MgSO_4$ solutions were added to a final concentration of 10 mM

SOC	20 mM sterile filtered (0.22 µm) Glucose was added to 1 l SOB medium
Stock solution	10 % (v/v) glycerol and 2 % (w/v) peptone were dissolved in 500 ml H_2O and autoclaved
5x ISO mix	500 mM Tris-HCl pH 7.5, 50 mM $MgCl_2$, 1 mM dNTP Mix, 50 mM DTT, 25 % (w/v) PEG 8000, 5 mM NAD filled up to 3 ml H_2O and were mixed.
Gibson master mix	100 µl 5x ISO mix, 0.2 µl T5 exonuclease, 6.25 µl Phusion DNA polymerase and 50 µl Taq DNA Ligase were mixed in 218.6 µl H2O
6x DNA loading dye	30 % (w/v) glycerol and a small piece of bromophenol blue were added to 3 ml H_2O, pH was adjusted by the addition of Tris-HCl (pH 8.8)
50x TAE buffer	2 M Tris base, 1 M glacial acetic acid and 100 mM EDTA were dissolved in 1 l H2O.
10x SDS-Running buffer	250 mM Tris base, 1.92 M glycine, 1 % (w/v) SDS for 1 l H_2O
4x SDS-Loading buffer	250 mM Tris-HCl pH 6.8, 20 % (v/v) glycerol, 8 % (w/v) SDS, 0.05 % (w/v) blue, 20 % (w/v) β-mercaptoethanol
1x SDS-Loading buffer	3 parts of H_2O mixed with 1 part 4x SDS-Loading buffer
Transfer Buffer	24.8 mM Tris base, 192 mM glycine, 0.025 % (w/v) SDS, 10 % (v/v) methanol
10x TBS	1.44 M NaCl, 248 mM Tris base for 1 l and pH was adjusted to 8.0
1x TBS	100 ml 10x TBS mixed with 900 ml H_2O
TBS-T	1x TBS, 0.05 % (w/v) TWEEN
10x PBS	1.37 M NaCl, 26.8 mM KCl, 80.9 mM Na_2HPO_4*2 H_2O and 17.6 mM KH_2PO_4 were dissolved in 1 l H_2O and the pH was adjusted to 7.4 with NaOH
1x PBS	100 ml 10x PBS mixed with 900 ml H_2O

Table 3: *Salmonella enterica* serevor Typhimurium strains used in this study.

Stock name	genotype	Source
SB300	WT (SL1344)	K. Kaniga, 1995
SB1751	*ΔinvA*	Wagner et al. 2010
SB762	WT (SL1344), *flhD::tet*	K. Kaniga, 1995
SB1901	*ΔinvA, flhD::tet*	Wagner et al. 2010
SB2098	P_{ara}*hilA*	Monjarás Feria, 2015
SB2085	P_{ara}*hilA*, Δ*prgHIJK*	Monjarás Feria, 2015
MIB3061	Δs*ipBCD*	this study
MIB3231	WT, SipA-Nluc^{myc}	this study
MIB3233	ΔinvA, SipA-Nluc^{myc}	this study
MIB3873	P_{ara}*hilA*, SipA-Nluc^{myc}	this study
MIB3875	P_{ara}*hilA*, *ΔprgHIJK,* SipA-Nluc^{myc}	this study
MIB4821	*ΔsipD,* SipA-Nluc^{myc}	this study
MIB4827	*ΔsipBCD,* SipA-Nluc^{myc}	this study
MIB4721	*ΔinvE,* SipA-Nluc^{myc}	this study
MIB3877	WT, SipA^{3xFlag} -HiBiT	this study
MIB3879	*ΔinvA,* SipA^{3xFlag} -HiBiT	this study
MIB4825	*ΔsipD,* SipA^{3xFlag} -HiBiT	this study
MIB4829	*ΔsipBCD,* SipA^{3xFlag} -HiBiT	this study
MIB4723	*ΔinvE,* SipA^{3xFlag} -HiBiT	this study
MIB4840	*Δtsp, flhD::tet*	this study

MIB4834	*ΔdegP, flhD::tet*	this study
MIB3508	*ΔpgtE, flhD::tet*	this study
MIB4751	*ΔinvG,* $PrgI_{M1K}$	this study
MIB3337	*ΔinvG*	this study
MIB5088	*ΔinvC, ΔinvG,* $PrgI_{M1K}$, InvJ336-HiBit-InvJ331-337, *flhD::tet*	this study
MIB4672	ΔinvG, $PrgI_{M1K}$, InvJ336-HiBit-InvJ331-337, *flhD::tet*	this study
MIB4324	InvJ336-HiBit-InvJ331-337, *flhD::tet*	this study
MIB5120	*ΔprgI*, InvJ336-HiBit-InvJ331-337, *flhD::tet*	this study
MIB5302	*ΔprgJ*, InvJ336-HiBit-InvJ331-337, *flhD::tet*	this study
MIB5304	*ΔprgI, ΔinvG,* InvJ336-HiBit-InvJ331-337, *flhD::tet*	this study
MIB5306	*ΔprgJ, ΔinvG,* InvJ336-HiBit-InvJ331-337, *flhD::tet*	this study
MIB5308	*ΔinvG*, InvJ336-HiBit-InvJ331-337, *flhD::tet*	this study
MIB5310	$PrgI_{C\Delta10}$, InvJ336-HiBit-InvJ331-337, *flhD::tet*	this study
MIB5090	*ΔinvG*, $PrgI_{C\Delta10}$, InvJ336-HiBit-InvJ331-337, *flhD::tet*	this study
MIB5118	*ΔinvC*, *ΔinvG*, $PrgI_{C\Delta10}$, InvJ336-HiBit-InvJ331-337, *flhD::tet*	this study
MIB5448	*ΔinvA*, *ΔinvG*, $PrgI_{C\Delta10}$, InvJ336-HiBit-InvJ331-337, *flhD::tet*	this study
MIB5450	*ΔinvA*, *ΔinvG*, $PrgI_{M1K}$, InvJ336-HiBit-InvJ331-337, *flhD::tet*	this study

Table 4: *Escherichia coli* strains used in this study.

Name	Description	Source
BL21 (DE3)	Host for overexpression from the T7 promotor: *huA2 [lon] ompT gal (λ DE3) [dcm] ΔhsdS λ DE3 = λ sBamHIo ΔEcoRI-B int:lacI::PlacUV5::T7 gene) i21 Δnin5*	Novagen
NEB5α	Host for plasmid construction: *fhuA2Δ(argF-lacZ) U169 phoA glnV44 Φ80Δ (lacZ)M15 gyrA96 recA1 relA1 endA1 thi-1 hsdR17*	NEB
λpir116	-	-
β2163 Δnic35	*(F-) RP4-2-Tc::Mu, ΔdapA:ermpir), [KmR ErmR], Δnic35*	Babic *et al.* 2008
MC4100	*F- [araD139]$_{B/r}$ Δ(argF-lac)169* &lambda- e14-flhD5301 Δ(fruKyeiR) 725 (fruA25)‡ relA1 rpsL150(strR) rbsR22 Δ(fimBfimE) 632(::IS1) deoC*	Peters *et al.* 2003
Ak00	MC4100, Δ*ompT*, Δ*rhaM-T*	Jan-Willem de Gier
Ak01	MC4100, Δ*ompT*, Δ*rhaM-T*, Δ*clpP*	Jan-Willem de Gier
Ak02	MC4100, Δ*ompT*, Δ*rhaM-T*, Δ*lon*	Jan-Willem de Gier
Ak03	MC4100, Δ*ompT*, Δ*rhaM-T*, Δ*clpQ-clpY*	Jan-Willem de Gier
Ak04	MC4100, Δ*ompT*, Δ*rhaM-T*, Δ*degP*	Jan-Willem de Gier
Ak05	MC4100, Δ*ompT*, Δ*rhaM-T*, Δ*degQ*	Jan-Willem de Gier
Ak06	MC4100, Δ*ompT*, Δ*rhaM-T*, Δ*bepA*	Jan-Willem de Gier
Ak07	MC4100, Δ*ompT*, Δ*rhaM-T*, Δ*tsp*	Jan-Willem de Gier
Ak08	MC4100, Δ*ompT*, Δ*rhaM-T*, Δ*ptr*	Jan-Willem de Gier
Ak09	MC4100, Δ*ompT*, Δ*rhaM-T*, Δ*tesA*	Jan-Willem de Gier
Ak10	MC4100, Δ*ompT*, Δ*rhaM-T*, Δ*ycaL*	Jan-Willem de Gier
Ak11	MC4100, Δ*ompT*, Δ*rhaM-T*, Δ*ydgD*	Jan-Willem de Gier
Ak12	MC4100, Δ*ompT*, Δ*rhaM-T*, Δ*yafL*	Jan-Willem de Gier
Ak13	MC4100, Δ*ompT*, Δ*rhaM-T*, Δ*yhjJ*	Jan-Willem de Gier

Ak14	MC4100, Δ*ompT*, Δ*rhaM-T*, Δ*nlpC*	Jan-Willem de Gier
Ak15	MC4100, Δ*ompT*, Δ*rhaM-T*, Δ*loiP*	Jan-Willem de Gier
Ak16	MC4100, Δ*ompT*, Δ*rhaM-T*, Δ*glpG*	Jan-Willem de Gier
Ak17	MC4100, Δ*ompT*, Δ*rhaM-T*, Δ*sppA*	Jan-Willem de Gier
Ak18	MC4100, Δ*ompT*, Δ*rhaM-T*, Δ*sohB*	Jan-Willem de Gier
Ak19	MC4100, Δ*ompT*, Δ*rhaM-T*, Δ*htpx*	Jan-Willem de Gier
Ak20	MC4100, Δ*ompT*, Δ*rhaM-T*, Δ*yfbL*	Jan-Willem de Gier

Table 5: Primers used in this study.

Name	Sequence 5'-3'
gib_890_ sipD_a_f	GTT ATT CCG CGA AAT ATA ATG ACC CTC TTG CGC GAA TAC GTT AAT GCT GAC G
gib_890_sipD_b_r	AAT ATT AAG CAT AAT ATC CCC AGT TCG CCA
gib_890_sipD_c_f	TGG CGA ACT GGG GAT ATT ATG CTT AAT ATT CTG CAA GGA TAA CAG AAG AG
gib_890_ sipD_d_r	CCG CGG TGG GGC TTT TTA TTG AGC TTG TTA ATA TTG ATA TTA ATA CC
gib_890_invE_a_f	GTT ATT CCG CGA AAT ATA ATG ACC CTC TTG CTG AGC AGG TGC ATT TTA TCG
invE_10b_r	TGA AAT ACC GGA GGT TGA GCC AGG AAT C
invE_10bc357_f	GAT TCC TGG CTC AAC CTC CGG TAT TTC AAA GCA TGA AAT GGC AGA ACA GC
gib_890_invE_d_r	CCG CGG TGG GGC TTT TTA TTG AGC TTG ATA ACA AAA ACC GGC AGT GGG
Gib_p890_SipA3xflag_f	CGT TGA TGG CTT GCA CAT GCA GCG TTC TAG AGA CTA CAA AGA CCA TGA CG
Gib_p890_HibitIacp_r	TAT TCA TCG CAT CTT TCC CGG TTA ATT AGC TAA TCT TCT TGA ACA GCC GC
gib_uni_SipA_r	ACG CTG CAT GTG CAA GCC ATC AAC G
Gib_uni_iacP_f	TTA ACC GGG AAA GAT GCG ATG AAT A
gib_uni_pT12_r	GGT GAA TTC CTC CTG AAT TTC
gib_uni_pT12_f	AGC TTG GCT GTT TTG GCG GAT G
Gib_HiBiT_pT12_f	GTG AGC GGC TGG CGG CTG TTC AAG AAG ATT AGC TAA GGA AGC TTG GCT GTT TTG G
Gib_HiBiT_FLAG_r	GAA CAG CCG CCA GCC GCT CAC TCC ACT CGA ACC TTT GTC ATC GTC ATC CTT GTA ATC G
gib_Myc_pT12b_f	GAG CAG AAA CTG ATT AGC GAA GAA GAT TTA CTA GAG TCG ACC TGC AGG CA
Gib_SipA_GDL_f	CGT TGA TGG CTT GCA CAT GCA GCG TAT GGG AGT CAA AGT TCT GTT TGC CCT GAT C
Gib_myc_GDL_r	CGT TGA TGG CTT GCA CAT GCA GCG TAT GGG AGT CAA AGT TCT GTT TGC CCT GAT C
Gib_SipA_CypL_f	CGT TGA TGG CTT GCA CAT GCA GCG TAT GAA GAC CCT GAT CCT GGC CGT G
Gib_myc_CypL_r	TTC TTC GCT AAT CAG TTT CTG CTC CTT GCA CTC GTC GGG CAC TTC CAG GG
Gib_SipA_greReL_f	CGT TGA TGG CTT GCA CAT GCA GCG TAT GGC CAG CAA GGT GTA CGA CCC CGA GCA G
Gib_SipA_RFL_f	CGT TGA TGG CTT GCA CAT GCA GCG TAT GGA AAA TAT GGA AAA CGA CGA GAA CAT C
Gib_myc_RFL_r	TTC TTC GCT AAT CAG TTT CTG CTC CAT CTT GGC CAC GGG TTT CTT CAG GAT CTC C
gib_SipA_NL_f	CGT TGA TGG CTT GCA CAT GCA GCG TAT GGT CTT CAC ACT CGA AGA TTT C
gib_myc_NL_r	TTC TTC GCT AAT CAG TTT CTG CTC CGC CAG AAT GCG TTC GCA CAG CCG CCA G
Gib_SipA_GL_f	CGT TGA TGG CTT GCA CAT GCA GCG TAT GGG AGT CAA AGT TCT GTT TGC CCT GAT CTG
Gib_myc_GL_r	TTC TTC GCT AAT CAG TTT CTG CTC GTC ACC ACC GGC CCC CTT GAT CTT GTC C
gib_uni_SopE_r	GGG AGT GTT TTG TAT ATA TTT ATT AG
Gib_SopE_RFL_f	CTA ATA AAT ATA TAC AAA ACA CTC CCA TGG AAA ATA TGG AAA ACG ACG AGA ACA TC

Gib_SopE_greReL_f	CTA ATA AAT ATA TAC AAA ACA CTC CCA TGG CCA GCA AGG TGT ACG ACC CCG AGC AG
Gib_SopE_GDL_f	CTA ATA AAT ATA TAC AAA ACA CTC CCA TGG GAG TCA AAG TTC TGT TTG CCC TGA TC
gib_SopE_NL_f	CTA ATA AAT ATA TAC AAA ACA CTC CCA TGG TCT TCA CAC TCG AAG ATT TC
Gib_SopE_GL_f	CTA ATA AAT ATA TAC AAA ACA CTC CCA TGG GAG TCA AAG TTC TGT TTG CCC TGA TCT G
Gib_SopE_CypL_f	CTA ATA AAT ATA TAC AAA ACA CTC CCA TGA AGA CCC TGA TCC TGG CCG TG
gib_pMalc5x_f	AAG CTT CAA ATA AAA CGA AAG GCT CAG
gib_pMalc5x_r	GGA TCC GTC GAC GAT ATC GCG GCC GCC CAT G
Gib_pMal5x_Nl_r	CTG AGC CTT TCG TTT TAT TTG AAG CTT GCC AGA ATG CGT TCG CAC
Gib_pMal5x_Nl_f	GCG GCC GCG ATA TCG TCG ACG GAT CCA TGG TCT TCA CAC TCG AAG ATT TC
gib_uni_pT12+_r	TGC CTG CAG GTC GAC TCT AG
gib_uni_pT12+_f	GGC TGT TTT GGC GGA TGA GAG
g_pT12+_InvB_f	CTA GAG TCG ACC TGC AGG CAG CTT AAT TAA GGA AAA GAT CTA TG
g_pT12+_InvB_r	CTC TCA TCC GCC AAA ACA GCC TCA TCT CAT TAG CGA CCG ACT AAA AAC
g_pT12no_SopE_f	CTT TTT AGA CTG GTC GTA ATG AAC ATA TAA AAG GAT CAT TAC C
gib_cMyc_SopE_r	TTC TTC GCT AAT CAG TTT CTG CTC GGG AGT GTT TTG TAT ATA TTT ATT AG
gib_uni_pT12noSD_r	TTC ATT ACG ACC AGT CTA AAA AG
gib_Myc_pT12b_f	GAG CAG AAA CTG ATT AGC GAA GAA GAT TTA CTA GAG TCG ACC TGC AGG CA
g_pT12no_SipA_f	CTT TTT AGA CTG GTC GTA ATG AAC AGA AGA GGA TAT TAA TAA TGG TTA C
gib_cMyc_SipA_r	AAA TCT TCT TCG CTA ATC AGT TTC TGC TCA CGC TGC ATG TGC AAG CCA TC
prha_seq_f	CTT TCC CTG GTT GCC AAT GG
prha_seq_r	GCT ACG GCG TTT CAC TTC TG
p890_seq_f	CGT CAC CAA ATG ATG TTA TTC C
p890_seq_r	GTT GAG AAG CGG TGT AAG TG
sipD_seq_f	CGC GCT TAA TCT GAA AGG TC
SipD_seq_r	GGC CTT TAA TTT CCC CTG AC
SipA520_seq_f	TTT AAG CAA AAT AGT TTC CTC TCA
gib_sicp_r	CTG CAG TAT GTT TTT GAG CGC
invE_seq_f	ATG CCA GCG AAT CGG TAA AC
invE_seq_r	GTG CGA TCA GGA AAT CAA CC
pmalc5x_uni_seq_f	CAG CGG TCG TCA GAC TGT CG
pmalc5x_uni_seq_r	CTC CGG GCC GTT GCT TCG C
478PLVX EF1a puro R	GAA TTC ACC GGA AAT AGA TCC TC
479PLVX EF1a puro F	GGA TCC CGC CCC TCT CCC
480 plv lgbit_fwd	GAT CTA TTT CCG GTG AAT TCA TGG TCT TCA CAC TCG AAG ATT TC
481 plvlgbit_rev	GAG GGA GAG GGG CGG GAT CCT TAA CTG TTG ATG GTT ACT CGG AAC
Gib_pMalc5x_HiBit_r	CTG AGC CTT TCG TTT TAT TTG AAG CTT GCT AAT CTT CTT GAA CAG CCG C
Gib_pMalc5x_HiBit_f	CAT GGG CGG CCG CGA TAT CGT CGA CGG ATC CGG CAG TTC AGG TGG TGG C
QC_prgI_Cd10_f	CGAACACGGTAAAAGTCTTTAAGGATTAATCAGTTATAAGGTGGATTATGTCG
QC_prgI_Cd10_r	CGACATAATCCACCTTATAACTGATTAATCCTTAAAGACTTTTACCGTGTTCG
gib_uni_pACYCcat_f	TAG GCT GCT GCC ACC GCT GAG
gib_lacP_ACYC_r	TTT CCA GTC GGG AAA CCT GTC GTG GGC GCC CAA TAC GCA AAC CG
gib_uni_lacP_f	CAC GAC AGG TTT CCC GAC TGG
gib_pACYCcat_BAD_r	CTC AGC GGT GGC AGC AGC CTA CTC ATG AGC GGA TAC ATA TTT GAA TG

MalE_dSigseq_QC_r	GAT TAC CAG TTT ACC TTC TTC GAT TTT CAT GAA TTC CTT GAA TTT CAT TAC GTG
MalE_dSigseq_QC_ f	GAT TAC CAG TTT ACC TTC TTC GAT TTT CAT GAA TTC CTT GAA TTT CAT TAC GTG

Table 6: Plasmids used in this study.

Plasmid	Description	Source
pNL1.1	NLuc	Promega
pCMS-RFL	RFLuc	Thermo Fisher Scientific
pMCS-GDL	GDLuc	Thermo Fisher Scientific
pMCS-GL	Gluc	Thermo Fisher Scientific
pCMS-GRL	GRLuc	Thermo Fisher Scientific
pMCS-CypL	Cluc	Thermo Fisher Scientific
pMalc5x	MBP for expression and purification	*New England Labs*
pLVX-EF1a-IRES-Puro	Lentiviral vector for bicistronic expression of a gene together with a puromycin-resistance marker	Takara
pBiT1.1-N	HSV-TK, LgBiT	Promega
CMV HiBit	HiBiT CMV-neo Flexi® Vectors	Promega
pT10	P_{rhaBAD}, *SC101 ori, aphA*	Wagner *et al.*, 2010
pMIB5752	pT10, InvB SipA^{myc}	this study
pMIB6436	pT10, InvB, SipA-GDLuc^{myc}	this study
pMIB6437	pT10, InvB, SipA-CLuc^{myc}	this study
pMIB6439	pT10, InvB, SipA-RLuc ^{myc}	this study
pMIB6440	pT10, InvB, SipA-RFLuc ^{myc}	this study
pMIB6441	pT10, InvB, SopE-RLuc^{myc}	this study
pMIB6443	pT10, InvB, SopE-RFLuc^{myc}	this study
pMIB6444	pT10, InvB, SopE-GDLuc^{myc}	this study
pMIB6445	pT10, InvB, SopE-NLuc^{myc}	this study
pMIB6446	pT10, InvB, SipA-GLuc^{myc}	this study
pMIB6447	pT10, InvB, SopE-GLuc^{myc}	this study
pMIB6448	pT10, InvB, SopE-CLuc^{myc}	this study
pMIB5566	pT10, InvB, SipA-NLuc^{myc}	this study
pMIB5563	pSB890, SipA-NLuc^{myc}	this study
pMIB6421	pT10, SscBSseF ^{3xFlag}HiBiT	this study
pMIB6645	psB890, SipA^{3xFlag} HiBiT	this study
pMIB6648	pSB890, *ΔsipD*	this study
pMIB5175	pSB890, *ΔinvE*	this study
pSB3531	pSB890, *ΔinvA*	Lara-Tejero et al., 2011
pMIB5079	pSB890, *ΔsipBCD*	this study
pMIB6434	pmalc5x, MBP-HiBiT	this study
1602	pLVX-EF1a-LgBiT-IRES-Puro	this study, Erwin Bohn

pMIB6644	pmalc5x, MBP-NLuc	this study
pMIB7112	pSB890, *ΔdegP*	this study
pMIB7113	pSB890, *Δtsp*	this study
pMIB5699	pSB890, *ΔpgtE*	this study
pMIB6882	pSB890, $PrgI_{M1K}$	Torres-Vargas et al., 2019
pMIB7498	psB890, $PrgI_{C\Delta 10}$	this study
pMIB5170	pSB890, *ΔinvG*	Torres-Varges et al., 2019
pMIB5292	pSB890, *ΔinvC*	this study
pMIB6220	pSB890, *ΔprgI*	this study
pMIB5642	pSB890, *ΔprgJ*	Torres-Varges et al., 2019
pMIB6215	pSB890, InvJ336-HiBit-InvJ331-337	this study
pMIB6429	pT10, InvJ- HiBiT	
placwoI	*pBR322 ori*, lac promotor without repressor lacI, constitutive expression	Krampen *et al.*, 2018
pMIB6831	placwoI mutation in SD5, N-terminal Fusion of Nanoluc to $MBP_{R8L\_S13L\_T16L}$	this study
pMIB6836	placwoI mutation in SD5, N-terminal Fusion of LargeBiT to $MBP_{R8L\_S13L\_T16L}$	this study
pMIB6649	placwoI mutation in SD5, N-terminal Fusion of LargeBit to $MBP_{R8L\_S13L\_T16L}$, ssrA tag C-terminal of LargeBiT	this study
pMIB6651	placwoI mutation in SD5, N-terminal Fusion of Nanoluc to $MBP_{R8L\_S13L\_T16L}$, ssrA tag C-terminal of Nanoluc	this study
pMIB6653	pT2 *CAT* and *P15A ori* part with MalE-Nanoluc from pMIB6831	this study
pMIB6654	*CAT* and *P15A* ori part with MalE-LgBit from pMIB6836	this study
pMIB6656	*CAT* and *P15A* ori part with MalE-Nanoluc-ssrA tag from pMIB6651	this study
pMIB6657	*CAT* and *P15A* ori part with MalE-LgBit ssrA from pMIB6649	this study
pMIB6779	Deletion of MalE signal sequence, Basevector: pMIB6656	this study
pMIB6780	Deletion of MalE signal sequence, Basevector: pMIB6657	this study

Table 7: Antibodies used in this study.

Antibody	Poly/Monoclonal	Dilution in TBS-T	Origin
α-Myc	**Monoclonal**	**1:1,000**	**Mouse**
α-InvJ	**Monoclonal**	**1:1,000**	**Mouse**
α-SipB	**Monoclonal**	**1:1,000**	**Mouse**
α-PrgK	**Polyclonal**	**1:5,000**	**Mouse**
α-MBP	**Monoclonal**	**1:10,000**	**Mouse**
α-RNA-polymerase (RpoB)	**Monoclonal**	**1:10,000**	**Mouse**
α-mouse 800	**Polyclonal**	**1:10,000**	**Goat**
α-rabbit 680	**Polyclonal**	**1:10,000**	**Goat**

Table 8: Nanoluc buffer and substrate kits used in this study.

Kit/ Reagent	Kit components	Source
Nano-Glo Luciferase Asssay System	Nanoglo Luciferase Assay Buffer Nanoglo Luciferase Assay Substrate (indicated in experimens as NLuc lytic substrate)	Promega (N1110)
Nano-Glo HiBiT Lytic Detection System	Nano-glo HiBiT Lytic Buffer Nano-glo HiBiT Lytic substrate LgBiT protein	Promega (N3030)
Nano-Glo HiBiT Extracellular Detection System	Nano-glo HiBiT Extracellular Buffer Nano-glo HiBiT Extracellular substrate LgBiT protein	Promega (N2420)
Nano-Glo Live cell assay system	Nano-Glo LCS Dilution Buffer Nano-Glo Live Cell Substrate	Promega (N2011)

4 Results

First, I will describe the development of the Nanoluc based secretion and injection assays and the different requirements we wanted them to fulfil. Second, I will focus on the establishment of a periplasmic secretion assay to gain insights into the process of substrate specificity switching.

4.1 Development of a quick and highly sensitive assay for the analysis of protein secretion and injection by bacterial type III secretion systems

The developed secretion and injection assay were based on the luciferase NanoLuc and a split variant of NanoLuc. Initially, we assessed the sensitivity, dynamic range and robustness of the assay. Then, its compatibility with HTP approaches was verified by screening different types of inhibitors. The integration of the larger bit of Nanoluc into the host cell chromosome helped to monitor T3SS effector injection over time.

4.1.1 Translational effector-luciferase fusion proteins provide a quick readout for type III secretion[8]

Cypridinia luciferase (Cluc), Gaussia princeps luciferase (Gluc), Gaussia dura luciferase (GDLuc), Nanoluc (NLuc), Renilla luciferase (Rluc), and Red Firefly luciferase (RFLuc) are broadly used, commercially available and have been tested in different types of applications (Lorenz *et al.*, 1991; Tannous *et al.*, 2004; Fan and Wood, 2007; Hall *et al.*, 2012). We evaluated these luciferases as translational reporters fused to SipA or SopE to determine which of them would be compatible with secretion through the T3SS-1. The luciferases were appended to the C-terminus of either effector protein without disturbing the N-terminal signal sequence or the chaperone binding domain. At the C-terminus of the luciferases, we fused a myc epitope-tag for independent detection of secretion via western blot analysis. The fusion proteins were expressed from a rhamnose inducible promotor system on a low copy number plasmid in wild type *S.* Typhimurium and in a secretion deficient mutant (Δ*invA*). After 5 hrs of growth under SPI-1 inducible conditions, we assessed the expression and the Type III dpendent secretion of the constructs by SDS PAGE, western blotting and immunodetection of the myc epitope tag in

[8] Parts in this chapter 4.1.1 have previously been published by Westerhausen *et al*., 2020. Fig. 19 with the respective information is unpublished.

whole bacterial cells and culture supernatant, respectively. We detected proteins for each effector-luciferase fusion at the expected molecular mass in whole cells and culture supernatant confirming their expression and secretion (Fig. 18A). Many of the fusion proteins could be detected in the whole cell fraction at low levels; but at higher levels in the supernatant fraction, indicating effective secretion. Cluc fusion proteins showed opposite behaviour not being efficiently secreted. Cluc and RFLuc-based fusion proteins displayed additionally bands likely corresponding to cleaved luciferase-myc. Overall, luciferases fused to SipA showed a higher secretion pattern than the SopE constructs.

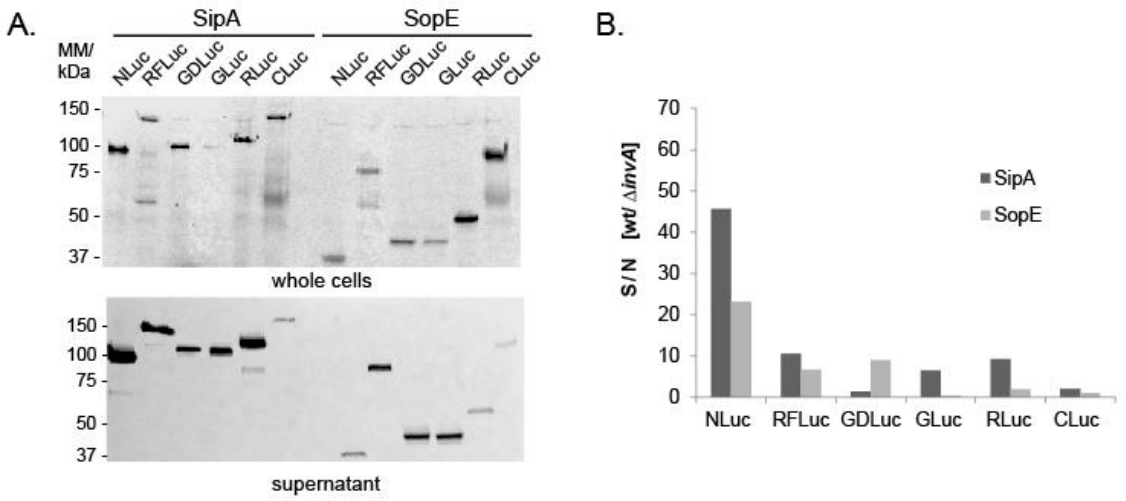

Fig. 18: Assessment of different luciferases as reporters for type III secretion. **A.** Proteins from whole cell lysates and culture supernatants of *S.* Typhimurium expressing the indicated SipA-Luc and SopE-Luc fusions were analyzed by SDS PAGE, western blot and immunodetection with an anti-myc antibody. **B.** The signal to noise (S/N) ratios (wt/Δ*invA*) of luciferase activities of secreted SipA-Luc and SopE-Luc fusions were plotted in a bar graph. Bar graphs represent the mean S/N of three independent measurements.

We evaluated the activity of the secreted luciferase-effector fusion protein in filtered culture supernatant of the *S.* Typhimurium wild type and Δ*invA* strains, respectively, for a better comparison, since each luciferase utilizes a different substrate leading to a different range of signal intensity (Fig. 18B). This was determined by luminometry using specific conditions for each luciferase. The Signal-to-Noise ratios (S/N) were calculated by dividing the signal of the wild type strain by that of the Δ*invA* mutant. The highest S/N ratios were observed for translational fusion constructs with NLuc (SipA-NLuc S/N= 45, SopE-NLuc S/N=22). In general, the SipA-luciferase fusions always displayed a higher ratio except for SipA-GDLuc.

Unlike SopE, SipA was postulated to constitute a highly abundant pre-formed effector pool before injection. Consequently, more SipA that SopE gets secreted (Winnen *et al.*, 2008). However, the effector protein SptP gets secreted later than SipA and SopE and reverses the

effect of these effectors on host cells. Hence SptP is believed to be secreted in higher abundance than SipA and SopE (Winnen *et al.*, 2008). To test whether we were capable to observe a different secretion pattern for the different effectors and demonstrate the versatility of NLuc as a secretion reporter, we constructed different effector fusions with NLuc and a split variant of NLuc. The split variant of NLuc is composed of one larger fragment (LargeBiT, LgBiT, 18kDa) and a smaller fragment referred to as HighBiT (HiBiT) with a very exceptionally high affinity for LgBiT (K_D=700 pM) (Schwinn *et al.*, 2018). Due to its small size, HiBiT, unlike the full length protein NLuc, should have a minimal influence on structural and functional features of the appended protein and should not lead to any sterical issues.

The constructs were expressed under the control of a rhamnose inducible promoter on a low copy number plasmid and transformed into wt, *flhd::tet* and Δ*invA, flhd::tet* strains. The *flhd::tet* strains were used in order to avoid export of effectors through the fT3SS. since it has been suggested that effectors of the T3SS could be also additionally exported by the fT3SS. The secretion was assessed by luminometry following growth of the bacterial cultures for 5 hrs under SPI-1 inducing conditions (Fig. 19).

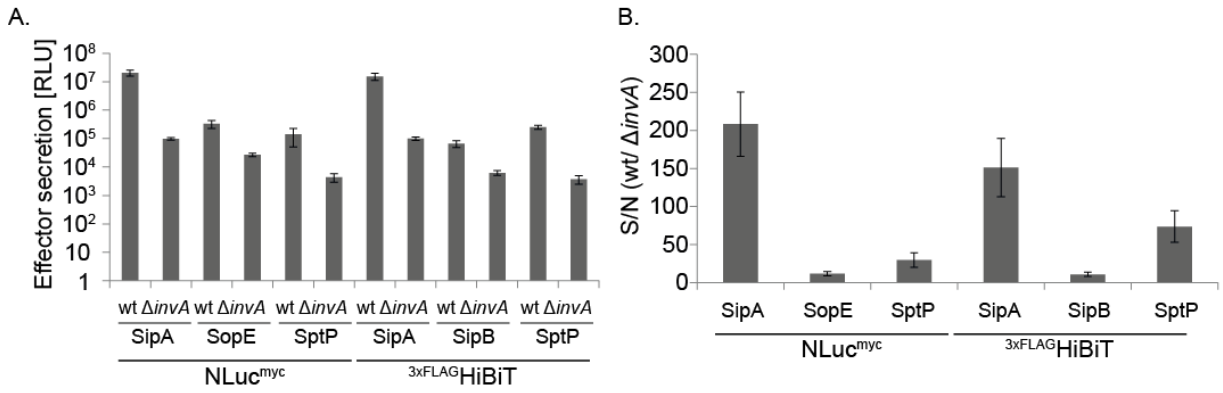

Fig. 19: NLuc and HiBiT as reporter proteins for T3SS effectors. **A.** Luminescence activities of the reporter proteins appended to different T3SS effectors were plotted in a log scale in bar graphs. **B.** S/N ratios (wt/Δ*invA*) of luciferase activities of secreted effector fusions were calculated and plotted in a bar graph. Bar graphs represent the mean S/N of four independent measurements.

The reporter luciferases coupled to SipA displayed the highest luminescence signal and the highest S/N (Fig. 19A). The signal intensity and the S/N of SptP could be improved up to 80 by using the split variant of NLuc. SipB^{3xFlag}-HiBiT with only about 10 exhibited the lowest S/N ratio (Fig. 19B).

We neither observed a higher luminescence signal nor a higher S/N for the SptP-luciferase fusion construct in comparison to the SipA-luciferase fusion constructs. However, all constructs were successfully secreted into the culture supernatant, proving that NLuc and split-NLuc can serve as secretion reporters.

To exclude any artifacts resulting from a plasmid based inducible expression system and to overcome plasmid-based experimental limits, SipA-NLuc-myc was introduced into the chromosome of wild-type and *ΔinvA S.* Typhimurium strains. We compared the expression and secretion of plasmid- and chromosome-encoded SipA-NLuc, respectively, by SDS PAGE, western blotting and immunodetectionas using as a reference the expression and secretion of the translocator SipB (Fig. 20A). The expression of SipA-NLuc from the chromosome was comparably lower than that from the plasmid, as expected. However, the T3SS-dependent secretion levels of both, the plasmid- and chromosome-encoded SipA-NLuc were identical.

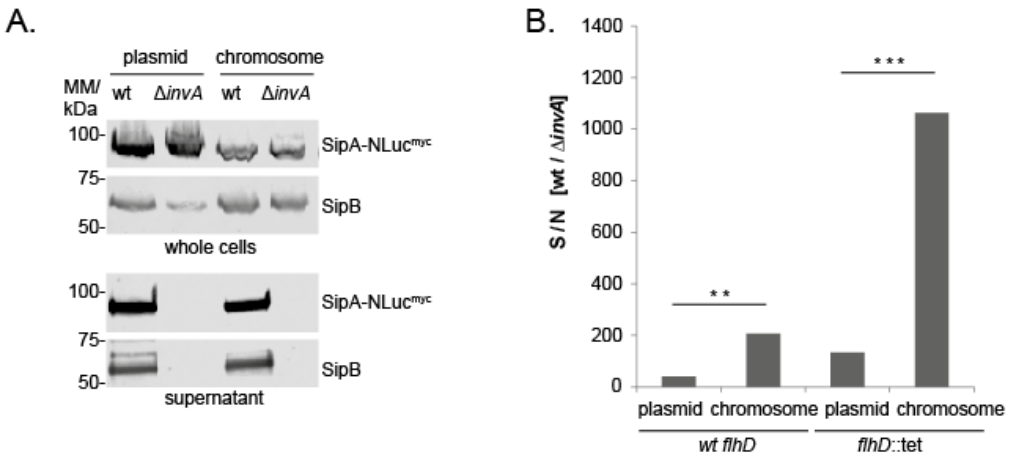

Fig. 20: Comparing plasmid- and chromosomal based expression of SipA-NLuc^{myc}. **A.** Immunodetection of SipA-Nluc^{myc} and SipB on western blot of SDS PAGE-separated culture supernatants and whole cell lysates, either expressing SipA-Nluc^{myc} from a plasmid or from the chromosome. **B.** S/N ratios (wt/Δ*invA*) of luciferase activities of secreted SipA-NLuc either expressed from a plasmid or from the chromosome, each with or without flagella (*flhD*), were plotted in a bar graph. Bar graphs represent the mean S/N of three independent measurements.

For the evaluation of the S/N ratio, the culture supernatant of the wild type *S.* Typhimurium and the Δ*invA mutant* was filtered, and the activity of the plasmid- and chromosome-encoded SipA-NLuc was measured (Fig. 20B). Expression of SipA-NLuc from the chromosome resulted in a S/N=200 well above the plasmid-based expression with a S/N=45. One reason for the strong discrepancy might be the stronger plasmid-based expression, leading to release of SipA-NLuc in the supernatant upon occasional cell lysis and increase of the noise signal.

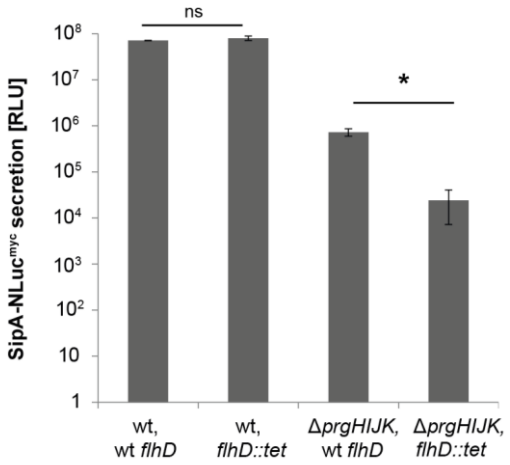

Fig. 21: T3SS effector secretion by flagellum. SipA-NLuc^{myc} secretion in *S.* Typhimurium P$_{ara}$*hilA* and in *S.* Typhimurium Δ*prgHIJK*, P$_{ara}$*hilA* with and without flagella (*flhD*), respectively. Bar graphs represent mean (± standard deviation) of three technical replicates. Asterisks indicate statistical significance of SipA-Nluc^{myc} secretion assessed by Student's *t*-test, *: $p \leq 0.05$.

Since the injectisome evolved from the flagellar T3SS, this is also capable to export proteins. Several studies indicate that substrates of one system can be secreted by the other system (Young and Young, 2002; Ehrbar *et al.*, 2004). The master regulator FlhD forms together with FlhC a complex regulating the transcription of several flagellar operons (Lucas *et al.*, 2000). We deleted the *flhD* gene, thereby inhibiting the expression of flagella in order to evaluate quantitatively the contribution of the fT3SS in the secretion of SipA-NLuc. We observed higher S/N for plasmid- and chromosomally encoded SipA-NLuc (S/N=140) and (S/N=1,000) in the absence of flagella (Fig. 20B). However, FlhD also regulates the T3SS-1 expression to some extent by indirectly modulating the SPI-1 master regulator HilA and leading to its activation. Consequently, in strains lacking *flhD* the expression of SPI-1 T3SS is reduced. To assess whether the increased S/N ratio in *flhD::tet* strains resulted from impeded secretion through the fT3SS or from an overall decreased expression of the T3SS-1, we created mutants of SipA-NLuc, in which HilA was expressed under the control of an arabinose inducible promotor, thus disconnecting HilA expression from FlhD control (Monjarás Feria *et al.*, 2015) (Fig. 21). Interestingly, we did not observe any difference between the wild type and the *flhD* deletion in the araHilA strain, respectively. However, mutants without functional T3SS-1 (Δ*prgIJHK)* and lacking *flhD* showed a 150-fold decreased S/N in comparison to Δ*prgIJHK* with *flhD*, indicating that a small amount of about 1% SipA-NLuc was secreted by the fT3SS. The secretion through the flagella which also occurs in Δ*invA* mutants are decreasing the S/N consequently and this explains the increased S/N in the *flhD* mutants.

4.1.2 Proving the sensitivity and suitability of the Nanoluc based secretion assay for kinetic measurements[9]

Western blot analysis is broadly used for detecting effector secretion through the T3SS. The availability of antisera against many T3SS proteins makes their tagging unnecessary and simplifies protein detection. However, western blots lack the sensitivity required for the detection of low abundant proteins, secretion kinetics or high-troughput screening hindering a thorough analysis of T3SS.

We compared the sensitivity between the secretion assay based on western blot and that based on NLuc. For this, bacterial cultures of SipA-NLuc wt and Δ*invA* mutant strains were grown for 5 h under SPI-1 inducing conditions. The culture supernatant was serially diluted and either directly transferred to a 384-well plate for luminescence measurement or TCA precipitated and subjected to SDS PAGE, western blot and immunodetection. We additionally probed the culture supernatant against the intermediate substrate SipB and the early substrate InvJ. While the intermediate substrate SipB was detectible down to 113 µl, we detected the proteins InvJ and SipA-NLuc only down to 225 µl of diluted supernatant culture on the western blot (Fig. 22A).

By using the luminometry, we were able to detect secreted SipA-NLuc in the culture supernatant down to 195 nl with an unchanged S/N of 200. By using a dilution corresponding to 24 nl, we still observed a S/N of 50 (Fig. 22 B). The difference of the mean between the wt and Δ*invA* strain defines the dynamic range. Within the serial dilution, we observed a linear dynamic range down to 195 nl.

Sensitivity is very crucial for kinetic measurements, as very low amounts of proteins are present at the very beginning of the type III mediated secretion. Once our assay revealed to be highly sensitive, we sought to assess the kinetics of type III-dependent secretion by using SipA-NLuc. We again used the wt and Δ*prgHIJK* strains, in which the master regulator HilA is expressed under the control of the arabinose inducible promotor. *S.* Typhimurium strains were grown until they reached A_{600} = 0.9 and expression of the pathogenicity island was induced by the addition of 0.02 % (w/v) arabinose. Culture samples were collected every 10 min for 120 min and kept on ice. Luminescence measurements of the samples were performed after the collection of all samples.

[9] This chapter 4.1.2 has previously been published in Molecular Microbiology by Westerhausen *et al*., 2020.

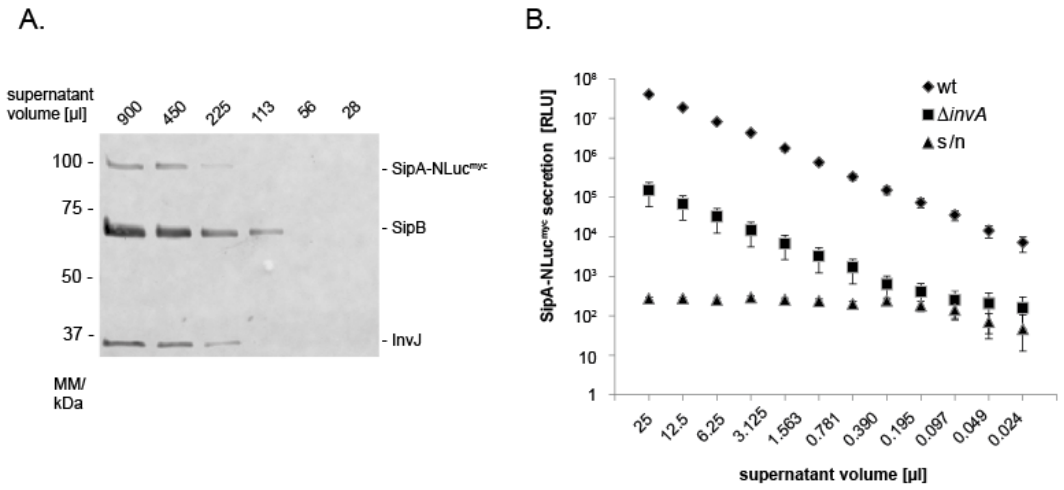

Fig. 22: Assessment of the sensitivity of the NLuc secretion reporter. **A.:** Immunodetection of the T3SS substrates SipB, InvJ and SipA-NLuc^{myc} on a western blot of SDS PAGE-separated, serially diluted culture supernatants. **B.:** Luminescence of secreted SipA-NLuc^{myc} in serially diluted culture supernatants of the *S.* Typhimurium wild type and a Δ*invA* mutant. Triangles show the corresponding signal to noise ratios for each dilution. Data represent the mean (± standard deviation) of three technical replicates.

In parallel, western blot and immunodetection of the structural base component PrgK was performed to independently monitor induction of the pathogenicity island.

Assembly of the T3SS was shown to start 15 mins post-induction of the SPI-1 (Monjarás Feria *et al.*, 2015). By considering the steps of effector translation and the substrate specificity switch, we predicted that secretion of the first effectors would start at least 30 min post-induction. In fact, we detected SipA-NLuc as soon as we were able to detect PrgK proving that the high sensitivity of our luminescence detection is not influenced by secondary effects like maturation or turn-over rates of NLuc (Fig. 23). Additionally, it enabled us to determine how rapidly step wise assembly and secretion of the T3SS occur.

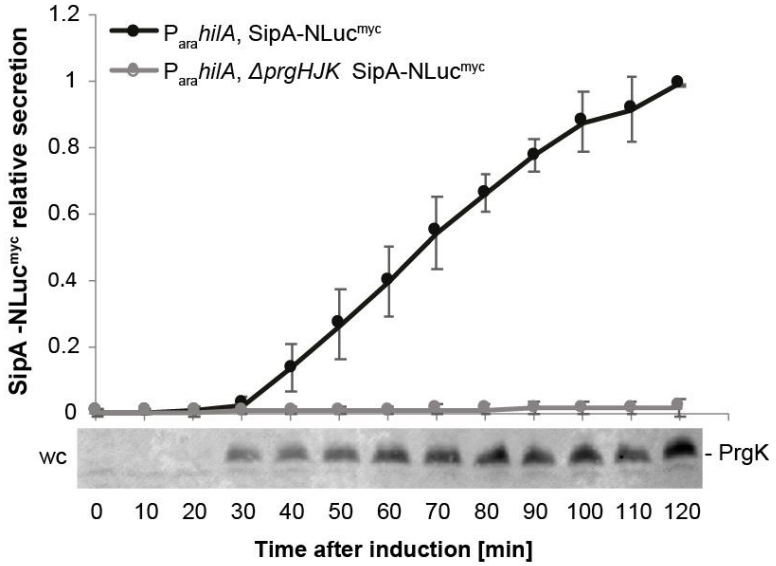

Fig. 23: SipA-NLuc^{myc} secretion kinetic upon SPI-1 induction. Normalized luminescence of secreted SipA-Nluc^{myc} at the indicated time points after induction of *hilA* with 0.02 % (w/v) arabinose. Experiments were normalized by setting the maximum luminescence of each experiment to 1. The data points represent mean (± standard deviation) of five independent measurements. At each time point, samples of whole cell (wc) lysates were taken for immunodetection of PrgK.

In order to prove that the stability of NLuc did not affect the kinetic reading described above, a recombinant maltose binding protein (MBP)-NLuc was produced in *E.coli* and purified by exploiting the MBP-tag. We investigated the activity of the purified MBP-NLuc fusion protein under different conditions for up to four hours (Fig. 24). MBP-NLuc was diluted in LB-NaCl and in *S.* Typhimurium wt supernatant after 5 hrs of growth. The samples were kept either on ice, at RT, or at 37°C. Aliquots were transferred to a 384-well plate and the activity was determined every hour by luminometry. Interestingly, MBP-NLuc showed a slight reduction in the luminescence when diluted in LB, independent of the incubation time, in comparison to when diluted in culture supernatant. However, the overall reduction in activity was not significant. For the dilution in LB-NaCl at 37°C a reduction of 15% was observed, which was the lowest luminescence signal detected after the 4 h incubation time. This data proves that NLucs stability did not affect the kinetic measurements.

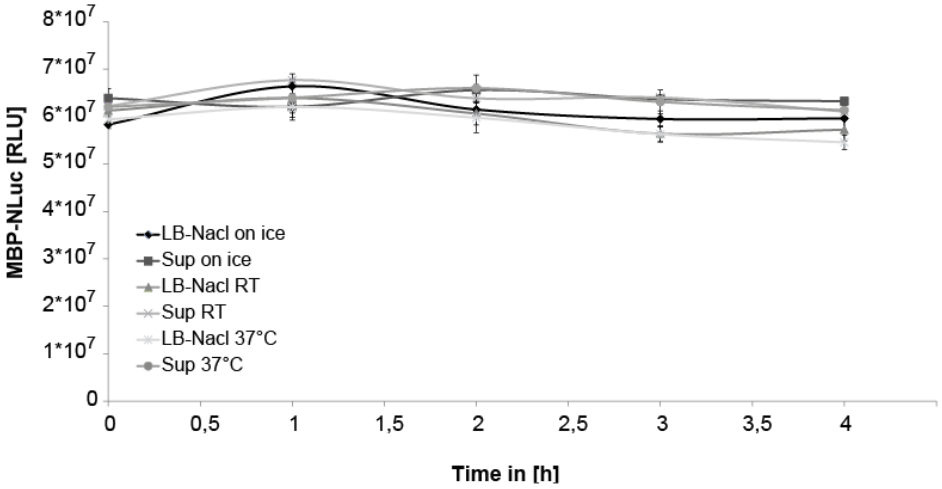

Fig. 24: Stability of MBP-NLuc in LB/ 0.3 M NaCl and in culture supernatant. The enzymatic activity of the purified MBP-NLuc was determined after incubation for 4 h at different conditions (on ice, room temperature (RT) and 37°C) in fresh LB/ 0.3 M NaCl and in filtered culture supernatant (Sup).

Overall, we showed the superior sensitivity of the NLuc-based assay over a traditional secretion assay. While the detection of secreted substrate proteins using a traditional assay requires larger volumes and accumulation of substrates in the culture supernatant for an extended period of time, the NLuc assay allows detection of secretion in very small volumes and at short intervals (10 min after collection of the supernatant). Our results show that once the system is induced, the assembly of the injectisome is a very quick process.

4.1.3 Assessing the SipA-NLuc secretion assay for high troughput screening[10]

Screening assays represent the initial step towards the identification of compounds against a desired biological target. High throughput (HTP) screening allows at least in part the automated testing of multiple compounds within a short time frame, thus accelerating the entire process. However, not every assay is suitable for HTP screens.

The SipA-NLuc based secretion assay showed a great sensitivity and very short handling times providing an excellent basis to develop a HTP assay for drug screening in a 384-well microplate format. However, in such growth conditions centrifugation or filtering is not feasible for separation of the bacterial cells and culture supernatant. In order to overcome this problem, we made use of the high-protein binding capacity of the microplates and tested whether secreted

[10] This chapter 4.1.3 has previously been published in Molecular Microbiology by Westerhausen *et al*.2020, and has been slightly modified. Fig.28 and the respective information is unpublished.

substrates would specifically bind to the plate wall after being secreted (Fig. 25A). For this, 50 µl of *S. Typhimurium* wild type and Δ*invA* mutant were grown in white high protein binding 384-well plates. Bacteria were washed out of the wells after 5 h of growth using a microplate washer. Then, PBS, NLuc buffer, and NLuc substrate were supplied to each well and SipA-NLuc bound to the wells was measured. Using this setup, a S/N = 37 could be achieved.

The Z' factor value is a defined parameter to evaluate the quality of a HTP assay. It includes the dynamic range and the data variation of a measured sample and control samples. A Z' factor of 1 is described as an ideal assay (Zhang, Chung and Oldenburg, 1999). For our SipA-NLuc assay, we calculated a Z' = 0.8, which is excellent for HTP screening (Fig. 25B).

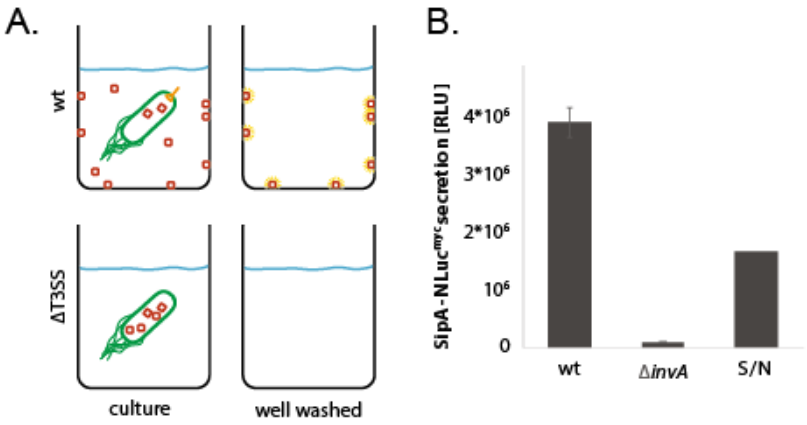

Fig. 25: Development of a SipA-NLuc-based HTP secretion assay. **A.** Overciew of the assay setup. Wild type (wt) and Δ*invA S*. Typhimurium strains expressing SipA-NLuc were grown in a 384-well microplate format. Secreted SipA-NLuc was able to bind to the walld of the high protein-binding microplate. Bacteria were washed out and luminescence was measured. **B.** Luminescence and signal to noise ratio of secreted SipA-NLuc based on the experimental setup shown in A. Bars represent the mean (± standard deviation) of three technical replicates. Experiment was performed by Melanie Nowak.

The luminescence signal of a sample can vary depending on its position in a multi-well plate a phenomenon known as "drift" or "edge" effect. Additionally, other systematic effects can influence the reproducibility of high-throughput assays (Iversen *et al.*, 2012). To find out how strong these effects influenced our read-outs, SipA-NLuc wt strains were transferred into each well of a high protein binding 384-well plate and grown for 5 hrs at 37 °C. Thereafter, bacteria were washed out using a microplate washer. Wall bound proteins were detected after the addition of PBS and NLuc Buffer substrate mixture by luminometry (Fig. 26). A difference in the luminescence signal was apparent in the wells of the last column of the plate (number 24), for which we observed an average signal of 87% (+/- 6 % stdev). With the exception of those wells, the overall column-wise signal difference for the wells was in the range of 106-93% (+/-

9%) and row-wise of 105-95% (+/-8%). These results indicated that the edge effect only applies to the wells of the last column (24) in which we observed the highest difference in signal intensity. The rest of the wells were not affected (Table 9 A and B).

Table 9: Statistics of the reproducibility assessment of the 384-well microplate format NLuc secretion assay. Data show luminescence of secreted, wall-bound SipA-NLuc. The average of the entire plate was set to 100%. Data represents the mean of either the wells of a column or the wells of a row in percentage.

Table 9 A

column	1	2	3	4	5	6	7	8	9	10	11	12	13	14	15	16	17	18	19	20	21	22	23	24
avg	98	103	101	103	106	103	103	103	102	104	100	100	100	103	103	101	100	99	96	97	97	100	93	87
CV	5	6	5	3	5	5	5	6	3	4	7	4	5	3	6	5	5	7	7	6	6	9	6	7

Table 9 B

row	A	B	C	D	E	F	G	H	I	J	K	L	M	N	O	P
avg	97	95	99	96	101	99	100	99	102	99	102	102	99	100	104	105
CV	7	6	5	8	6	6	6	6	8	7	6	7	6	5	7	6

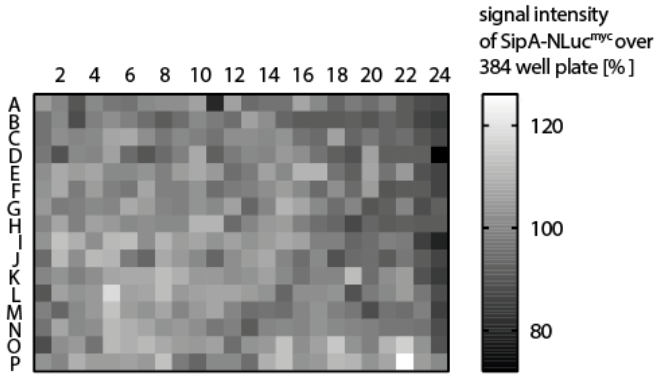

Fig. 26: Assessing variation of the luminescence signal across the plate. Signal variation of secreted SipA-NLuc assayed over an entire 384-well microplate. The experimental set up is shown in A. Luminescence was measured after washing out the bacterial cells. Experiment was performed by Melanie Nowak.

Moreover, as a proof-of-concept we tested the high-throughput capability of our assay by screening for inhibitors of bacterial growth, the T3SS and Nanoluc activity among 37 different commercially available compounds. These compounds included well-known antibiotics, polyphenols, antioxidants and a luciferase inhibitor. These were added directly to the SipA-NLuc expressing strains in a 384-well maxi-sorp plate and the amount of wall-bound secreted fusion protein was measured. The results of the plate screening with the wall-bound assay are shown in the plate layout (Fig. 27). We were able to immediately identify two strong inhibitors, quercetin (3 mg/ml) and scutellarin (1 mg/ml), that suppressed the luminescence signal down to 10%. Both compounds are well-known for their antibacterial effects (Tsou *et al.*, 2016). Additonally, we have noticed that quercetin precipitates secreted proteins (data not shown), and this could also explain the observed reduction in signal activity. Surprisingly, the Luciferase Inhibitor I, which was developed against the ATP-dependent *Photuris pennsylvanica* (*lucPpe*)

and *Photinus pyralis* (*lucPpy*) luciferase activity (Auld *et al.*, 2008, 2009), did not display any inhibitory effect against the Nanoluc activity (>100% maintained activity).

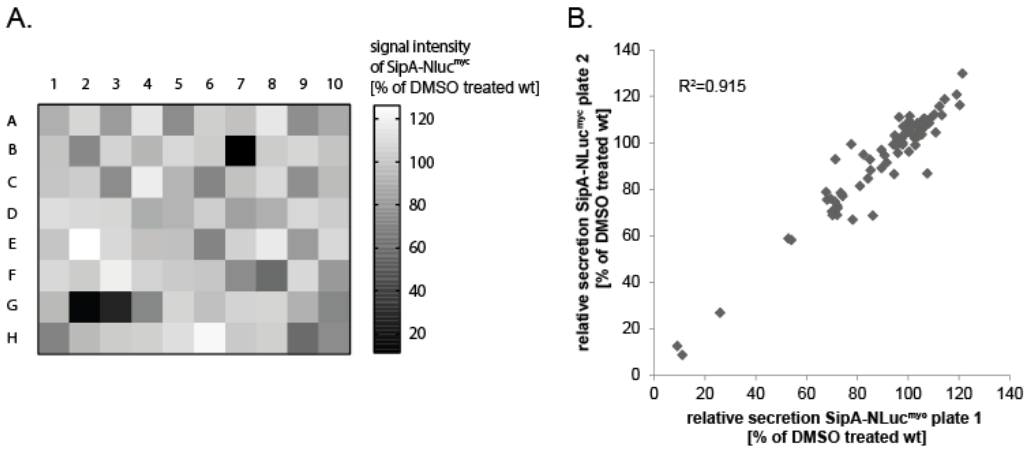

Fig. 27: SipA-NLuc secretion in response to treatment with 37 different bioactive compounds. **A.:** the assay was conducted by detecting the secreted SipA-NLuc bound to the wall of the high protein binding microplate. The DMSO-treated control was set to 100%. The layout of the plate is shown in table 10. **B.:** Comparison of the results of two independent compound screens as in A. The R^2 value was calculated from a linear regression. Experiment was performed by Melanie Nowak.

In Fig. 27 B we have exemplified the measurements of two representative plates in a plate to plate dot-plot to illustrate the reproducibility of our high-throughput screen. We observed a R^2-value of 0.915, which represents the high reproducibility.

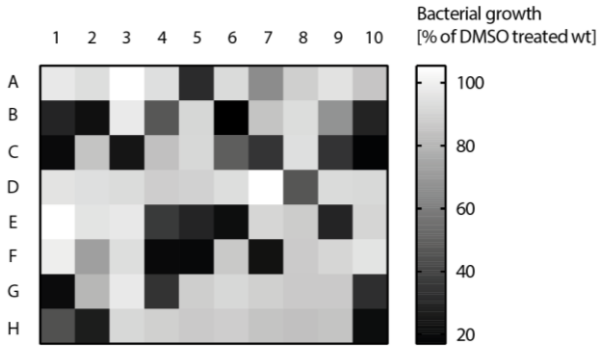

Fig. 28: Bacterial growth in response to treatment with 37 different bioactive compounds. The assay was conducted in a 384 well plate by measuring the optical density at a wavelength of 600 (A_{600}). The DMSO treated control was set to 100 %. Experiment was performed by Melanie Nowak.

Table 10: Layout of compound screening test plate incl. SipA-NLuc secretion of one measurement. The values represent the SipA-NL RLU normalized for the treatment with 1% DMSO (set to 100%) that was used as a solvent for all compounds.
Rationale for selecting these 37 bioactive compounds: The compounds were selected to serve as controls for the development of many different high-throughput assays. Hence, they were selected to cover many different biological activities and molecular targets. Among them are antibiotics, antimycotics, broadly acting cytotoxic substances, membrane-active substances, and substances targeting the cytoskeleton of eukaryotic cells. All compounds where present in replicates. The concentrations where chosen such that a biological activity can be expected. Experiment was perfoemd by Melanie Nowak.

	1	2	3	4	5	6	7	8	9	10
A	Amphotericin B 20 µg/mL	Brefeldin A 11 µM	Rotenone 50 µg/mL	SB203580 10 µg/mL	Carbenicillin 20 µg/mL	Hydroxyurea 50 µg/mL	PDTC 10 µg/mL	Resveratrol 10 µg/mL	BAY 11-7085 40 µg/mL	Amphotericin B 20 µg/mL
SipA-NLuc luminescence/DMSO control [%]	91	108	81	111	76	104	98	113	72	84
B	Ciprofloxacin 4 µg/mL	Chloramphenicol 20 µg/mL	Sulfamethazine 10 µg/mL	Linezolid 50 µg/mL	Carbamazepine 20 µg/mL	CCCP 50 µg/mL	Quercetin 30 µg/mL	Anisomycin 0.45 µM	Fusidic acid 100 µM	Ciprofloxacin 4 µg/mL
SipA-NLuc luminescence/DMSO control [%]	99	73	107	93	108	103	11	100	106	96
C	2-Theonyltri-fluoroacetone 20 µg/mL	Erythromycin 10 µg/mL	Tetracyclin 10 µg/mL	Luciferase inhibitor I 50 µg/mL	Doxorubicin 11 µM	Ampicillin 100 µg/mL	Rifampicin 10 µg/mL	SB203580 10 µg/mL	Penicillin G 20 µg/mL	2-Theonyltri-fluoroacetone 20µg/mL
SipA-NLuc luminescence/DMSO control [%]	105	104	73	117	93	70	99	106	73	105
D	Sodium Orthovanadate 4 µg/mL	Fluconazole 20 µg/mL	Theaflavin 5 µg/mL	Amphotericin B 20 µg/mL	Amphotericin B 20 µg/mL	Brefeldin A 11µM	Rotenone 50 µg/mL	Linezolid 50 µg/mL	Streptomycin 10 µg/mL	Cycloheximide 1 µg/mL
SipA-NLuc luminescence/DMSO control [%]	111	108	107	89	92	97	77	89	105	102
E	Antimycin A 50 µg/mL	Fludioxonil 10 µg/mL	Acycloguanosine 50 µg/mL	Ciprofloxacin 4 µg/mL	Ciprofloxacin 4 µg/mL	Chloramphenicol 20 µg/mL	Sulfamethazine 10 µg/mL	Luciferase Inhibitor I 50 µg/mL	Carbenicillin 20 µg/mL	Cytochalasin D 5 µM
SipA-NLuc luminescence/DMSO control [%]	89	126	108	98	97	72	103	114	82	103
F	Hydroxyurea 50 µg/mL	PDTC 10 µg/mL	Resveratrol 10 µg/mL	2-Theonyltri-fluoroacetone 20 µg/mL	2-Theonyltri-fluoroacetone 20 µg/mL	Erythromycin 10 µg/mL	Tetracyclin 10 µg/mL	Simvastatin 8 µM	Carbamazepine 20 µg/mL	BAY 11-7085 40 µg/mL
SipA-NLuc luminescence/DMSO control [%]	107	103	118	106	104	99	76	56	105	76
G	CCCP 50 µg/mL	Quercetin 30 µg/mL	Scutellarin 10 µg/mL	Penicillin G 20 µg/mL	Sodium Orthovanadate	Fluconazole 20 µg/mL	Theaflavin 5 µg/mL	Cycloheximide 1 µg/mL	Doxorubicin 11 µM	Penicillin G 20 µg/mL
SipA-NLuc luminescence/DMSO control [%]	88	10	26	72	105	101	103	103	87	70
H	Ampicillin 100 µg/mL	Rifampicin 10 µg/mL	Anisomycin 0.45 µM	Streptomycin 10 µg/mL	Antimycin A 50 µg/mL	Fludioxonil 10 µg/mL	Acycloguanosine 50 µg/mL	Cytochalasin D 5 µM	Simvastatin 8 µM	Tetracyclin 10 µg/mL
SipA-NLuc luminescence/DMSO control [%]	71	97	101	104	107	120	98	102	56	73

We additionally monitored the bacterial growth in response to treatment with the 37 different compounds in order to exclude growth inhibitory effects of the compounds impacting the luminescence detection (Fig. 28). The compounds were added again directly to the wild-type strain culture in a 384-well plate and the A_{600} measured after 5 hrs of growth. We did detect bacterial growth inhibition although the luminescence signal was only slightly reduced: The antibiotics ampicillin, rifampicin, carbenicillin, ciproflaxocin, tetracycline, penicillin and the PMF inhibitor CCCP led to a strong growth inhibition, but did not affect the luminescence detection. NLuc has been shown to be very stable at different conditions. Therefore, it is conceivable that these compounds lysed the bacteria releasing the cytoplasmic content including SipA-NLuc. This released SipA-NLuc could be still capable to convert furimazine into light still resulting in a signal.

Overall, the SipA-NLuc assay proved to be highly adaptable to a high throughput screening format in 384-well plates, featuring a high S/N ratio, a low error across the plate, a great reproducibility and requiring only short hands-on time. However, an additional control of growth should always be included to rule out false positive signals due to the high stability of NLuc even in lysed cells.

4.1.4 PMF-dependence of type III secretion and assessment of effects of different type of inhibitors by SipA-NLuc secretion assay[11]

It has been known for long that secretion through the T3SS depends on two sources of energy, on the hydrolysis of ATP by the system's ATPase (FliI in flagella, InvC in injectisomes) and on the PMF (Akeda and Galán, 2005; Paul *et al.*, 2008; Minamino *et al.*, 2012; Lee and Rietsch, 2015), which itself is composed of the ΔpH, i.e. the proton concentration gradient across the membrane, and the ΔΨ, the electric potential difference between the periplasm and cytoplasm. The contribution of these two PMF components to T3SS function can be dissected with specific inhibitors.

Carbonyl cyanide 3-chlorophenylhydrazone (CCCP) is a PMF uncoupler (ionophore) and discharges both the ΔpH and the ΔΨ by transporting protons through the membrane (Paul *et al.*, 2008). At acidic pH, potassium benzoate is a weak acid and can enter the membrane and discharge the ΔpH (Lee *et al.*, 2014). Valinomycin can shuttle potassium ions across the membrane which collapses the electric potential difference ΔΨ (Shen and Blocker, 2016).

[11] This chapter 4.1.4 has previously been published in Molecular Microbiology by Westerhausen *et al.*, 2020.

Evaluating the contribution of each PMF component to T3SS function requires the careful analysis of secretion kinetics, for which the classical, semi-quantitative western blot-based secretion assay is not well suited, but for which the NLuc-based secretion assay proved very powerful. To further show this, CCCP, potassium benzoates, and valinomycin, respectively, were added to the bacterial culture at different concentrations, 60 mins after induction of SPI-1, and samples of culture supernatants were taken every 10 mins for subsequent analysis of the luminescence of secreted SipA-NLuc.

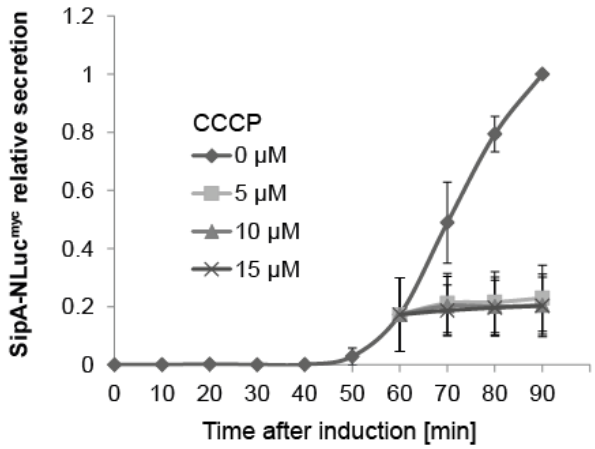

Fig. 29: Assessment of the dependence of type III secretion on the PMF by using the NLuc secretion assay. Normalized secretion of SipA-NLuc in *S.* Typhimurium P_{ara}*hilA* after induction of *S*PI-1 by addition of 0.02% arabinose. CCCP was added to a final concentration of 0, 5, 10 and 15 µM, respectively, 60 min after induction of *S*PI-1. Data represent mean (±standard deviation) of three technical independent replicates.

While SipA-NLuc secretion progressed over time in the control sample (Fig. 29), addition of the inhibitors led to sudden changes in secretion kinetics: CCCP blocked secretion instantly, even at concentrations of 5 µM, showing the critical relevance of the PMF for type III secretion (Fig. 29). Discharching the ΔpH by potassium benzoate resulted in a concentration-dependent instant reduction of secretion (Fig. 30 A). At a concentration of 20 mM potassium benzoate completely abolished secretion while at a concentration of 5mM and 10mM enabled partial secretion with a luminescence signal of 60% and 10% that of the untreated control, respectively. Collapsing the electric potential by valinomycin led to a strongly reduced luciferase signal after 10 min, after which secretion proceeded in a concentration-dependent manner (Fig. 30 B): in the presence of 20 µM valinomycin, no significant change in secretion rate was observed, while 40 µM and 60 µM valinomycin, respectively, led to a signal of 70% and 40% that of the untreated control.

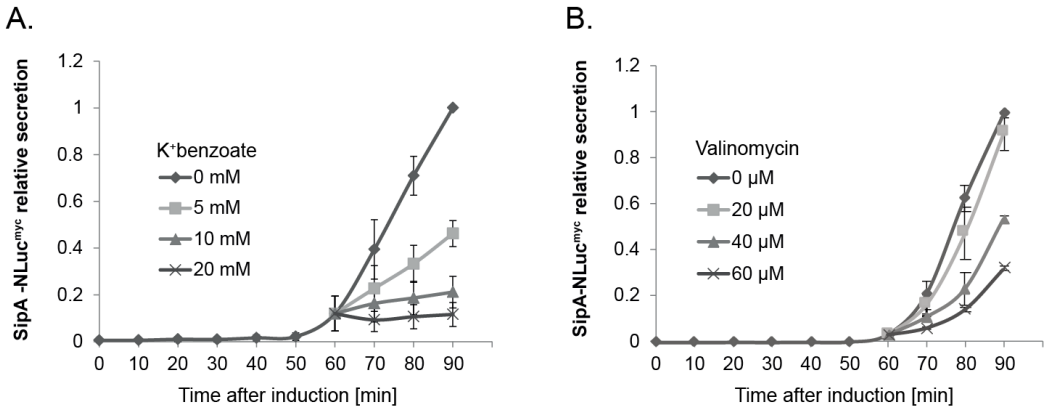

Fig. 30: Assessment of the dependence of type III secretion on the ΔpH and ΔΨ by using the NLuc secretion assay. **A.** Secretion of SipA-NLuc in *S*. Typhimurium P_{ara}*hilA* strain. *S*PI-1 was induced by addition of 0.02% arabinose. K^+ benzoate was added to a final concentration of 0, 5, 10 and 10 mM, respectively, 60 min after induction of *S*PI-1. **B.** As in A, by adding Valinomycin to a final concentration of 0, 20, 40 and 60 µM. Data were normalized to control and represent mean (±standard deviation) of three technical independent replicates.

These results show that both components of the PMF, ΔpH and ΔΨ, contribute to energizing secretion in the SPI-1-encoded T3SS of *S*. Typhimurium. By enabling the detection of very rapid effects of the PMF-compromising compounds on secretion, our sensitive and highly time-resolved NLuc secretion assay also allowed ruling out the possibility that the dependence of type III secretion on the PMF is the consequence of a secondary effect of PMF reduction. These results open the door to further experiments aimed at dissecting which components of the T3SS are powered by the PMF.

4.2 Development of NLuc-based host cell injection assays[12]

The assessment of secretion of T3SS substrates into the culture supernatant is very useful to investigate the basic secretion mechanism of the injectisome. However, the intended biological function of the T3SS is the injection of effector proteins into host cells. Since the SipA-NLuc-based secretion assay proved to be very sensitive and simple, we aimed to adapt the assay to monitor the injection of SipA-NLuc into host cells (Fig. 31).

[12] This chapter 4.3 has been previously published in Molecular Microbiology by Westerhausen *et al*., 2020, and has been slightly modified. Fig.34 and the respective information is unpublished.

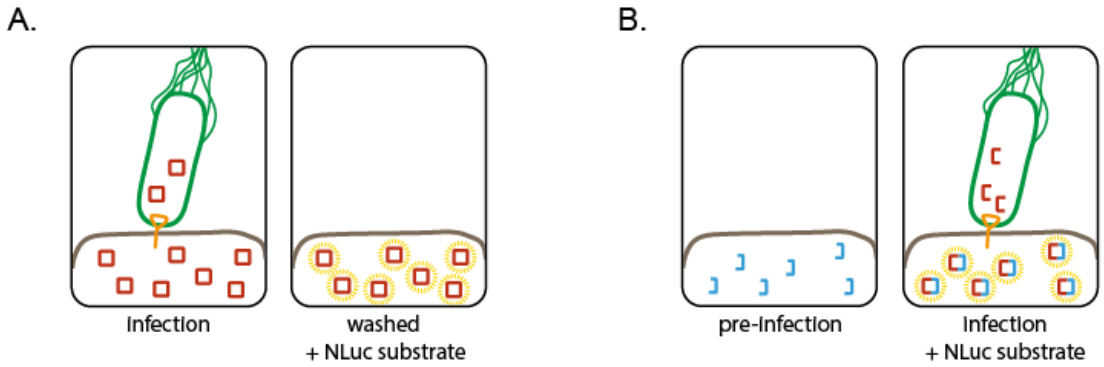

Fig. 31: Development of NLuc-based host cell injection assays. **A.** Cartoon showing setup of NLuc injection assay. *S.* Typhimurium strains expressing SipA-NLuc are allowed to infect HeLa cells for 60 min. During this thime, SipA-NLuc is injected into HeLa cells by the T3SS injectisome. Bacteria are then washed away using a microplate washer and NLuc luminescence measured. **B.** Cartoon showing setup of split-NLuc (HiBiT) injection assay. *S.* Typhimurium strains expressing SipA-HiBiT is allowed to infect HeLa cells (expressing LgBiT) for 60 min. During this time, SipA-HiBiT is injected into HeLa cells by the T3SS injectisome. Luminescence of the complemented split-NLuc is measured after washing away bacteria with a microplate reader.

In a first and simple approach, we infected HeLa cells in 96-well plates at a MOI of 50 with SipA-NLuc-expressing *S.* Typhimurium, using either wild type bacteria or secretion-deficient Δ*invA* mutants. After 60 min, the attached bacteria were gently washed off with PBS using a microplate washer and subsequently, the HeLa cell-associated luminescence was measured using live cell buffer (Fig. 31A). The non-secreting Δ*invA* mutants (Fig. 32A) showed a HeLa cell-associated luminescence of 8% that of the wild type, corresponding to a S/N = 12. To determine whether the HeLa cell-associated signal truly resulted from the injected SipA-NLuc, we assessed luminescence in a set of mutants that are capable of secreting but not injecting SipA-NLuc into host cells: A needle tip-deficient Δ*sipD*, a translocon-deficient Δ*sipBCD*, and a gatekeeper-deficient Δ*invE* mutant. While secretion of SipA-NLuc into the culture supernatant was increased between 2 and 5-fold in the Δ*sipD*, Δ*sipBCD*, and Δ*invE* mutants (Fig. 32 A), which are reportedly unlocked for secretion of late substrates like SipA (Kubori and Galán, 2002; Lara-Tejero *et al.*, 2011), the HeLa cell-associated luminescence following infection with the same mutants was strongly reduced to 9-24% that of the wild type strain (Fig. 32B). From these results we can conclude that more than 90% of the luminescence signal obtained from infection with wild type *S.* Typhimurium results from the injected SipA-NLuc and that only little signal may stem from bacteria attached to HeLa cells or to the plate after washing.

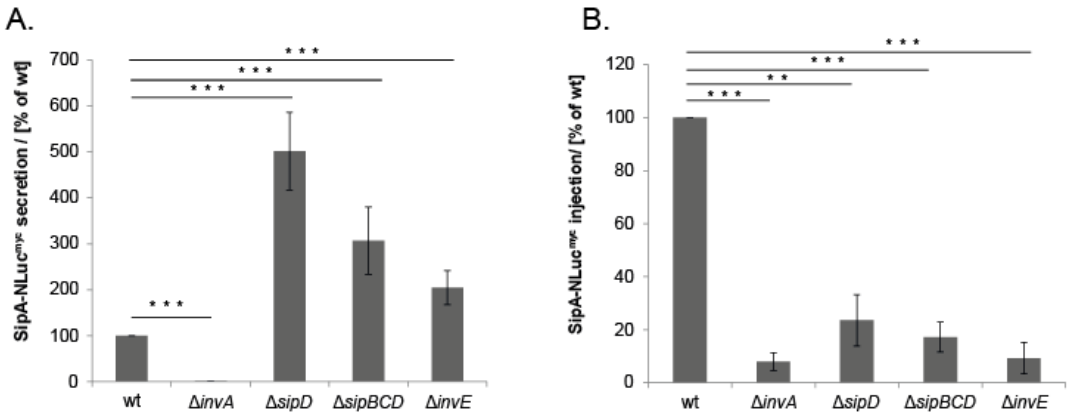

Fig. 32: SipA-NLuc secretion and injection by different T3SS mutants. **A.** Luminescence of SipA-NLuc secreted by the *S.* Typhimurium wild type and indicated mutants in the absence of host cells. The luminescence of the wild type was set to 100%. **B.** Luminescence of SipA-NLuc injected into HeLa cells by the *S.* Typhimurium wild type and indicated mutants. The experimental setup is as described in Figure 31A. The luminescence of the wild type was set to 100%.

Overall, this NLuc-based injection assay proved very useful for the quick and simple assessment of the translocation of effectors into host cells as experimental end-point. However, it did not allow assessment of the kinetics of injection.

To overcome this limitation, we employed the split version of NLuc. To this end, SipA was fused to HiBiT while LgBiT was stably expressed by the HeLa cell line. Complementation of LgBiT with HiBiT to a functional luciferase should only occur inside the HeLa cells after translocation of SipA-HiBiT (Fig. 32 B). We first tested the secretion of SipA-HiBiT into the culture supernatant by supplementing the assay buffer with LgBiT. Similar to what was observed for SipA-NLuc, secretion of SipA-HiBiT into the culture supernatant was increased between 2- and 6-fold in the Δ*sipD*, Δ*sipBCD*, and Δ*invE* mutants, respectively, when compared to the wild type (Fig. 33A). However, in contrast to the SipA-NLuc-based injection assay, none of the T3SS mutant strains yielded any detectable luminescence in the split NLuc assay (Fig. 33B), making the assay highly suitable for monitoring the specific injection of T3SS effectors into host cells even in absence of a washing step.

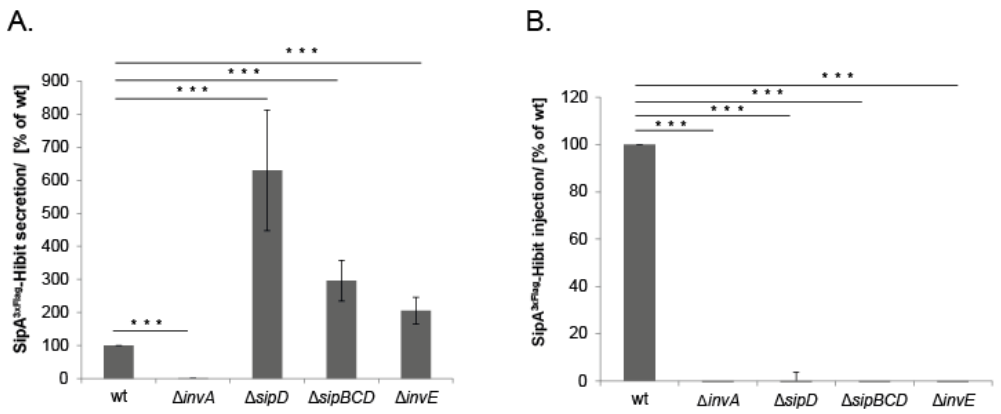

Fig. 33: SipA-HiBiT secretion and injection by different T3SS mutants. **A.** Luminescence of LgBiT-complemented SipA-HiBiT secreted by the *S.* Typhimurium wild type and indicated mutants in the absence of host cells. The luminescence of the wild type was set to 100%. **B.** Luminescence of SipA-HiBiT injected into LgBiT-expressing HeLa cells by the *S.* Typhimurium wild type and indicated mutants. The experimental setup is as described in Figure 31A. The luminescence of the wild type was set to 100%.

This allowed us to follow the kinetics of SipA-HiBiT injection over time directly in the microplate reader. Unfortunately, in these conditions we detected an overtime increase of the luminescence signal also in the injection mutant strains (Figure 34B). We speculated that HeLa cells that had not survived the infection procedure lysed and released cytosolic LgBiT into the extracellular environment, thus resulting in a background signal.

In order to overcome this problem, we used a mutated version of HiBiT, called DrkBit (Yamamoto *et al.*, 2019). In DrkBit, the fifth amino acid is mutated to alanine, which still allows the binding to LgBit but inhibits the substrate conversion thus quenching rather than emitting luminescence. When we supplemented the infection medium with purified DrkBit (Promega) and monitored the injection kinetics over time, we observed a specific signal only in the wt strain (Fig. 34C), indicating that the background signal, which was previously observed for the translocation deficient strains (Fig. 34A), was completely quenched by the addition of DrkBit. These data support the hypothesis that this unspecific signal stems from extracellularly released LgBiT and may also explain the strong decreasing signal that we observed within the first 10 min in the translocation mutant Δ*sipD* (Figure 34C). Indeed, in previous experiments, this mutant displayed the highest secretion (Fig. 33 A) as well as the highest unspecific luminescence signal associated with Hela-cells (Fig. 32B). Of note, the wt specific signal increased exponentially, but it is conceivable that it reaches a peak followed by a drop once the effector pool of SipA is depleted and bacteria are internalized into host vacuoles.

In conclusion, we successfully established host cell injection assays based on NLuc and its split variant. While SipA-NLuc was not optimal to assess injection by *S.* Typhimurium T3SS due to lack of specificity leading to a high background signal, the SipA-HiBiT assay provided the required specificity, especially in combination with DrkBiT, allowing real-time measurements.

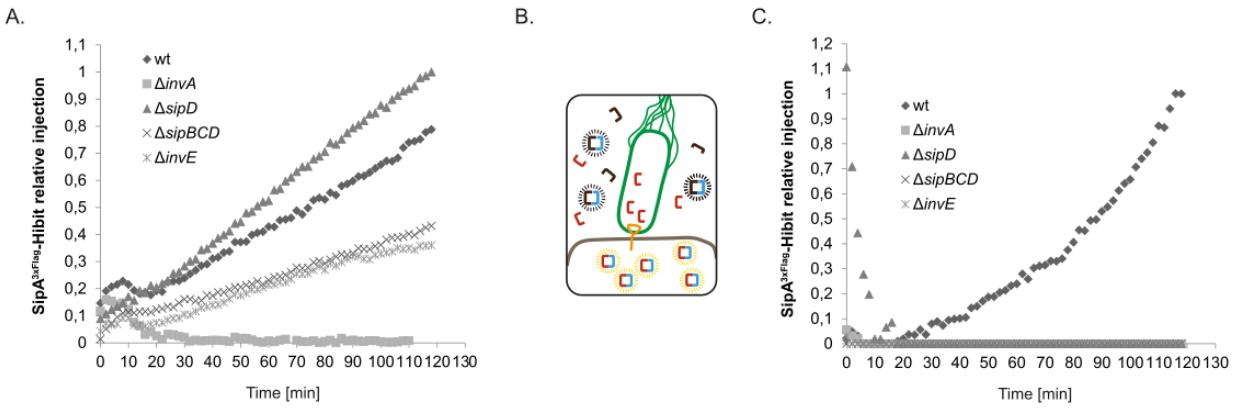

Fig. 34: Injection kinetics with SipA-HiBiT. **A.** Injection kinetics without DrkBiT. Luminescence of SipA-HiBiT injected into LgBiT-expressing HeLa cells by the *S.* Typhimurium wild type and the mutant strains. At timepoint zero, HeLa cells were infected with *S.* Typhimurium after which cells were incubated inside a microplate reader in the presence of NLuc substrate. Luminescence was followed at 2 min intervals. The results show the mean of two independent technical triplicates. **B.** Cartoon showing *S.* Typhimurium expressing SipA-HiBiT injected into HeLa cells by T3SS injectisome. The background signal is quenched by DrkBiT bound to free LgBiT (blue: LgBiT, black: DrkBiT, red: SipA-HiBiT) **C.** Same as in B, but DrkBit was added to the infection medium before incubation and reading. Data represents mean of three independent technical triplicates

4.3 Development of a periplasmic secretion assay for investigating substrate specificity switching

The Type III secretion system is assembled in a hierarchical manner. Once the basal body associates with the cytoplasmic components, early substrates are secreted and assemble the needle, followed by intermediate substrates that form the needle tip and the translocon in the host cell membrane. At last, late substrates are translocated into the host cell.

What is the difference in the system between the secretion of early, intermediate, and late substrates? What kind of mechanism prevents the secretion of intermediate substrates prior to the assembly of the needle?

Few proteins involved in ensuring the hierarchical secretion of substrates have been identified so far: The gatekeeper protein InvE and the autocleavage protein SpaS. The flexibility of SpaS C-terminus induced by its autocleavage is known to be required for secretion of intermediate substrates (Monjarás Feria *et al.*, 2015). It is also known that the secretion of the late substrates

is not executed before the release of the gatekeeper protein InvE (Kubori and Galán, 2002). In our current model, we propose that upon host cell contact InvE is no longer capable to bind to the major export apparatus protein InvA. This allows the chaperone-late substrate complexes to bind to InvA in order to be secreted. However, we do not believe that InvE is already bound to InvA at the stage of early substrate secretion. This notion is supported by the observation that early substrate secretion in *Yersinia* requires the release of YscX and its chaperone YscY, which are presumably involved in recruiting chaperone-early substrate complexes to YscV (InvA homolog). Hence, it is conceivable that YscX acts as gatekeeper protein for early substrate secretion (Diepold *et al.*, 2012).

If the secretion of intermediate substrates is dependent on the binding of InvE to InvA, it has to be triggered somehow or prevented prior to secretion of early substrates. We believe that the substrate specificity switching protein SpaS promotes the interaction of InvE with InvA. However, how SpaS-dependent substrate specificity switching is induced remains elusive.

In the fT3SS, the needle length regulator FliK (InvJ homolog) was shown to interact with the C-terminus of the SpaS homolog FlhB to induce substrate switching *in vitro* (Minamino and Macnab, 2000; Ho *et al.*, 2017). The execution of needle length control, which causes a halt in needle elongation, correlates with the timing of the switch and secretion of intermediate substrates. However, whether it is a prerequisite for substrate switching remains a matter of debate. Work in our lab showed earlier that needle length control acts independently of substrate specificity switching (Monjarás Feria *et al.*, 2015). On the other hand, genetic evidence suggests that timely and efficient substrate specificity switching depends on the execution of the needle length control. In 1994, Kutsukake *et al*. isolated fT3SS mutants that were capable to secrete intermediate substrates autonomously and independently of FliK (Kutsukake, Minamino and Yokoseki, 1994). Edqvist et al. reported that similar mutations in YscU, the Yersinia homolog of SpaS, enabled secretion of intermediate substrates in ruler protein deficient strains (Edqvist *et al.*, 2003). These so-called suppressor mutants carried specific mutations at the C-termini of SpaS homologs. Our lab was able to confirm the partial suppression of the Δ*invJ* phenotype by a C-terminal amino acid mutation of SpaS also in *S.* Typhimurium (unpublished data by Monjarás Feria and Bachmann). A closer look at the structure revealed that these suppressor mutations conceivably exerted steric strain on the interaction between $SpaS_{CN}$ and $SpaS_{CC}$ thus favouring autonomous switching.

On this basis we wondered whether SpaS switches between two states, one incompetent and the other competent for substrate specificity switching, and whether these suppressor mutations somehow stabilize the competent state of SpaS, thus triggering switching in absence of execution of needle length control. If substrate specificity switching is a stochastic event, of very low probability in wt SpaS and higher probability in the *invJ* suppressor mutants, then it should be possible to investigate whether switching requires ongoing secretion of early substrates or whether itcould already switch before any secretion starts. Further, it could be assessed whether the switch is a one-way switch or can go forth and back.

In order to test these hypotheses and investigate switching independently of needle length control, we sought to generate needle deficient strains and determine whether T3SS substrates are secreted in these needle deficient strains. However, in absence of a needle, if secretion does take place, it would lead to the accumulation of substrates in the periplasm rather than the extracellular space. Hence, we first needed to establish a periplasmic secretion assay that allows the specific and sensitive quantification of the T3SS secretion of early and intermediate substrates in the periplasm. As fusion of the early substrate InvJ to NLuc compromised its secretion (Westerhausen et al. 2020), we decided to use the split variant of NLuc for the periplasmic secretion assay and the small peptide HiBiT as fusion partner for the T3SS substrates. Simultaneously, we needed to achieve a stable expression of LgBiT in the periplasm for complementation. NLuc without a targeting sequence has already been shown to be evenly expressed in the cytoplasm of mammalian cells (Hall *et al.*, 2012). We did not expect a different behaviour in bacteria. Hence, to ensure the translocation to the periplasm, we decided to fuse the N-terminus of LgBiT to the periplasmic maltose binding protein MBP. The localization of MBP-LgBiT in the periplasm was investigated by two different approaches: Luminescence detection and Western Blot analysis.

The currently available Nano-Glo buffer and substrate kits can detect luminescence converted by NLuc fusion proteins in the intracellular and extracellular space, respectively (intracellular: Nano-Glo luciferase assay system kit also known as lytic kit for NanoLuc and Nano-Glo HiBiT lytic detection system for the NanoBiT system , extracellular: Nano-Glo HiBiT extracellular detection system for NanoBiT). These kits were mainly developed for mammalian cells which do not have an exterior protective cell wall (Schwinn *et al.*, 2018). We assumed that our bacteria with two membranes and a peptidoglycan layer in between were unlikely to be lysed by the intracellular Nano-Glo buffers. However, we speculated that these buffers might destabilize the outer membrane making the periplasm accessible. Nevertheless, we could not exclude a partial lysis or at least penetration of the kit components to the cytoplasm of the bacteria (Fig. 35A).

Thus, we considered to test the extracellular kit, which would penetrate the outer but not the inner membrane (Fig. 35B). To enhance accessibility of the extracellular kit to the periplasm, we treated the bacteria with EDTA, which chelates LPS-bound divalent ions thus destabilizing the outer membrane (Alakomi *et al.*, 2006).

To determine the optimal setup for luminescence detection, we purified MBP-HiBiT for external addition before the measurements. As detection of the luminescence signal of NLuc does not require any complementation, we performed tests also with cells expressing the translational fusion protein MBP-NLuc as a proof of concept for signal detection.

To determine the localization of MBP-LgBiT/MBP-NLuc by western blotting, we treated bacteria with a Ca^{2+}-chelator, EDTA, and lysozyme under osmotic conditions. This treatment releases the bacterial outer membrane with the digested peptidoglycan layer (outer membrane plus periplasm, OMP) and generates spheroplasts. The spheroplast fraction provides information about the cytoplasmic location of MBP-LgBiT/MBP-NLuc, while the OMP fraction informs about the presence of the fusion proteins in the periplasm.

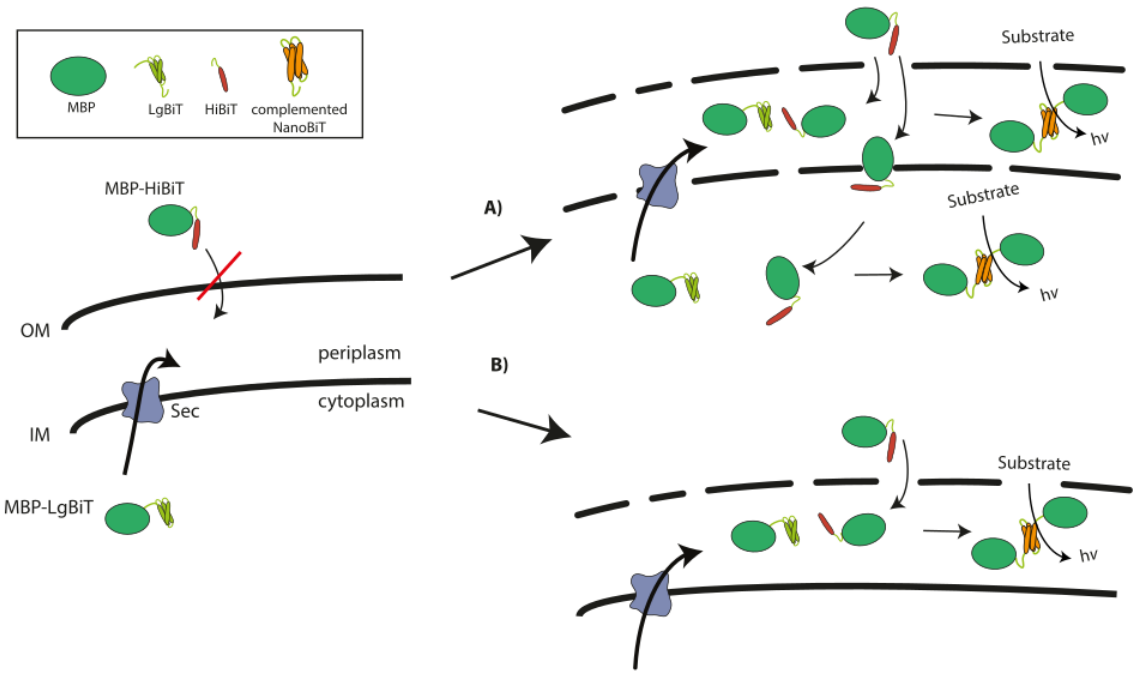

Fig. 35: The luminescence detection setup for MBP-LgBiT. The most suitable luminescence detection setup was determined by external supplementation of purified MBP-HiBiT, which needs to traverse the outer membrane for complementation. MBP-LgBiT is intracellularly expressed and translocated to periplasm by the Sec translocon. Two detection kits are available for NanoBiT, Nano-Glo HiBiT lytic detection system **(A)** and the Nano-Glo HiBiT extracellelular detection system **(B). A)** The lytic buffer detection system in combination with EDTA treatment might not only destabilize the outer membrane but also the inner membrane. In this scenario MBP-HiBiT complements with MBP-LgBiT for luminescence detection not only in the periplasm but also in the cytoplasm. However, it is conceivable that the inner membrane is less affected by the buffer treatment and that the large size of MBP may prohibit MBP-HiBiT to penetrate the inner membrane thus enabling specific detection of

NanoBiT in periplasm. **B)** The extracellular detection system in combination with EDTA treatment might selectively destabilize the outer membrane enabling MBP-HiBiT to pass through the outer membrane and the detection of NanoBiT in periplasm. **Abbreviations:** MBP: Maltose binding protein, LgBiT: large subunit (LargeBiT) of NLuc, HiBiT: high affinity binding small subunit of NLuc (HighBiT), OM: outer membrane, IM: inner membrane NanoBiT: NanoLuc binary technology.

4.3.1 Co-translational targeting of MBP fusion proteins

The periplasmic maltose binding protein (MBP) encoded by the *malE* gene has the typical signal sequence for being targeted to the Sec-translocon: A positively charged N-terminus and a hydrophobic central part followed by a polar region (Blaudeck *et al.*, 2003; Miot and Betton, 2004). The signal sequence has been shown to slow down the folding of MalE to enable post-translational recruitment to the Sec-translocon (Park *et al.*, 1988; Hardy and Randall, 1991). Substrates of the T3SS are also targeted to the T3SS in a post-translational way (Lloyd *et al.*, 2001; Ramamurthi and Schneewind, 2003). This poses the problem that folded MBP-LgBiT fusion constructs could already complement in the cytoplasm with HiBiT-tagged T3SS effectors. In order to overcome this problem, we sought to co-translationally target the MBP fusion constructs to the periplasm.

A correlation between the hydrophobicity of the core region in the signal sequence of the periplasmic protein alkaline phosphatase (PhoA) and SRP-dependent co-translational targeting has already been demonstrated in *E. coli* (Valent *et al.*, 1995). Correspondingly, we exchanged the amino acids in the central part of the MBP signal sequence with leucine residues and calculated the ΔG_{app} values (Table 11) according to Hessa *et al.* and Schibich *et al.* (Hessa *et al.*, 2007; Schibich *et al.*, 2016). We set a sliding window of 12-17 aa, since it has been reported that SRP prefers to bind to ribosomes exposing 12-17 aa stretches with several hydrophobic residues (Schibich *et al.*, 2016; Krampen *et al.*, 2018). As a reference value for SRP targeting, we calculated the ΔG_{app} values for the PhoA signal sequence mutations (Valent *et al.*, 1995).

Table 11: Amino acid substitution to increase the hydrophobicity of MBP. Valent et al. replaced the hydrophobic core of PhoA signal sequence with Ala (less hydrophobic) and Leu (more hydrophobic) to monitor the correlation between hydrophobicity and SRP binding. The amino acid exchange was performed by Michaela Morlock. ΔG_{app} of the signal sequence was determined using the prediction server v1.0. Length correction was set on off.

Name	Signal Sequence	ΔG_{app} (12-17 aa) in kcal/mol
PhoA$_{1A9L}$	MKQSTL**LLLLLLLL**TPVTKA	-3.499
PhoA$_{3A7L}$	MKQSTL**LLLLL**A**L**ATPVTKA	-2.576
PhoA$_{5A5L}$	MKQSTL**L**A**L**A**L**A**L**ATPVTKA	-1.445
PhoA sigseq$_{wt}$	MKQSTIALALLPLLFTPVTKA	-0.763

MBP sigseq$_{wt}$	MKIKTGARILALSALTTMMFSASALA	0.046
MBP $_{R8L}$	MKIKTGA**L**ILALSALTTMMFSASALA	-0.351
MBP$_{S13L}$	MKIKTGARILAL**L**ALTTMMFSASALA	-1.149
MBP$_{R8L_S13L}$	MKIKTGA**L**ILAL**L**ALTTMMFSASALA	-1.594
MBP$_{S13L_T16L}$	MKIKTGARILAL**L**AL**L**TMMFSASALA	-1.651
MBP$_{R8L_S13L_T16L}$	MKIKTGA**L**ILAL**L**AL**L**TMMFSASALA	-2.064

When arginine 8, serine 13 and threonine 16 were exchanged with leucine residues, a ΔG_{app} value of -2.064 kcal/mol was obtained (Table 11). This value is below the ΔG_{app} of PhoA$_{5A5L}$, which proved to be the minimum hydrophobic value for SRP-dependent translocation, but above the one of PhoA$_{3A7L}$, which resulted in a too strong binding to SRP and affected the targeting at a later stage (Valent *et al.*, 1995). The MBP$_{R8L_S13L_T16L}$ fusion constructs were expressed in *Salmonella* on a high copy number plasmid (placwoI (Krampen *et al.*, 2018)), and targeting to the periplasm was analysed by Western blotting with antisera against MBP as described above. This revealed that, despite being increasingly targeted to the periplasm, the MBP-fusion proteins were still detectable in the cytoplasm (Data not shown, data can be found in Michaela Morlock' s Master thesis, 2017). These data indicated that the increased hydrophobicity did contribute to improve the co-translational targeting of the fusion proteins to the Sec-Translocon. However, non-translocated fusion proteins were still detectable in the cytoplasm possibly due to the limited amount of SRP or saturation of the Sec translocon, resulting in inefficient translocation. We concluded that we needed to optimize the setup to target the MBP fusion proteins exclusively to the periplasm.

4.3.2 Further optimization of co-translational targeting of the MBP fusion proteins

Michaela Morlock' s data revealed that the expression of the MBP-fusion proteins from a high copy number plasmid (placwoI (Krampen *et al.*, 2018)) resulted in cytoplasmic localization (Data not shown, data can be found in Michaela Morlock' s Master thesis, 2017). We assumed that over-expression saturated the Sec-translocon thus hindering translocation of every single fusion protein to the periplasm. To overcome this, we cloned the MBP fusion proteins into low copy plasmids with a p15A origin of replication (pT2, (Wagner *et al.*, 2010)). Additionally, we introduced a *Salmonella* specific ssrA tag on the C-terminus of NLuc and LgBiT, respectively. The ssrA tag ensures the degradation of proteins located in the cytoplasm by the ATP dependent proteases ClpXP or ClpAP (Farrell, Grossman and Sauer, 2005). Constructs lacking the MBP signal sequence served as a negative control.

Following transformation of the plasmids encoding the different constructs in wild type *S.* Typhimurium, luminescence measurements of whole bacterial cells were carried out. Purified MBP-HiBiT was externally supplemented to the MBP-LgBiT samples for the detection of luminescence.

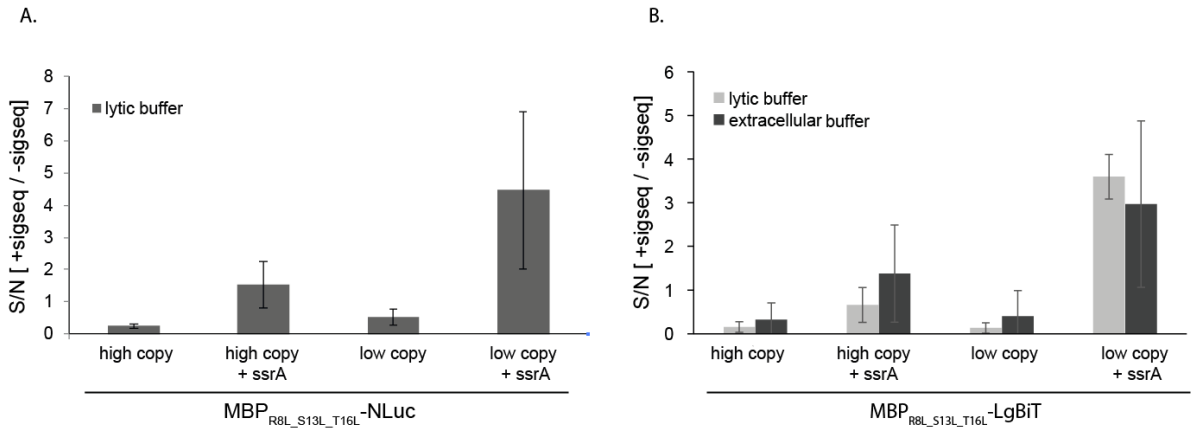

Fig. 36: Assessing luminescence of different constructs for periplasmic localization. **A.** Signal/ Noise ratio (S/N) of MBP-NLuc with signal sequence and without signal sequence was calculated upon luminescence measurement of whole cells treated with PBS and 0.1.mM EDTA for 30 minutes. Luminometry was carried out with Nano-Glo luciferase assay system kit (lytic buffer). **B.** Signal/ Noise ratio (S/N) of MBP-LgBiT was analysed by luminometry. The Nano-Glo HiBiT lytic detection system and the Nano-Glo HiBiT extracellular detection system were used for luminescence detection.
Every graph represents mean S/N (± standard deviation) of three independent measurements.

The signal to noise (S/N) ratio was determined by dividing the $MBP_{+sigseq}$-NLuc (or $MBP_{+sigseq}$-LgBiT) values by the values of $MBP_{-sigseq}$-NLuc (or $MBP_{-sigseq}$-LgBiT), and plotted in bar graphs (Fig. 36 A and B).

Overall, similarly modified NLuc and LgBiT constructs displayed similar S/N: The ssrA-tag appended to the C-terminus of LgBiT and NLuc significantly enhanced the S/N ratio, while expression of the fusion proteins from a low copy plasmid had a minor effect. The combination of both increased the S/N for MBP-NLuc to 5 and for MBP-LgBiT to 4 regardless of the buffer used for detection (Fig. 36). The variance between the lytic and the extracellular detection buffer in the S/N results of the LgBiT constructs was negligible when taking into account the standard deviation of the experiments. Of note, the expression of MBP-$LgBiT^{ssrA}$ from a low copy plasmid confirmed our initial assumption that the HiBiT lytic detection buffer in combination with the external supplementation of MBP-HiBiT does not penetrate the inner membrane.

Western Blot analysis revealed that the fusion proteins MBP-NLuc and MBP-LgBiT were still detectable in the cytoplasm irrespective of the modifications, with the exception of $MBP_{+/-sigseq}$ -$LgBiT^{ssrA}$ expressed from the low copy plasmid (Fig. 37). The constructs with $MBP_{+sigseq}$

showed overall a slightly decreased cytoplasmic localization while those with $MBP_{-sigseq}$ displayed a slightly increased cytoplasmic localization in agreement with the performed modification. The data also seemed to indicate that some of the $MBP_{-sigseq}$ constructs were translocated to the periplasm. Since MBP without signal sequence should not be able to translocate to the periplasm, we can exclude a translocation of $MBP_{-sigseq}$ constructs to the periplasm and hence have to assume that spheroplasting was not perfectly performed in these samples. Additionally, we detected a band of a similar size to, but distinct from native MBP in the periplasm. The signal intensity of this band increased with the intensity of the MBP-fusion proteins in the periplasm suggesting that our MBP fusion proteins are, at least in part, cleaved by a specific periplasmic protease. The $MBP_{-sigseq}$ -$NLuc^{ssrA}$ from the low copy plasmid was not localized in the cytoplasm suggesting a complete degradation in absence of translocation to the periplasm. Both $MBP_{+sigseq}$ -$LgBiT^{ssrA}$ and $MBP_{-sigseq}$ -$LgBiT^{ssrA}$ expressed from the low copy plasmid were neither detectable in the spheroplast nor in the periplasmic fraction. However, in the periplasmic fraction, we did observe again a band of about ~ 40 kDa suggesting that $MBP_{+sigseq}$ -$LgBiT^{ssrA}$ is translocated but cleaved in the periplasm.

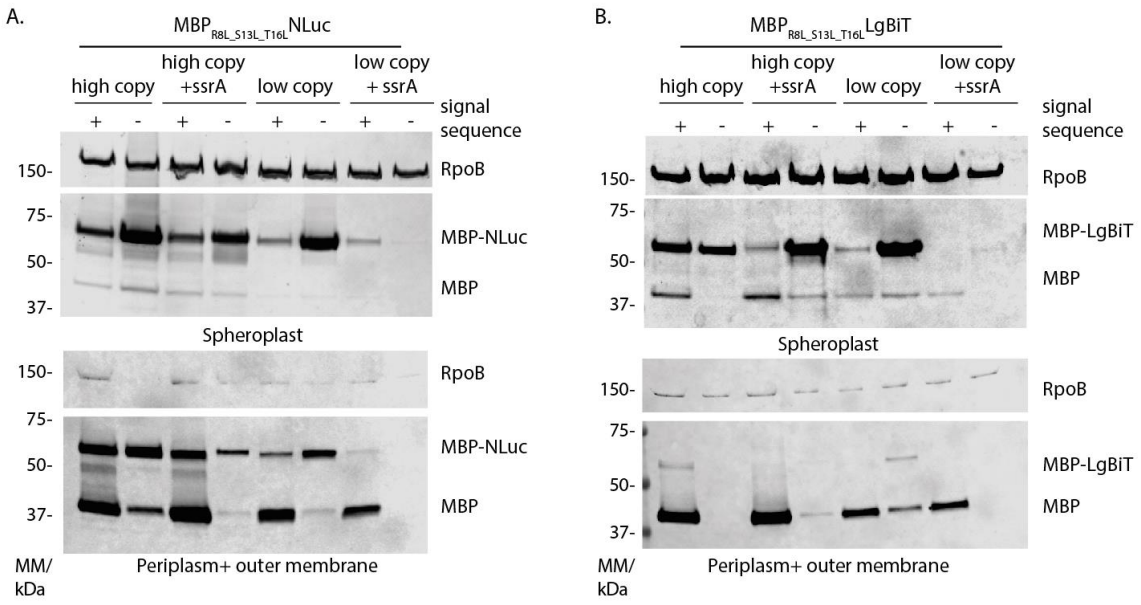

Fig. 37: Western blot analysis of the different MBP-NLuc and MBP-LgBiT fusion proteins. **A and B.** Wild type *S.* Typhimurium strains carrying different MBP-NLuc plasmids (A) and different MBP-LgBiT plasmids (B) were grown for 5 h. Afterwards 0.5 ODU of the cultures were collected and used to generate spheroplasts as in the text. Expression of the MBP fusion constructs in the cytoplasmic and periplasmic / outer membrane fractions was analyzed by SDS PAGE, Western blot and immunodetection with an anti-MBP antibody. The anti- RpoB antibody was used to detect the RNA-polymerase ß (RpoB), which served as loading control.

Overall, the results of the Western blot analysis and the luminometry suggested that MBP-NLuc and MBP-LgBit with a ssrA appendage and expressed from a low copy plasmid are decreasingly localized in the cytoplasm. A correspondingly increased localization in the periplasm was not detected most likely because the periplasmic-localized MBP-fusion proteins are cleaved by periplasmic proteases.

4.3.3 Overcoming periplasmic degradation of MBPs fusion proteins

The lack of the MBP fusion proteins and the presence of a fragment of about 40 kDa in the periplasmic fractions (Fig. 37) led us to assume that our MBP fusion proteins were translocated into the periplasm but cleaved by some proteases. The periplasmic space of bacteria comprises many different proteases (Miot and Betton, 2004). In an effort to find the protease responsible for the cleavage of our fusion constructs, we collaborated with Jan Willem de Gier from the Stockholm University, who provided us with 20 different periplasmic and cytoplasmic protease deficient *E. coli* strains (Table 12). Initial tests were performed by transforming the low copy plasmid (p15A ori, pT2) harboring $MBP_{R8L\_S13L\_T16L}$-$NLuc^{ssrA}$ and $MBP_{R8L\_S13L\_T16L}$-$LgBiT^{ssrA}$ as well as the MBP fusion constructs without signal sequence in these mutant strains (Note: all strains had an additional deletion of *ompT*) (Table 12).

Table 12: List of proteases lacking in the tested *E.coli* strains. The indicated "characteristic features" are restricted to those relevant to the scopes of this thesis.

Protease	Localization	Characteristic feature	Reference
OmpT	Periplasm	Serine protease, outer membrane protease with TMD, 10 antiparallel strands in a β-barrel structure, degrades antimicrobial peptides, complete biological function not known	(Kramer, Dekker and Egmond, 2000; Baaden and Sansom, 2004)
ClpP	Cytoplasm	ATP dependent serine protease, part of the two-component machinery with ClpA or ClpX, ClpP acts as protease, ClpA/X as unfoldase, active under stress and normal conditions (for protein turnover)	(Frees *et al.*, 2007; Truscott, Bezawork-Geleta and Dougan, 2011)
Lon	Cytoplasm	ATP dependent serine protease, degrades misfolded proteins but also normal proteins for protein turnover, implicated role in cell division, capsule synthesis, DNA damage recovery and virulence of SPI-1	(Kuroda *et al.*, 2001; Boddicker and Jones, 2004; Tsilibaris, Maenhaut-Michel and Van Melderen, 2006)
ClpQY (HslVU)	Cytoplasm	ClpQ acts as serine protease, ClpY ATPase and chaperone that activates ClpQ, role in protein quality control and protein turnover	(Kanemori, Yanagi and Yura, 1999; Ramachandran *et al.*, 2002)

DegP (HtrA)	Periplasm	Serine protease, role in Outer membrane protein (OMP) biogenesis for membrane integrity, degrades misfolded OMPs, it is proposed to possess protease and chaperone activity dependent on the temperature, it is suggested that C-terminal protein tags enhance recognition by degPs chaperone activity	(Iwanczyk *et al.*, 2007; Soltes *et al.*, 2017)
DegQ	Periplasm	Serine protease, HtrA family member, proposed to have chaperone and protease activity, dispensable role in protein quality in periplasm	(Malet *et al.*, 2012)
BepA	Periplasm	Zn^{2+} -dependent metalloprotease, ehances the assembly and elimination of β-barrel structure in OMPs together with BAM machinery	(Shahrizal *et al.*, 2019)
Tsp (Prc)	Periplasm	Serine protease, Tail-specific protease degrades substrates with nonpolar C-termini or ssrA tags, contributes to peptidoglycan enlargement	(Silber, Keiler and Sauer, 1992; Su *et al.*, 2017)
Ptr (Protease III)	Periplasm	Mg^{2+} -dependent endopeptidase, degrades small peptides with mass less than 7 kDa	(Finch *et al.*, 1981)
TesA	Periplasm	Thioesterase, lysophospholipase A, role in inner and outer membrane homoestasis	(Kovačić *et al.*, 2013)
YcaL	Periplasm	Metallo protease, role in degradation of BAM substrates	(Soltes *et al.*, 2017)
YdgD	Periplasm	Serine protease, role in cell wall biosynthesis	(Weski and Ehrmann, 2012)
YafL	Periplasm	Cysteine protease, Cell wall peptidase, role in peptidoglycan synthesis	(Lütticke *et al.*, 2012)
YhjJ	Periplasm	Zn^{2+} -dependent metallopeptidase, role in autophagy	(Sudhakar *et al.*, 2019)
NlpC	Periplasm	Cysteine protease, cell wall peptidase, role in peptidoglycan synthesis	(Ishikawa *et al.*, 1998; Singh *et al.*, 2012)
LoiP (YggG)	Periplasm	Metalloprotease, attached to outer membrane associated with BAM complex	(Lütticke *et al.*, 2012; Soltes *et al.*, 2017)
GlpG	Periplasm	Rhomboid-type serine protease, role in diverse biological processes e.g. activates membrane bound signaling proteins for several signaling pathways	(Dalbey, Wang and van Dijl, 2012; Guo *et al.*, 2016)
SppA	Periplasm	Signal peptide peptidase A, inner membrane bound serine protease, hydrolyses accumulated cleaved signal peptides of proteins translocated to periplasm	(Suzuki *et al.*, 1987; Wang *et al.*, 2008)
SohB	Periplasm	Serine protease, multicopy suppressor of htrA proteases like DegP	(Baird *et al.*, 1991)
HtpX	Periplasm	Membrane bound Zn^{2+} metalloprotease, degrades overexpressed SecY	(Sakoh, Ito and Akiyama, 2005; Dalbey, Wang and van Dijl, 2012)
YfbL	Periplasm	uncharacterized	-

We assessed the S/N ratio of the constructs with signal sequence and without signal sequence in the *E. coli* strains by luminometry. These analyses revealed that the luminescence signals were similar amongst most of the *E. coli* mutants in comparison to the wt, except for Δ*clpP*, Δ*degP* and Δ*tsp*. The luminescence signals of these mutants were plotted in a bar graph and the S/N ratio was calculated (Fig. 38 and 39).

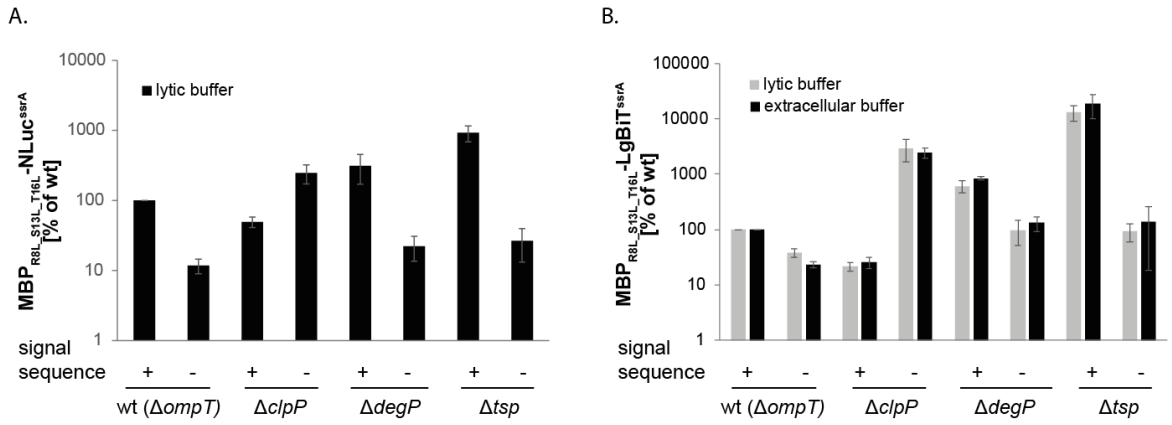

Fig. 38: Luminescence activity of the MBP fusion constructs in the wt (Δ*ompT)*, Δ*clpP*, Δ*degP* and Δ*tsp E.coli* mutants. **A.** MBP-NLuc^{ssrA} constructs were transformed in the respective *E.coli* strains. Luminometry was carried out with Nano-Glo luciferase assay system kit (lytic buffer) of EDTA-treated samples. MBP$_{+sigseq}$-NLuc^{ssrA} in the wt strain was set to 100 %. **B.** MBP-LgBiT^{ssrA} constructs were transformed in the indicated *E.coli* strains and analysed by luminometry. The Nano-Glo HiBiT lytic detection system and the Nano-Glo HiBiT extracellular detection system were used for luminescence detection. The graph is shown in log scale. MBP$_{+sigseq}$-LgBiT^{ssrA} in the wt strain was set to 100 %. Every graph represents mean signal (± standard deviation) of three independent measurements.

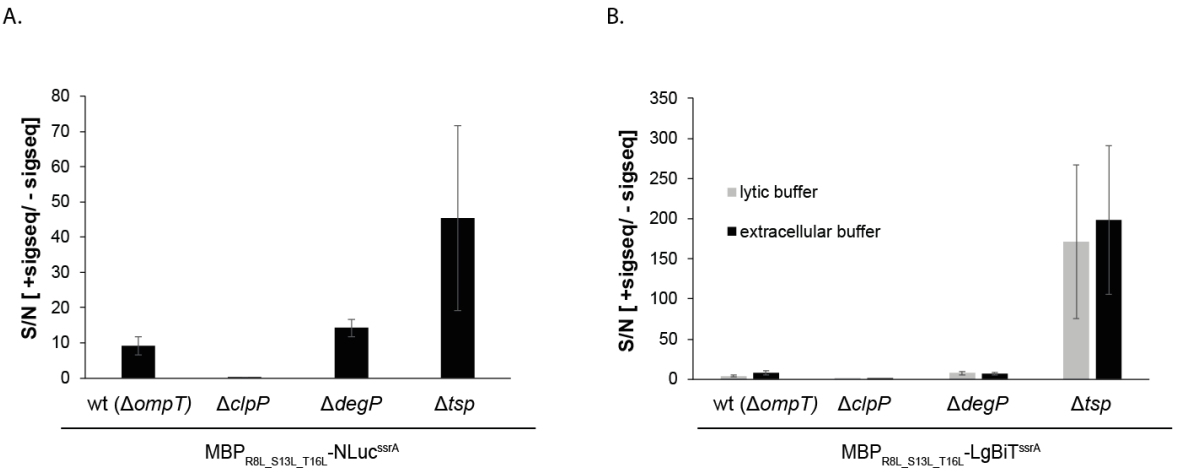

Fig. 39: Assessment of the S/N ratios of different MBP fusion constructs in wt (Δ*ompT)*, Δ*clpP*, Δ*degP and* Δ*tsp E.coli* mutants. **A.** Signal/ Noise ratio (S/N) of MBP-NLuc^{ssrA} was calculated upon luminescence measurement of whole cells treated with PBS and EDTA. Luminometry was carried out with Nano-Glo luciferase assay system kit (lytic buffer). **B.** Signal/ Noise ratio (S/N) of MBP-LgBiT was analysed by luminometry. The Nano-Glo HiBiT lytic detection system and the Nano-Glo HiBiT extracellular detection system were used for luminescence detection. Every graph represents mean S/N (± standard deviation) of three independent measurements.

The wt *E.coli* strain expressing MBP-NLuc^{ssrA} exhibited a slightly increased S/N ratio of 1.8-fold when compared to the corresponding *Salmonella* wt strain. However, this increase was negligible when the standard deviation was included. For MBP-LgBiT^{ssrA}, we did not detect any difference between the wt strains.

Tsp deficient mutants are reported to have a partial cell wall defect (Weski and Ehrmann, 2012). We detected the highest signal and the highest S/N ratio in the Δ*tsp* mutants. MBP$_{+sigseq}$-LgBiT^{ssrA} showed a 20-fold higher luminescence with the extracellular buffer and a 10-fold higher luminescence signal with the lytic buffer in comparison to the wt strain (Fig. 38A). MBP$_{+sigseq}$-NLuc^{ssrA} yielded a 10-fold higher luminescence signal in the Δ*tsp* mutant than in the wt strain (Fig. 38B). In this mutant, we observed S/N ratios of about 170±95 with the lytic buffer and of about 200±92 with the extracellular buffer for MBP-LgBiT^{ssrA} whereas the S/N ratio for MBP-NLuc^{ssrA} was 45±26. Presumably, the high signal and high S/N ratio in the Δ*tsp* mutant stems from its altered membrane permeability which enhances the uptake of external substances such as the lytic buffer and substrates through the bacterial outer membrane. Discrepancy in the observed S/N ratios between MBP-NLuc^{ssrA} (5 fold increase to wt) and MBP-LgBiT^{ssrA} (40 fold increase to wt) could conceivably also be the result of the increased outer membrane permeability in the Δ*tsp*, which would enhance the uptake of externally added MBP-HiBiT into the periplasm. MBP-NLuc^{ssrA} was only detected with the Nano-Glo luciferase detection kit, which proved to be partly lytic in previous experiments, thus decreasing the S/N ratio. In the Δ*tsp* mutant, due to the altered outer membrane permeability, the uptake of the lytic buffer would presumably be increased, resulting in a higher decrease of the S/N ratio.

The luminescence signal of the fusion constructs in the Δ*degP* mutant showed a 3-fold increase (MBP$_{+sigseq}$-NLuc^{ssrA}), a 6-fold increase (MBP$_{+sigseq}$-LgBiT^{ssrA}) with the lytic buffer and a 8-fold increase with extracellular buffer in comparison to the wt strain. The S/N ratios for MBP-NLuc^{ssrA} and MBP-LgBiT^{ssrA} in Δ*degP* were 1.5 to 2-fold higher than the ones of the wt strain. DegP is a protease contributing to the OMP biogenesis and well known to degrade substrates of the OMP assembly machinery (Soltes *et al.*, 2017). Our data suggest that it could potentially play a role in degrading other periplasmic proteins as well.

The serine protease ClpP forms a complex with the unfoldases ClpA or ClpX. In cooperation, ClpXP or ClpAP degrade aggregated cytoplasmic proteins tagged with ssrA (Olivares, Baker and Sauer, 2018). Correspondingly, in the Δ*clpP* mutant we observed a stronger luminescence signal for MBP$_{-sigseq}$-NLuc^{ssrA} and MBP$_{-sigseq}$-LgBiT^{srA} than that for their plus signal sequence counterparts and for the same constructs in the wt background. Accordingly, the increased signal of the MBP$_{-sigseq}$ fusion proteins resulted in a reduced S/N ratio. Contrary to our

expectations, in this mutant we detected a decreased signal for the $MBP_{+sigseq}$-fusion constructs and a higher luminescence intensity for MBP-LgBiT^{ssrA} when using the lytic buffer as compared to the signal detected with the extracellular buffer. These results suggest that the impaired quality control in the *clpP* mutant could result in problems with targeting and that still not all proteins are targeted correctly.

In order to verify the results obtained with the luminescence measurement, we performed a western blot analysis of the different protease deficient mutants. We observed a similar localization pattern for MBP-NLuc and MBP-LgBiT in the different protease deficient mutants compared to the corresponding wt strains (appendix). In some of the mutants we did not detect MBP-fusion proteins either in cytoplasm or in periplasm. However, we did detect a stronger signal for cleaved MBP. We proposed that deletion of those proteases activated other protease machineries, which degraded even more efficiently the MBP fusion proteins (appendix). As observed for the luminescence activities (Fig. 38 and 39), the Δ*clpP*, Δ*degP* and Δ*tsp* mutants displayed interesting localization patterns (Figure 40).

In the Δ*clpP* mutant, $MBP_{-sigseq}$-NLuc^{ssrA} and $MBP_{-sigseq}$-LgBiT^{ssrA} strongly accumulated in the cytoplasm, but was also detected in the periplasmic fraction as their plus signal sequence counterparts (Fig. 40). It is conceivable that the cytoplasmic accumulation of the constructs without signal sequence in this mutant is strong enough to enable the detection of these fusion proteins in the periplasmic fraction upon lysis of the spheroplasts during their generation (Fig. 40). This hypothesis is supported by the observation that $MBP_{-sigseq}$ fusion proteins when expressed from a high copy number plasmid were also detected in the periplasmic fraction (Fig. 37). In addition, the poor separation of the spheroplasts from the periplasmic / outer membrane fraction may contribute to the enhanced appearance of the $MBP_{-sigseq}$ fusion proteins in the periplasm.

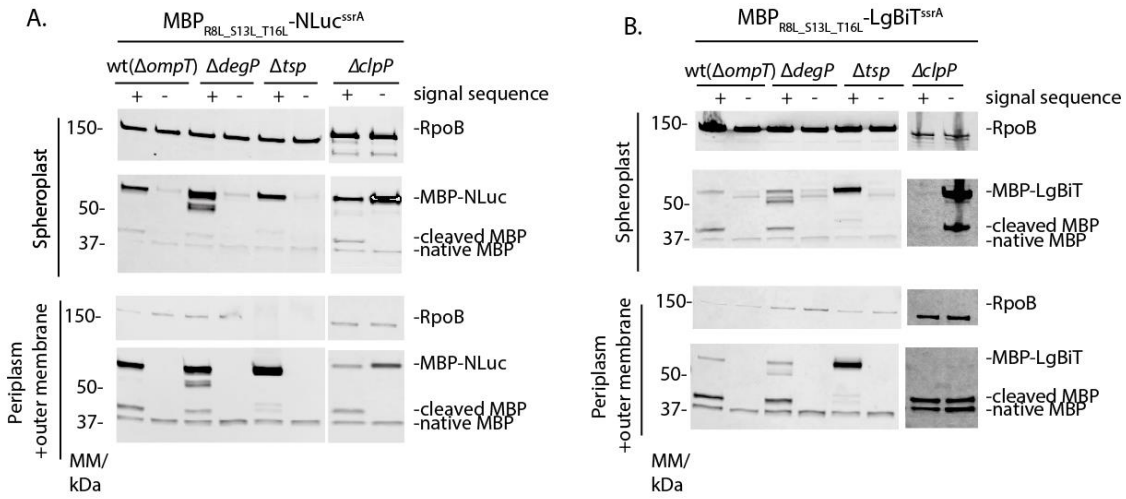

Fig 40: Western Blot analysis of the *ompT, degP, tsp* and *clpP* mutants. **A.** MBP$_{+sigseq/-sigseq}$-NLuc^{ssrA} plasmids were transformed into *E*. coli mutants and spheroplasting was performed. The MBP fusion constructs in the cytoplasmic and periplasmic/outer membrane fractions were analyzed by SDS PAGE, Western blot and immunodetection with an anti-MBP antibody. The anti-RpoB antibody was used to detect the RNA-polymerase ß (RpoB), which served as loading control. **B.** MBP$_{+sigseq/-sigseq}$-LgBiT^{ssrA} plasmids were transformed in the indicated *E*. coli mutants. Cytoplasmic and periplasmic fractions were obtained by spheroplasting and the MBP fusion constructs in these fractions were analysed as indicated in (A).

As previously seen in *Salmonella* (Fig. 39), the MBP-LgBiT constructs were weakly detectable in comparison to the MBP-NLuc constructs irrespective of the mutant. This suggested that NLuc is more stable than LgBiT in bacterial cells. LgBiT is the large subunit of NLuc and lacks one β-strand, which is provided by the complementation with the smaller subunit HiBiT. Although these subunits have been optimized for stability (Dixon *et al.*, 2016), it is conceivable that the missing β-strand makes LgBiT more unstable than the full length protein NLuc.

In the wt *E.coli*, we detected MBP$_{+sigseq}$-LgBiT in the cytoplasm as well as in the periplasmic fraction (Fig. 40 B). In contrast, MBP$_{+sigseq}$-LgBiT was not localized in any fraction of the *Salmonella* wt strain (Fig. 37 B). This observation suggests that the MBP fusion proteins are more stable in a bacterial strain that lacks *ompT*. This was used in our experiments as wild type *E. coli* strain since the different protease deficient mutants were generated in an *ompT* mutant background. Alternatively, it is possible that there was a technical issue in the immunodetection of the Western blot of *Salmonella* strains caused by the intense signal of the accumulated MBP$_{sigseq}$-LgBiT in the spheroplast fraction and cleaved MBP in periplasm fraction (Fig. 37 B). The similar S/N ratios for wt *Salmonella* (Fig. 37) and wt *E.coli* (Fig. 39) make the latter possibility plausible.

For the MBP$_{+sigseq}$ fusion proteins we detected two fragments that corresponded to the molecular mass of MBP in all *E: coli* strains (Fig. 40). The largest fragment was only detectable in the translocated MBP$_{+sigseq}$ fusion proteins indicating that this fragment resulted from the cleavage of the MBP fusion proteins while the lower fragment represented native MBP as it was detectable in every construct irrespective of their signal sequence. The size of the larger fragment indicates that the cleavage of the fusion proteins does not directly occur at the C-termini of MBP but rather somewhere within the linker that connects MBP with the reporter protein.

Deletion of the *tsp* gene is reported to cause membrane permeability in *E.coli* (Weski and Ehrmann, 2012). Additionally, the protease Tsp has been described to cleave periplasmic proteins with nonpolar C-termini and a ssrA tag (Silber, Keiler and Sauer, 1992; Keiler, Waller and Sauer, 1996). Correspondingly, the cleavage of the MBP fusion proteins with the ssrA tag was significantly diminished but not completely abolished in the Δ*tsp* mutant (Fig. 40). A

complete disappearance of the cleaved MBP was not expected because both reporter proteins, NLuc and LgBiT, do not have nonpolar C-termini and MBP fusion proteins without the ssrA tag were nonetheless previously cleaved in initial experiments (Fig. 37). These data suggest that the increased signal intensity and the high S/N ratio previously observed in Δ*tsp* mutant (Fig. 38 and 39) does not stem from the increased membrane permeability of this mutant, but rather from a role for Tsp in the cleavage of the MBP constructs.

The MBP fusion proteins in the Δ*degP* mutant appeared to be differently cleaved resulting in a fragment below the expected mass of the MBP fusion constructs. Although DegP was primarily assigned a role as protease in OMP biogenesis, its chaperone activity was reported by experiments with the periplasmic protein MalS (Spiess, Beil and Ehrmann, 1999). The appearance of the fragment of about ~ 50 kDa in the Δ*degP* mutant supports the notion that DegP may serve as chaperone and suppress another cleavage of the MBP fusion proteins. However, we did not detect a decreased signal or reduced S/N ratio in the Δ*degP* mutant (Fig. 38 and 39) opposing the idea of DegP as chaperone of the MBP fusion proteins, unless the cleavage occurred directly in MBP without influencing the reporter proteins. This would mean that in the Δ*degP* mutant native MBP should be cleaved as well, but it is not (Figure 40). A possible explanation could be that, in absence of DegP, MBP is cleaved only when fused to the reporter proteins, thus not affecting the integrity of native MBP.

The protein with a mass of ~50 kDa was detected not only in the periplasmic fraction but also in the spheroplasts of the Δ*degP* mutant. This might have been the result of incomplete spheroplasting of the mutant cells as suggested also by the observation that RpoB used as lysis control was barely detectable in the periplasmic fraction.

To sum up, we could identify three *E.coli* mutants in which the MBP fusion proteins behaved differently from those expressed in the wt strain. $MBP_{\text{-sigseq}}$ fusion proteins accumulated in the Δ*clpP* mutant. The use of this mutant also revealed that, contrary to our expectations, the lytic buffer penetrates the inner membrane to some extent (Fig. 38 B). The role of DegP remains unclear since the Western blot analysis suggests that it stabilizes the fusion proteins (Fig. 40), but the luminescence activity results oppose this notion (Fig. 38 and 39). The Δ*tsp* mutant exhibited a significantly increased luminescence activity and periplasmic MBP fusion proteins, prompting to a role for Tsp in the cleavage of the MBP fusion constructs in the periplasm (Fig. 38). These data also indicate that Tsp alone cannot entirely account for the cleavage suggesting that yet another protease, which was not covered in our screening, is involved in this process.

4.3.4 *Salmonella* periplasmic protease deficient mutants: Tsp targets MBP-fusion constructs in periplasm

Based on the above presented data, we could identify a role for Tsp in the periplasmic cleavage of our MBP fusion proteins. In order to verify its role in *S.* Typhimurium, we generated a *tsp* deletion mutant in this species. Additionally, we chose to test also the effects of deletion of *degP* and *pgtE* (*Salmonella OmpT* protease homolog) in *S.* Typhimurium in the light of our observations in the *E. coli* strains. Upon transformation of the MBP fusion constructs in these *Salmonella* mutant strains, cells were grown for 5 hrs at 37°C. Subsequently, 0.5 ODU of these cultures were treated with PBS and EDTA for luminometry and with sucrose, lysozyme and EDTA for spheroplasting. Both the spheroplasts and the periplasmic/outer membrane fractions were analyzed by SDS PAGE followed by Western blotting and immunodetection.

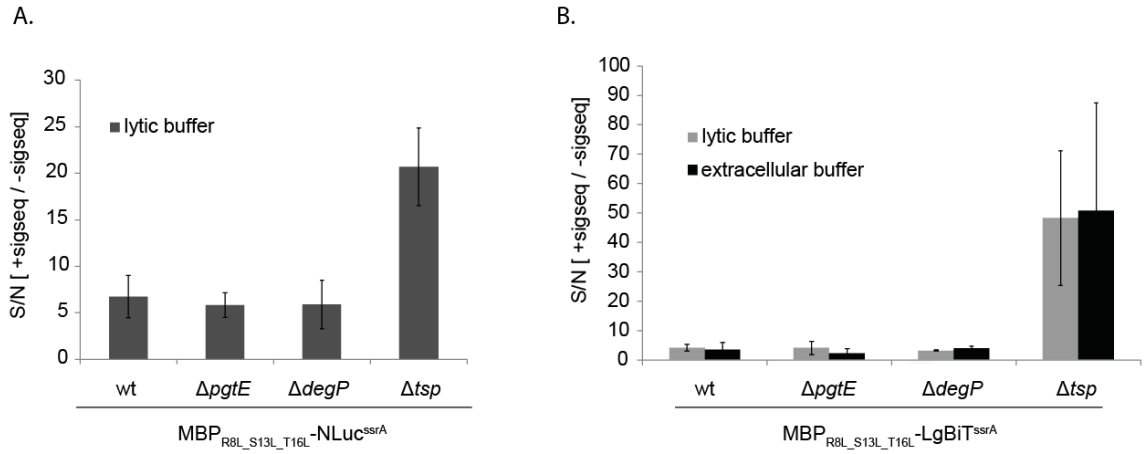

Fig. 41: S/N ratios of MBP-NLuc^{ssrA} and MBP-NLuc^{ssrA} in *S.*Typhimurium mutants. **A.** Signal to noise ratio of NLucs activity was determined with Nano-Glo luciferase detection kit (lytic buffer) of whole cells. **B.** Signal to noise ratio of LgBiTs activity was determined with lytic and extracellular buffer of whole cells upon complementation with MBP-HiBiT. Bar graph represents mean S/N (± standard deviation) of three independent measurements.

Similarly to what we detected in the *E. coli* strains, the MBP fusion protein constructs displayed the highest S/N ratio in the *Salmonella* Δ*tsp* mutant. Although, the S/N ratio was not as high as that in the *E.coli* mutant, we observed for MBP-NLuc^{ssrA} an increase of approx. 3-fold. For MBP-LgBiT^{ssrA}, we detected an increase of approx.12-fold with the lytic buffer and an increase of 14-fold with the extracellular buffer compared to the wt strain (Fig. 41). Both, Δ*pgtE* and Δ*degP* did not show any significant difference in comparison to wt. Of note, the *E. coli tsp* mutant had an additional deletion in the *ompT* gene. Although the luminescence activity of the MBP fusion constructs did not seem to be affected in the single *ompT* deletion mutant, it is conceivable that the combined deletion of *tsp* and *ompT* somehow enhances the luminescence signal.

Also the Western Blot results resembled those obtained for the corresponding mutants in *E.coli*. The MBP fusion constructs in the Δ*tsp* mutant showed a reduction in cleaved MBP accompanied by a stronger localization of the MBP fusion proteins in the periplasm. These data confirm the role of Tsp in the degradation of our fusion constructs.

We previously detected a second fragment of ~50 kDa below the expected mass of the MBP fusion proteins in the *E.coli* Δ*degP* mutant and assumed that a cleavage occurs directly in MBP (Fig. 40). Strikingly, we also detected the second protein fragment of ~50 kDa in *Salmonella* wt, Δ*pgtE* and Δ*tsp* to some extent, but not as strong as in Δ*degP* (Fig. 42). This result indicates that, contrary to our assumptions, DegP does not act as a chaperone for the MBP fusion

constructs, but rather another protease machinery is turned on in the *degP* mutants further enhancing degradation.

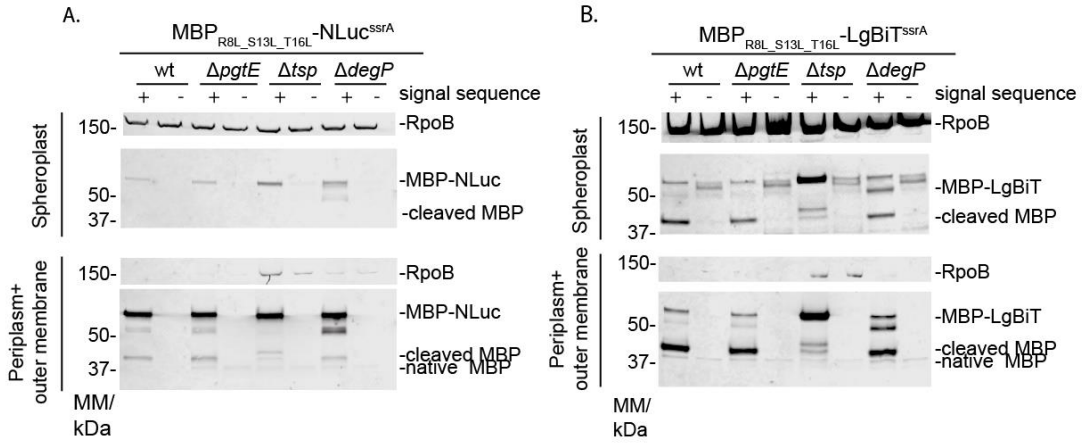

Fig. 42: Western Blot analysis of MBP-NLuc^{ssrA} and MBP-LgBiT^{ssrA} in the *S*.Typhimurium mutants. **A** and **B.** Immunodetection of MBP-NLuc^{ssrA} (A) and MBP-LgBiT^{ssrA} (B) constructs in spheroplasts and in the periplasmic/ outer membrane fraction. The two fractions were analysed by SDS PAGE, Western blot and immunodetection with an anti-MBP and anti-RpoB antibodies. RpoB served as loading control for the cytoplasmic fraction and lysis control for the periplasmic/outer membrane fraction.

In conclusion, we carried out four different types of modifications to reduce the localization of the MBP fusion constructs in the cytoplasm and to enhance their translocation to the periplasm. First, we increased the hydrophobicity by replacing amino acids in the signal sequence of MBP with leucine residues for co-translational targeting. Second, we changed the expression strength by introducing the constructs into a low copy plasmid to avoid saturation of SRP and / or the Sec translocon. Third, we appended a specific degradation tag at the C-terminus of the proteins to promote their degradation in the cytoplasm. Last, by testing different protease deficient mutants, we identified the protease Tsp as partly responsible for the cleavage of MBP-NLuc^{ssrA} and MBP-LgBiT^{ssrA} in the periplasm. As a result, MBP$_{R8L_S13L_T16L}$LgBiT^{ssrA} expressed from a low copy plasmid was stably localized in the periplasm of the *Salmonella* Δ*tsp* strain. Moreover, correlating with the periplasmic localization was the luminescence activity of MBP$_{R8L_S13L_T16L}$LgBiT^{ssrA}, which we detected upon external addition of MBP-HiBiT using the extracellular detection buffer.

This optimized setup was subsequently used to investigate the occurrence of T3SS secretion in needle deficient mutants, as described below.

4.3.5 Biological perspective of the periplasmic secretion assay: investigation of needle deficient mutants provides insights of assembly process

Once we had successfully established a periplasmic secretion assay, we changed the perspective back to T3SS to assess whether strains that lack the needle are still capable to secrete substrates into the periplasm. To uncouple substrate switching from needle length control, we sought to generate needle deficient strains that retain the ability to secrete T3SS substrates.

The needle subunit protein PrgI has been demonstrated not to be essential for a functional T3SS export apparatus (Diepold *et al.*, 2012; Wee and Hughes, 2015). However, simple deletion of *prgI* would conceivably result in T3SS substrates captured in the barrel structure of the secretin protein InvG and unable to reach the periplasm (Fig. 43). Knowledge about the function of InvG is restricted to its role in coupling the inner and outer membrane components of the T3SS and ensuring outer membrane translocation (Hu *et al.*, 2019). It has been proposed that secretion of early substrates does not depend on this coupling (Schraidt *et al.*, 2010). Strains lacking InvG were reported to show a loose attachment of the needle to the two inner membrane ring proteins PrgH and PrgK (Sukhan *et al.*, 2001; Schraidt *et al.*, 2010). We created mutants lacking InvG and carrying a point mutation in PrgI ($PrgI_{M1K}$) that inhibits translation of PrgI and thereby needle polymerization. The $PrgI_{M1K}$ mutation was chosen to avoid polar effects on the *prg* operon that could have arisen upon complete deletion However, the $PrgI_{M1K}$ strain has already been shown to result in impaired secretion of the inner rod protein PrgJ (Torres-Vargas *et al.*, 2019). Concomitantly, the needle protein lacking the C-terminus was demonstrated to have a polymerization defect which did not supposedly cause secretion defects in *Shigella* (Kenjale *et al.*, 2005). We took advantage of this needle polymerization deficiency and generated also strains lacking the last 10 C-terminal aa residues of PrgI ($PrgI_{C\Delta10}$). Furthermore, to ensure that the detected luminescence values correlated with the localization of T3SS substrates in the periplasm and not the cytoplasm, we introduced a deletion of the T3SS ATPase *invC* and a deletion of the export apparatus protein *invA* in the needle deficient strains. Mutants harboring an *invC* or *invA* deletion should be incapable to secrete T3SS substrates through the export apparatus and would hence serve as negative controls.

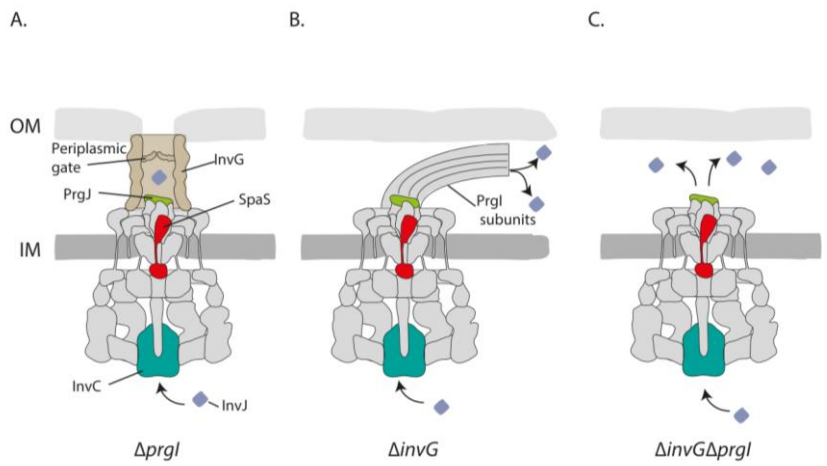

Fig. 43: Overview of different deletions and their resulting phenotypes. **A.** PrgI is proposed to traverse the periplasmic gate of secretin. Correspondingly, substrates in Δ*prgI* strains should not be able to pass through the periplasmic gate and would remain caught in the barrel structure of InvG. **B.** Sukhan et al. detected reduced amounts of PrgI in *ΔinvG* mutants and assumed that the attached needles would remain in the periplasmic space being unable to traverse the outer membrane (Sukhan *et al.*, 2001). **C**. The combination of *invG* and *prgI* deletion phenotypes supposedly results in secretion of InvJ to the periplasm.

Although we sought to assess secretion of intermediate substrates independently of needle length control, as a proof of concept for the secretion capability of the mutant strains, we attempted to detect periplasmic secretion of the needle length regulator InvJ fused to HiBiT, which occurs independently of the substrate specificity switch.

We initially assessed whether any of the strains were capable to secrete InvJ-HiBiT to the extracellular environment. As expected, we did not detect any significant secretion in the supernatant when strains lacked the export apparatus components InvA or InvC, the secretin InvG, the needle component and adaptor proteins PrgI and PrgJ, respectively (Fig. 44 A).

To test initially whether we can detect InvJ-HiBiT in the periplasm, LgBiT, 17.6 kDa is supplemented for complementation of InvJ-HiBiT, we treated 0.5 ODU harvested cells with EDTA to destabilize the outer membrane. The luminescence activity of InvJ-HiBiT was determined after the addition of the extracellular or lytic buffer substrate mixture containing external LgBiT.

Unexpectedly, irrespective of the buffer used, we detected high values for the positive wt control strain in whole cells (Fig. 44B). We expected a low signal because this strain is capable to secrete InvJ-HiBiT to the extracellular environment. The observed high signal might be due to the fact that, when harvested, the bacteria were at different stages of the T3SS assembly process. Therefore, it is conceivable that the signal stems from bacteria with incomplete needles starting to secrete early substrates to the periplasm. The acquired raw values (data not shown) of InvJ-HiBiT secretion were extremely low with the extracellular buffer and the standard

deviation was remarkably high hindering correct analysis of the data (Fig. 44 B). Since the extracellular buffer does not contain any detergents, EDTA treatment might not be sufficient to allow the passage of LgBiT through the outer membrane.

The overall signal was as well low when using the lytic buffer in whole cells (Fig. 44 B). Especially the $PrgI_{M1K}$ strains did not show any significant InvJ-HiBiT secretion in comparison to the corresponding Δ*invA* control strain. The lytic buffer containing detergents might lead to a leaky inner membrane, allowing the penetration of LgBiT into the cytoplasm.

Since we detected an overall low secretion in the different strains and in order to assure that these results were not impacted by the size of LgBiT, hindering passage through the outer membrane or inner membrane with the lytic buffer, we performed spheroplasting as described above under SPI-1 inducing conditions and determined the luminescence activity in the outer membrane and periplasmic fraction of the different background strains upon the addition of external LgBiT (Fig. 45).

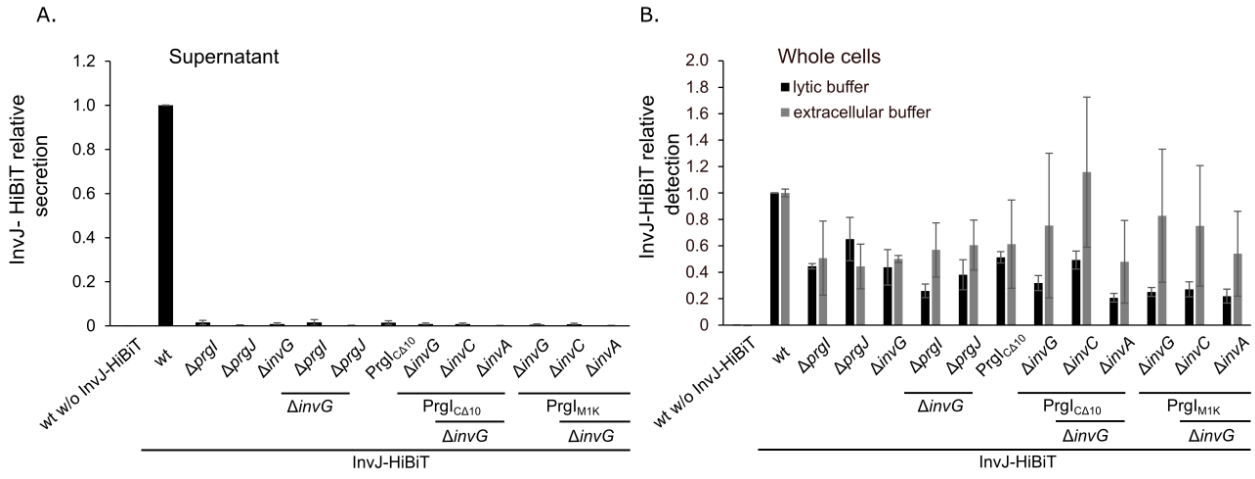

Fig. 44: Assessing InvJ-HiBiT secretion in absence of different T3SS components and in different *prgI* background strains. Wild type (wt) with and without InvJ-HiBiT were used as controls. **A.** InvJ-HiBiT detection in the supernatant after 5 hrs of growth at 37°C under SPI-1 inducing conditions. **B.** Bacterial cultures were grown as in A. Detection of InvJ-HiBiT was carried out in whole cells with lytic and extracellular buffer with the addition of external LgBiT upon treatment with EDTA for enhancing the permeability of the buffers. Wt constitutively expressing InvJ-HiBiT was set to 1. Bar graphs represent mean (± standard deviation) of three independent technical replicates.

The analysis of the secretion of InvJ-HiBiT in the periplasmic and outer membrane fraction of the different mutants revealed differences with that performed on whole cells after treatment with either lytic or extracellular buffer. While we did not detect any significant differences among the Δ*prgI,* Δ*prgJ* and Δ*invG* mutants with the lytic buffer, Δ*prgI* showed a 2-3 fold increased secretion in comparison to Δ*prgJ* and Δ*invG* in the periplasmic fraction. The

differences in luminescence activity between whole cells and the periplasmic fraction could be the result of lysis induced by the lytic buffer. We could hence conclude that the lytic buffer results in a leaky inner membrane and that by spheroplasting the periplasmic fraction is better isolated from the cytoplasm and provides a more specific and reliable signal.

The increased InvJ-HiBiT secretion in Δ*prgI* and decreased secretion in the Δ*prgJ* mutant prompt to speculate that InvJ secretion is PrgI but not PrgJ independent. However, the InvJ secretion in Δ*prgJ* is 2-fold the one detected in the negative control Δ*invA* indicating that secretion in the Δ*prgJ* mutant does occur albeit to a low degree. The secretion level of InvJ-HiBiT is similar in the Δ*prgJ* and Δ*invG* mutants.

The additional deletion of *invG* in the Δ*prgI* strain reduced the secretion of InvJ-HiBiT to 2-fold in comparison to the single *prgI* deletion. We previously speculated that InvJ-HiBiT might be captured in the barrel structure of the secretin impeding the detection of HiBiT if we would not delete it. This result opposes this notion.

While we also detected a 2-fold reduction in the signal of the $PrgI_{C\Delta10}$, Δ*invG* mutant strain in comparison to $PrgI_{C\Delta10}$, secretion was restored back to the $PrgI_{C\Delta10}$ mutant level by the additional deletion of *invC* in the double $PrgI_{C\Delta10}$ Δ*invG* mutant. Based on these data, it is conceivable that InvC and hence ATP hydrolysid is not required for the secretion of InvJ into the periplasm, but rather its deletion facilitates the entry of the early substrate InvJ into the export gate rescuing the Δ*invG* phenotype.

However, the restoring effect of Δ*invC* was not detected in the $PrgI_{M1K}$ strain. In fact, by including the standard deviation in the $PrgI_{M1K}$ Δ*invGC* , the $PrgI_{M1K}$ Δ*invG*, the $PrgI_{C\Delta10}$ Δ*invGC* and $PrgI_{C\Delta10}$ Δ*invG* strains, we observed similar levels of InvJ-HiBiT secretion to the periplasm. Therefore, it is likely that the single $PrgI_{M1K}$ mutant strain would show the same InvJ secretion phenotype as $PrgI_{C\Delta10}$ strain. This would support the notion that InvJ secretion is PrgI independent.

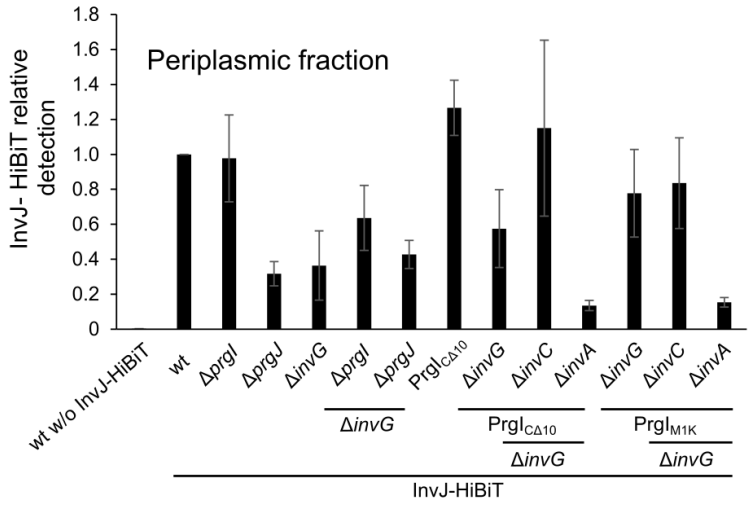

Fig. 45: Luminescence activity of the periplasmic and outer membrane fraction. Bacterial cultures were grown for 5 hrs under SPI-1 inducing conditions. Spheroplasing was performed by using EDTA and lysozyme under osmotic conditions. The luminescence signal was detected upon addition of extracellular buffer and substrate mixture with external LgBiT for complementation. Wt constitutively expressing InvJ-HiBiT was set to 1. Bar graphs represent mean (± standard deviation) of three independent technical replicates.

In an effort to use the periplasmic secretion assay with the above tested mutants, $MBP_{R8L\_S13L\_T16L}$-$LgBiT^{ssrA}$ and $MBP_{-sigseq}$-$LgBiT^{ssrA}$ fusion constructs were transformed into those mutants that had delivered the most significant results.

We assessed the luminescence activity of the complemented NanoBiT by luminometry. For this purpose, bacteria were grown for 5 hrs at 37°C and, afterwards, 0.5 ODU were collected and treated with EDTA to permeabilize the outer membrane. Samples were transferred to a 384-well plate and the corresponding luciferase reagents were supplemented without the external addition of the NanoBiT fusion partner for the detection of luminescence activity.

As seen previously, the signal intensities of mutants expressing $MBP_{-sigseq}$-$LgBiT^{ssrA}$ were increased in comparison to mutants expressing $MBP_{+sigseq}$ -$LgBiT^{ssrA}$ (data not shown). We speculate that $MBP_{-sigseq}$-$LgBiT^{ssrA}$ is expressed at higher levels or more stably within the cytoplasm impacting the analysis of the S/N ratios. Therefore, we decided to exclude strains carrying $MBP_{-sigseq}$-$LgBiT^{ssrA}$ from the analysis.

In whole cells, for each mutant we observed similar relative detection values irrespective of the buffer used (Fig. 46A). The lytic buffer could detect the signal in the cytoplasm as well. As we assume that MBP-$LgBiT^{ssrA}$ is still translocated in a post-translational manner to the periplasm, it is likely that complementation also occurs in the cytoplasm. The similar relative detection with the lytic and extracellular buffer could indicate that the extracellular kit components might pass the inner membrane aided by the EDTA treatment. In support of this notion, we detected the highest signal with the extracellular buffer in the Δ*invA* strain, which is unable to secrete.

For a better separation of the periplasmic and outer membrane fraction from the cytoplasm, we performed spheroplasting with EDTA and lysoyzme under osmotic conditions and assessed the NanoBiT complementation in the periplasmic fraction by luminometry (Fig. 46 B).

Although the difference between the Δ*prgI* and the $PrgI_{C\Delta10}$ strain was negligible in the previous experiment, it became clearer by endogenously expressing both NanoBiT fusion proteins. $PrgI_{C\Delta10}$ displayed a 2-fold increased NanoBiT activity when compared to Δ*prgI*. It is conceivable that $PrgI_{C\Delta10}$ increases the stability of InvJ or prevents its degradation through protein-protein interaction.

Additional deletion of *invG* or *invC* decreased the detection level of NanoBiT complementation in the $PrgI_{C\Delta10}$. Unlike what we previously observed with external supplementation of LgBiT (Fig. 45), the slight difference between the single *invG* and the double *invGC* deletion was negligible in cells endogenously expressing both NanoBiT fusion proteins. Deletion of *prgJ*, *invG* and *invGC* showed a similar level of NanoBiT activity (about 20%). This suggests that InvC is not as important as InvA for secretion of InvJ. Additionally, this result also supports the notion that InvJ secretion is PrgJ- and InvG- dependent. The single deletion of *invG* and *invC* would be required to clarify the assembly order and the importance of InvC in the early substrate secretion.

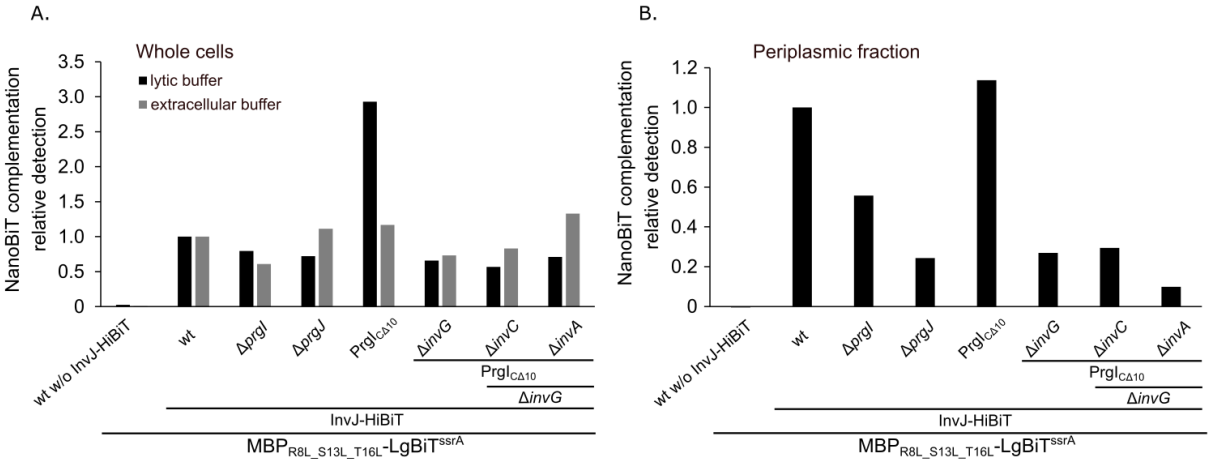

Fig. 46: Assessing NanoBiT complementation in absence of different T3SS components and in different PrgI background strains in whole cells and in periplasmic fraction. Wild type (wt) with and without InvJ-HiBiT were used as controls. **A.** Bacterial cultures were grown for 5 hrs under SPI-1 inducing conditions. Detection of NanoBiT complementation was carried out in whole cells with lytic and extracellular buffer without the addition of external LgBiT upon treatment with EDTA for enhancing the permeability of the buffers. **B.** Bacterial cultures were grown as in A. Spheroplasing was performed by using EDTA and lysozyme under osmotic conditions. The luminescence signal was detected upon addition of extracellular buffer and substrate mixture without external addition of NanoBiT fusion partner protein for complementation. Wt constitutively expressing InvJ-HiBiT was set to 1. Bar graphs depict one representative technical duplicate. Experiment was performed by Melanie Nowak.

The above presented NanoBiT assay was based on complementation of $MBP_{R8L\_S13L\_T16L}LgBiT^{ssrA}$ and InvJ-HiBiT. We previously demonstrated that $MBP_{R8L\_S13L\_T16L}LgBiT^{ssrA}$ is degraded by the protease Tsp. We could show that deletion of *tsp* increased the periplasmic localization of the MBP-fusion constructs and thereby the signal intensity (Fig. 41 and 42). Hence, we sought to test whether we could observe increased NanoBiT complementation in the Δ*tsp* strain. For this purpose, InvJ-HiBiT was expressed under the control of a rhamnose inducible promoter on a low copy number plasmid, and $MBP_{R8L\_S13L\_T16L}LgBiT^{ssrA}$ constitutively expressed from a low copy plasmid in *S.* Typhimurium wt and Δ*tsp* strains. We assessed whole cells using EDTA treatment in combination with lytic and extracellular buffer. The periplasmic fraction was obtained upon spheroplasting under osmotic conditions. The relative signal intensity in all samples was determined by luminometry.

The detection of the NanoBiT complemtentation was increased 20-fold with lytic and extracellular buffer in the Δ*tsp* mutant (Fig. 47). In the periplasmic fraction, we observed increased NanoBiT detection up to 150-fold. We can conclude that deletion of *tsp* in the needle deficient mutants can increase the detection signal and conceivably help discriminate subtle differences among the strains thus enabling to draw clearer conclusions.

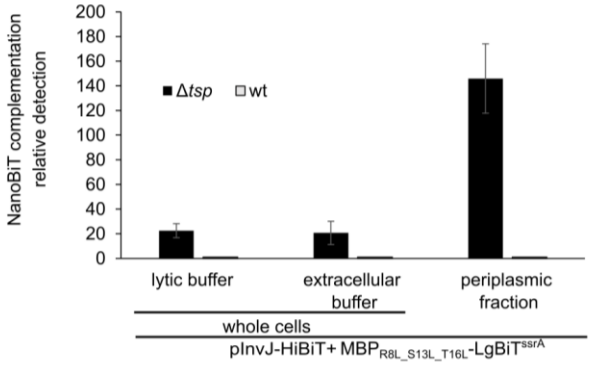

Fig. 47: Assessing NanoBiT complementation in whole cells and periplasmic fraction. Wild type (wt) and Δ*tsp* strains were transformed with low copy plasmid expressing InvJ-HiBiT and low copy plasmid expressing $MBP_{R8L\_S13L\_T16L}LgBiT^{ssrA}$. Bacteria were grown for 5 hrs under SPI-1 inducing conditions. Harvested cells were treated with EDTA for whole cells measurement or with EDTA and lysozyme under osmotic conditions for obtaining the periplasmic fraction. Data were acquired with the lytic kit or extracellular kit in whole cells. The luminescence activity of the periplasmic fraction was detected with thr extracellular kit. Bar graph represents mean S/N (± standard deviation) of three independent measurements.

In summary, we gained an overview of the secretion capability of the needle deficient mutants. Although assessment of luminometry detection in whole cells was of limited use due the permeability of the buffers especially when the NanoBit protein fragments were endogenously expressed, we could determine the activity of the complemented NanoBit proteins in the periplasm by cell fractionation analysis. In these conditions, we detected increased InvJ secretion and increased NanoBiT activity in the $PrgI_{C\Delta10}$ mutant, suggesting that secretion of $PrgI_{C\Delta10}$ increases the stability of InvJ-HiBiT in the cytoplasm or prevents its degradation in comparison to complete deletion of *prgI*. Furthermore, secretion of InvJ appeared to be PrgJ- and InvG- dependent. This could indicate that the secretion of InvJ occurs simultaneously with PrgI and is not executed prior to PrgJ secretion and InvG assembly. Interestingly, we could detect InvJ-HiBiT secretion in *invC* mutant strains suggesting that the ATPase function might be dispensable for the secretion of early substrates. The additional deletion of *tsp* resulted in increased signal intensity of NanoBiT and could help to gain better insights into the assembly and secretion process of the T3SS proteins.

5 Summary and Discussion[13]

Gram-negative bacteria exploit different types of secretion systems for pathogenicity, nutrient uptake but also as a survival mechanism against their many competitors. One of these systems is the T3SS. The T3SS secretes proteins into the host cell to promoting bacterial survival and replication. Many assays have been developed in the recent years to investigate its structure and molecular mechanism. Most of these assays are time consuming and not sufficiently quantitative, thus largely unsuitable to assess secretion/injection kinetics or identify inhibitors in a high throughput (HTP) manner.

The scientific aim of this thesis was to develop a versatile tool that can be differently used depending on the scientific purpose. We present three simple, quick and quantitative applications to investigate different aspects of protein secretion by using as read out luciferase activity (Fig. 48). Nano-Luciferase (NLuc) has the benefits of being bright and small and thus suitable for different types of application. As illustrated below, fusion of NLuc to different T3SS substrates enabled to elucidate the mechanism of secretion and injection (Fig. 48).

In the next chapters, I will describe the three applications of the use of NLuc activity as a reporter for secretion into I) extracellular environment, II) host cell III) the bacterial periplasm.

5.1 Development of the NLuc based secretion assay into extracellular environment[14]

Only few assays are available to assess the secretion by the T3SS system independently of host cell contact. While fluorescence reporters like GFP are usually the first choice for molecular analysis as they benefit from an intrinsic signal, they have proven unsuitable for the study of Type III dependent secretion: Their very stable β-barrel structure was reported to block the export gate of the T3SS (Enninga *et al.*, 2005; Radics, Königsmaier and Marlovits, 2014). The split variant of GFP was shown to be secreted by the T3SS but resulted in tight folding and slow complementation (VanEngelenburg and Palmer, 2008). Western blot-based assays allow to detect secreted proteins in the supernatant after a precipitation step, but lack the required sensitivity to analyse secretion kinetics and are not suitable for HTP screening. The carboxypeptidase G2 (CPG2) was established as reporter enzyme for T3SS effectors and used to screen T3SS inhibitors (Yount *et al.*, 2010; Tsou *et al.*, 2016). However, the fluorogenic substrate of CPG2 is not commercially available and this limits its use.

[13] Parts of the chapter 5 have been previously published in Molecular Microbiology by S.Westerhausen et al.
[14] Parts of 5.1 has been previously published in Molecular Microbiology by (Westerhausen *et al.*, 2020)

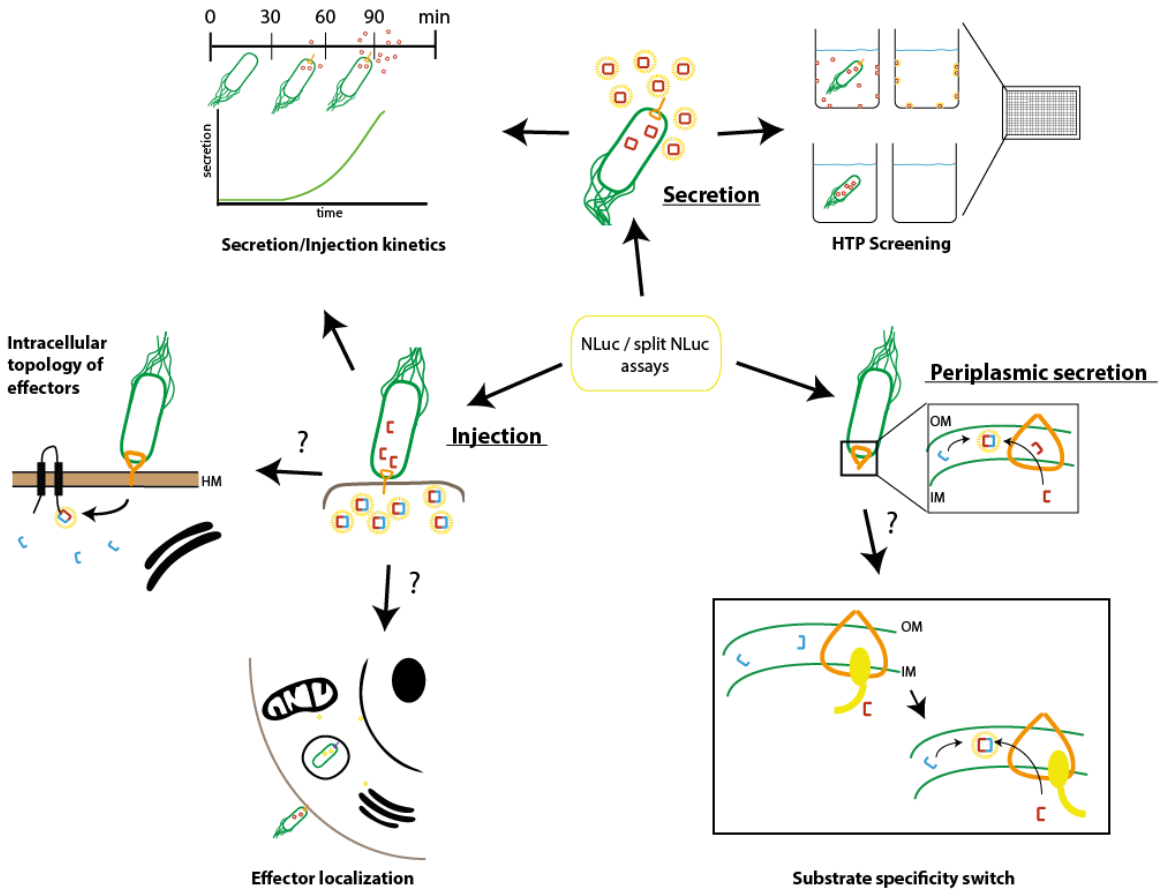

Fig. 48: Different applications of NLuc and its split variant. We have used both reporters to determine the extracellular and periplasmic secretion of T3SS effectors as well as their injection into host cells. The secretion and injection assays enabled monitoring over time effector dynamics. We showed that the secretion assay is suitable for HTP screens as well. Whether the injection assay can be used to determine the topology or localization of effectors in the host cell remains to be tested. The periplasmic secretion will prove useful to study the substrate specificity switch.

We developed a luciferase-based Type III secretion assay that enables overcoming the major limitations of previously developed assays. Although NLuc requires a substrate for signal detection, the measured signal directly correlates with the amount of the accumulated protein. We have shown this by simply performing a serial dilution. The serial dilution has also demonstrated the superior sensitivity and high dynamic range of NLuc, which allows detecting down to 24 nl of the culture supernatant in a linear correlation. This sensitivity allows studying the kinetics of secretion. We used a simple set-up in which accumulation of SipA-NLuc was measured in the culture supernatant over time. We note that a better system could have been developed by utilizing a microfluidic platform. This would have enabled direct reading of secretion into the flowing medium thus facilitating a better resolved analysis of the secretion mechanism.

The experiments with NLuc showed that its secretion is supported by fusion to a range of intermediate and late T3SS substrates. However, it failed to be secreted when fused to the early substrate InvJ (Westerhausen *et al.*, 2020) and to the intermediate substrate SipB. It is conceivable that the mode of early substrate secretion did not allow sufficient unfolding to support secretion of InvJ. The homolog of InvJ in *Yersinia* was shown to be secreted when fused to PhoA (Diepold *et al.*, 2012), pointing either to a higher unfolding capacity of the *Yersinia* T3SS or to a weaker folding of PhoA. This limitation could be overcome by using the split variant of NLuc. The 11 amino acid-long HiBiT was accommodated well by InvJ (Westerhausen *et al.*, 2020). However, HiBiT fused to SipB resulted in a low S/N ratio. Whether the C-terminal position of HiBiT in the SipB fusion protein played a role in the observed low S/N ratio needs to be investigated. However, it is very unlikely that the folding capacity or flexibility of HiBiT affected SipB secretion.

While the NLuc-based secretion assay proved to be simple, versatile and robust, the stability of NLuc resulted in false-positive signals due to lysis of bacteria in the HTP screen. Indeed, upon addition of some antibiotics like ampicillin, rifampicin, carbenicillin and ciproflaxocin we detected a strong reduction in growth and assumed that bacteria treated with these compounds were lysed releasing the already expressed SipA-NLuc in the extracellular environment. Consistent with this notion, NLuc was stable up to 4 hrs in the culture supernatant at 37°C in our experiments. Hence, in general, HTP screens should always be followed by an additional orthogonal assay to exclude additional effects of the tested compounds.

5.2 Development of SipA-NLuc injection assay: secretion into host cell[15]

Most of the T3SS assays developed so far are dedicated to the analysis of effector injection into host cells. While assays based on split variants of fluorescence reporters are very limited in their use to investigate injection kinetics, they have proven to be very suitable to study localization dynamics (VanEngelenburg and Palmer, 2008). The CCF2-based β-lactamase assay enables the analysis of effector translocation kinetics as well as effector localization but suffers from the high cost of CCF2 and a low dynamic range (Enninga *et al.*, 2005; Mills *et al.*, 2008). In addition, the β-lactamase cleaved products accumulate and complicate the analysis of the injection. We could establish a NLuc-based assay that allows simple and quick analysis without the compounded effects of accumulated products. While this assay does not support the study of the localization of effector-NLuc fusion proteins at high-resolution, microscopic

[15] This section has been published in Westerhausen et al. 2020

setups exist that could enable monitoring of single cells over an extended period of time (Horibe *et al.*, 2018). This could also be enabled by the recently developed live substrates Endurazine and Vivazine. These substrates allow detection up to 72 hrs post injection in live cells and are suitable for effectors that are translocated at a later stage of the infection cycle. However, due to the 10-fold decreased brightness within the first hour in comparison to fumirazine, they are less suitable to monitor the initial phase of injection.

The cytoplasmic expression of LgBiT in the host cell should only generate luminescence when HiBiT-fused T3SS effector proteins localize in the cytoplasm following injection. This simple setup of detection proved to be effective when cells, prior measurements, were washed gently thus removing bound bacteria as well as lysed host cells. When we tried to monitor the injection kinetics without including a washing step, we detected an unspecific signal in translocation deficient mutants. We could overcome this problem by externally supplementing DrkBiT, a HiBiT mutant variant (Yamamoto *et al.*, 2019), prior measurements. DrkBiT bound to extracellular LgBiT released by lysed host cells and completely quenched the unspecific signal. This allowed the simple, cheap and quick monitoring of kinetics over time in correlation to secreted substrate.

The split NLuc assay could potentially be used also to analyse the localization and topology of effector proteins inside the host cells by targeting LgBiT to specific organelles. The utilization of low- affinity SmBiT instead of high-affinity HiBiT could prove useful to investigate effector-host protein interaction *in vivo* by bimolecular complementation without affecting the appended proteins affinity (Dixon *et al.*, 2016).

5.3 Development of a periplasmic secretion assay for investigating substrate specificity switch

More than 20 different proteins form the T3SS. The hierarchical order of the assembly and secretion of the proteins ensures the correct functioning of the secretion system. How this is achieved is still under investigation.
Several proteins were suggested to ensure a hierarchical secretion. It is believed that the autocleavage protein SpaS, the needle adaptor protein PrgJ and the needle length regulator InvJ play an important role in the secretion of intermediate substrates while InvE is proposed to regulate the secretion of late effectors.

The needle adaptor protein PrgJ was reported to be involved in needle length regulation and substrate specificity switch based on the observation that deletion of InvJ resulted in mutants

with long needles and unable to secrete intermediate substrates. Consequently, it was proposed that PrgJ and InvJ are secreted simultaneously and that the assembly of PrgJ times needle length followed by secretion of intermediate substrates (Marlovits *et al.*, 2006; Lefebre and Gálan, 2014). However, this timer model was challenged by experiments performed under native, rather than overexpression conditions.

Many studies in *Yersinia* as well as of the flagellar T3SS proposed that the autocleavage of the homolog protein of SpaS was the inducer for switching secretion from early to intermediate substrates (Ferris *et al.*, 2005; Riordan and Schneewind, 2008). This notion was opposed by the findings that autocleaved SpaS is incorporated into the base and is not *per se* the inducer but its autocleavage has to take place to enable regulation of the switching process (Monjarás Feria *et al.*, 2015).

The N-terminus of the needle length regulator InvJ has been shown to dictate needle length. Reports in *Yersinia* demonstrated that deletions of the N-terminal sequence of YscP resulted in shorter needles while insertions in longer needles, suggesting that a part of YscP is attached to the basal body whereas the other part acts as molecular ruler (Journet *et al.*, 2003). Recent data by Kinoshita support this notion in flagella and link needle length control by the needle length regulator FliK with substrate specificity switching. FliK is postulated to suppress and induce substrate specificity switching by interacting with the autocleavage protein FlhB (Minamino *et al.*, 2004; Kinoshita *et al.*, 2017).

Interestingly, studies of the fT3SS and *Yersinia* injectisome reported the identification of *flhB* and *yscU* (homologs of SpaS) mutants able to regulate substrate specificity switching independently of the needle length regulator (Kutsukake, Minamino and Yokoseki, 1994; Edqvist *et al.*, 2003). These suppressor mutants were capable to secrete intermediate substrates despite their longer needles. Vice versa, autocleavage defective mutants were able to execute needle length control , but unable to secrete intermediate substrates (Monjarás Feria *et al.*, 2015).

In the light of these findings, we proposed a model in which substrate specificity switching and needle length regulation are two independent events. This model implies that neither the secretion of intermediate substrates nor needle capping by the tip protein stops needle elongation, but rather an unknown mechanism. This may involve either an active stopping of early substrate secretion or a conformational change of the assembling needle that prohibits further assembly at its distal end (Wagner *et al.*, 2018).

But which kind of mechanism induces the substrate specificity switching and how is SpaS involved in the regulation?

The suppressor mutations in the homologs of SpaS are located in the region between the $SpaS_{CN}$ and the $SpaS_{CC}$ domain. We speculated that these mutations exert a steric strain that favours and increases the likelihood of autonomous, uninduced switching. Moreover, we asked ourselves whether substrate specificity switching is rather the result of a stochastic event and can occur also in a system with unfinished needle and if a molecular switch truly exists, is it a "one-way" direction or can be turned off again?

In order to investigate the mechanism behind the substrate specificity switching in a T3SS lacking assembled needles, we sought to develop a periplasmic secretion assay. In case of a premature switch, we could detect secretion of the T3SS substrates to the periplasm of the needle deficient strains.

This assay needed to be not only sensitive and specific, but also able to monitor kinetics over time to follow the switch between the substrates. The setup comprised bacterial cells carrying HiBiT-tagged T3SS substrates and expressing the MBP-LgBiT fusion protein for complementation of NanoBiT in the periplasm. It also required the use of different Nano-Glo detection kits with different outer membrane penetration properties. We decided to use the split variant of NLuc for the final assay, since full length NLuc compromised the secretion of the early substrate InvJ. However, for proof of concept experiments, we also used NLuc, since we did not know whether we could achieve complementation of LgBiT by external addition of HiBiT.

In the next section, I will discuss about the single components of the periplasmic secretion assay and their suitability for the assay.

5.3.1 MBP is not an optimal fusion partner for the periplasmic secretion assay

MBP and the T3SS substrates are post-translationally targeted, posing the problem of a possible complementation in the cytoplasm prior to translocation to the periplasm. To overcome this, we aimed at co-translational targeting MBP to the periplasm by increasing the hydrophobicity of its signal sequence for recognition by SRP. Despite obtaining increased amounts of MBP-LgBiT in the periplasm, we still detected MBP-LgBiT in the cytoplasm. We assumed that the Sec-translocon is saturated by the overexpression of MBP-LgBiT. Hence, we expressed MBP-LgBiT from a low copy plasmid and inserted an additional ssrA -tag to promote degradation of the fusion protein in the cytoplasm. Strains expressing a mutant MBP-LgBiT with no signal

sequence ($MBP_{-sigseq}$LgBiT) served as negative control. While expression from the low copy plasmid alone did not enhance the S/N (Signal: $MBP_{+sigseq}$/ Noise: $MBP_{-sigseq}$) ratio, we detected increased S/N ratios for MBP-LgBiT expressed from a low copy plasmid and harbouring the ssrA-tag. These data suggested that not a saturation of the Sec-translocon was the reason for the localization of MBP-LgBiT in the cytoplasm but rather the occurrence of residual post-translational targeting to the periplasm. SRP has been reported to bind to very hydrophobic proteins with low ΔG_{app} (Schibich *et al.*, 2016). The exchange of amino acids with leucine residues within the signal sequence has been reported to increase the hydrophobicity and correspondingly SRP targeting (Valent *et al.*, 1995; Schibich *et al.*, 2016). Nonetheless, 60 % of $PhoA_{5A5L}$ (5 leucine residues exchanged) and 40% of Pho_{A3A7L} (7 leucine residues exchanged) were still bound to SecB as determined by cross-linking experiments (Valent *et al.*, 1995). As SRP occurs in a very limited amount in the cell (Schibich *et al.*, 2016), it could very well be the limiting factor for the co-translational targeting and cause the remaining proteins to be post-translationally targeted.

This notion is supported by the ΔG_{app} for the optimized $MBP_{R8L\_S13L\_T16L}$ which was between the predicted ΔG_{app} of $PhoA_{5A5L}$ and $PhoA_{3A7L}$. We could estimate that about 50% of $MBP_{R8L\_S13L\_T16L}$ is co-translationally targeted to the periplasm and the remaining 50% post-translationally. It is conceivable that the appended 11 amino acid-long ssrA-tag changed this ratio in favour of co-translational targeting and increased the S/N ratio by serving as degradation signal for the cytoplasmic ClpXP machinery (Truscott, Bezawork-Geleta and Dougan, 2011).

Besides inefficient co-translational targeting, we also faced the problem of periplasmic degradation of the translocated $MBP_{R8L\_S13L\_T16L}$-LgBiT fusion protein. To identify the responsible protease(s), we tested 20 different protease deficient *E.coli* strains provided by Jan-Willen de Gier from Stockholm University. In this context, another interesting finding was that deletion of *clpP* seemed to result in an increased translocation of $MBP_{-sigseq}$ to the periplasm. It also appeared that $MBP_{-sigseq}$ displayed a higher protein expression rate. The signal sequence of MBP has been suggested to slow down the folding to increase binding to the chaperone SecB for post-translational targeting (Collier *et al.*, 1988). It is conceivable that in absence of a signal sequence, the accelerated folding increases protein translation and hence protein production. Intriguingly, a mechanochemical coupling between translation and folding was recently reported whereby folding supposedly affects the translation rate (Waudby, Dobson and Christodoulou, 2019). Additionally, it has been reported that the signal sequence destabilizes MBP (Beena, Udgaonkar and Varadarajan, 2004). This could also be the contributing factor to the increased appearance of $MBP_{-sigseq}$ in the cytoplasm. It is likely that the increased accumulation of $MBP_{-sigseq}$ in the cytoplasm led to its detection in the periplasm: In these

conditions a slight lysis of the cells could result in an increased amount of $MBP_{-sigseq}$ in the periplasm.

Overall, these results indicate that MBP is not an optimal fusion partner for the purpose of a periplasmic secretion assay: Most likely the use of the signal sequence of MBP alone would have been sufficient for targeting the reporter proteins to the periplasm.

5.3.2 Tail specific protease deficient mutants would positively affect the periplasmic secretion assay by enhancing the signal

We found out that the periplasmic tail specific protease, Tsp contributes partially to the cleavage of the MBP-proteins in the periplasm in *E.coli* as well as in *Salmonella* strains. The ssrA-tag significantly increased the S/N ratio by promoting degradation of the MBP-fusion constructs in the cytoplasm, but probably also activated the quality control proteases of the periplasm. Indeed, Tsp belongs to the periplasmic proteases known to cleave proteins with a ssrA-tag (Silber, Keiler and Sauer, 1992).

The *tsp* defective strains are also known to have a reduced membrane integrity leading to increased membrane permeability to different reagents (Weski and Ehrmann, 2012). This feature could be exploited to ease processing of the samples prior to the luminescence measurement: The EDTA treatment that we performed to enhance substrate permeability was no longer required in a Δ*tsp* strain. Although a strain with a membrane defect could have been impaired in growth, we did not detect any growth defect in comparison to the wt in agreement with previous reports (Weski and Ehrmann, 2012).

Since we were only looking for the assembly of the basal body, which is attached to the inner membrane, we did not believe that outer membrane defect would in any way negatively affect the outcome of a periplasmic secretion assay. Indeed, we detected increased NanoBiT complementation in the periplasmic fraction of the Δ*tsp* mutant and thereby could conclude that secretion of InvJ was not affected at all. Hence, deletion of *tsp* in the tested mutants could enable us to clarify the roles of the different tested proteins by increasing the sensitivity of our assay.

5.3.3 Evaluation of the different NanoGlo-Kits in context of periplasmic secretion assay

To assess the various functions of the T3SS, each assay and its components had to meet different requirements. For the detection of secreted effectors into the extracellular environment it was desirable to keep the bacterial cells intact. Similarly, the injection assay needed to be adapted to detect proteins in the host cell but not in the bacteria. For monitoring injection kinetics both organisms needed to remain alive. In these cases, we were able to achieve good results and overcome the limitations posed by NLuc and NanoBiT technology by introducing small modifications like separation of bacteria and supernatant or external supplementation of DrkBiT. For the periplasmic secretion assay, we needed to render the outer membrane permeable leaving the inner cytoplasmic membrane intact. For this purpose, we had to re-evaluate the use of the different available NanoGlo detection kits.

We speculated that the NanoGlo HiBiT lytic detection system containing non-ionic detergents and a cell permeable substrate like Furimazine would behave similarly to the NanoGlo luciferase, optimized for use in mammalian cells. In contrast, the NanoGlo HiBiT extracellular kit, which presumably contains no detergents and a non-permeable substrate, should leave the outer membrane intact.

However, neither when we externally supplemented MBP-HiBiT for complementation nor when both NanoBiT proteins were endogenously expressed we detected differences between the lytic and extracellular kit. Although the extracellular kit does not contain any detergents, it is likely that the EDTA treatment prior measurements facilitated the entry of the extracellular substrate through the inner membrane and yielded an unspecific signal (Fig. 46).

Overall, the data based on external supplementation of MBP-HiBiT for complementation with periplasmic detection of periplasmic LgBiT fusion proteins led us to assume that the lytic buffer did not affect the integrity of the inner membrane (Fig. 41). However, upon supplementation of LgBiT for complementation with InvJ-HiBiT we detected a signal also into the cytoplasm (Fig. 44). This suggests that the HiBiT lytic detection system also results in lysis of bacterial cells. Alternatively, the data could indicate a size restricted entry through pores induced in the inner membrane. Cytoplasmic expression of DrkBiT or its external addition to suppress unspecific signal could be used to follow up these possibilities.

The extracellular detection system is suitable for detection of periplasmic proteins if a small complementation partner (e.g. HiBiT) is added upon EDTA destabilization of the membrane resulting in high S/N ratios (Fig. 41), but not suitable for detection of periplasmic proteins if a complementation partner as large as LgBiT is required (Fig. 44). In this case EDTA and

lysozyme treatment under osmotic conditions are helpful to separate the periplasmic fraction from the cytoplasm for luminometry of the periplasmic fraction. Separation of the periplasmic fraction for luminescence detection yielded the most conclusive results also when both NanoBiT fragments were endogenously expressed (Fig. 46 B).

What we did not yet include in our setup are long duration measurements, which would be as well important to monitor substrate secretion before and after the substrate specificity switch. We speculate that the NanoGlo live cell detection system that was used for effector injection would probably be better suited to this purpose. However, further testing is required to prove this assumption.

5.3.4 Is the secretion of early substrates dependent on various T3SS components ensuring the hierarchical secretion?

Once the technical aspects of the periplasmic secretion assay were set, we could focus on the biological perspective of the assay: The targeting of T3SS substrates to the periplasm independently of needle length control. We decided to append HiBiT to the early substrate and needle length regulator InvJ: Independently of the switching mechanism, InvJ-HiBiT was supposed to be detected in secretion competent strains. We first tested secretion of InvJ-HiBiT into the periplasm by external addition of LgBiT, afterwards by constitutively expressing $MBP_{R8L\_S13L\_T16L}$-$LgBiT^{ssrA}$ from a low copy plasmid in the bacterial cells.

We chose strains carrying either different mutations of the needle subunit protein PrgI or a complete deletion of PrgI since PrgI has been demonstrated to be dispensable for a functional export apparatus (Diepold *et al.*, 2012; Wee and Hughes, 2015). We assumed that complete deletion of the needle subunit protein PrgI could result in polar effects of the *prg* operon, and therefore we made use of additional allelic variants that either prevented PrgI translation ($PrgI_{M1K}$) or needle polymerization ($PrgI_{C\Delta10}$) (Kenjale *et al.*, 2005).

As needle elongation is proposed to open the periplasmic gate of the secretin InvG, we speculated that, in absence of a functional needle, secreted T3SS substrates could remain trapped in the barrel structure of the secretin and be unable to reach the periplasm (Hu *et al.*, 2019). Since the role of InvG is supposedly restricted to ensuring outer membrane translocation and coupling the needle to the two inner membrane rings PrgH and PrgK without affecting secretion of early substrates, we additionally deleted *invG* (Sukhan *et al.*, 2001; Schraidt *et al.*, 2010). As controls, we created secretion deficient mutants by deleting the T3SS ATPase *invC* and the export apparatus protein *invA*.

Against our expectations, mutants harbouring a single *prgI* deletion or single deletion of the last 10 aa ($PrgI_{C\Delta10}$) displayed an increased InvJ-HiBiT secretion, whereas the single or the additional deletion of *invG* in *prgI* mutant variants, reduced its secretion. Similarly, we detected a reduced signal in *prgJ* mutants. Deletion of the ATPase did not diminish InvJ-HiBiT secretion, but deletion of InvA did.

Assembly of PrgJ was long time believed to time substrate specificity switching in the so-called "timer model". The inner rod or needle adaptor is formed by only one helical turn of PrgJ, ruling out the possibility that the duration of inner rod assembly could provide the required time for needle assembly (Torres-Vargas *et al.*, 2019). Additionally, it was reported that the inner rod and the needle subunits do not assemble independently of each other. While mutations as well as a complete deletion of the molecular ruler were shown not to affect the assembly of the inner rod into the export apparatus proteins (Wee and Hughes, 2015; Torres-Vargas *et al.*, 2019), it appeared that deletion of PrgJ affected InvJ secretion to a certain extent. While Western blot analysis of the periplasmic fraction did not reveal such an effect (Wee and Hughes, 2015), the sensitive detection of the NanoBiT assay clearly showed a reduced secretion. Overexpression of PrgJ resulted as well in reduced secretion of InvJ (Wee and Hughes, 2015). It was proposed that overexpression of the early substrate PrgJ results in reduced secretion of InvJ because of competition for secretion. Consequently, secretion of InvJ should either not be affected or increase upon deletion of PrgJ. This is not what we observed. Similarly, in *Yersinia*, Diepold et al. detected reduced secretion of the molecular ruler into the periplasm in inner rod deletion strains (Diepold *et al.*, 2012). Recent data suggest that the inner rod enhances the activity of a specific peptidoglycan lytic enzyme, EtgA, which is required for the assembly of the EPEC T3SS. This ensures the tight control of EtgA activity to prevent uncontrolled lysis of the peptidoglycan layer (Burkinshaw *et al.*, 2015). It is conceivable that, even in other T3SSs, clearing of the peptidoglycan layer is required for efficient assembly of the injectisome and substrate secretion. Based on its localization and interaction with the export gate proteins, PrgJ could also exert some kind of gating function. In fact, it has been proposed that PrgJ initiates needle polymerization (Hu *et al.*, 2019). Strains with impaired needle polymerization could conceivably also display impaired needle length regulation as it was shown that elongated needles produced by overexpression of PrgI result in a reduced secretion of InvJ relative to the needle polymerization (Wee and Hughes, 2015). Consequently, the correlation between PrgI and InvJ could mean that decreased or abolished needle polymerization could conceivably result in increased InvJ secretion. Consistent with this notion, in the different *prgI* mutants we detected an increased secretion of InvJ into the periplasm.

The recruitment of the secretin InvG to the export apparatus has remained controversial. Recent interaction maps between secretin and the two inner membrane ring proteins PrgH and PrgK, as well as the secretion of PrgJ before InvG assembly favour an inside-out model whereby InvG is recruited to an already assembled export apparatus with IM ring forming proteins (Burkinshaw *et al.*, 2015; Wagner *et al.*, 2018; Torres-Vargas *et al.*, 2019). However, against our expectations, secretion of InvJ-HiBiT to the periplasm was compromised in secretin deletion strains. *In-vivo* crosslinking of SpaP-PrgJ also appeared somewhat reduced in *invG* mutants (Torres-Vargas *et al.*, 2019), indicating that deletion of *invG* could result in a phenotype similar to that observed upon deletion of *prgJ*.

Understanding how far PrgJ, PrgI and InvG regulate secretion and how the hierarchical assembly is established requires further investigation.

The energy source of the T3SS remains controversial. Several studies using artificial systems reported that the PMF is the main energy source as the secretion of different substrates occurred in an ATPase independent manner in mutants with increasing PMF (Minamino and Namba, 2008; Erhardt *et al.*, 2014). However, ATPase deficient mutants displayed only very inefficient substrate secretion. It was proposed that the activity of the ATPase is required for the release of the chaperones from the effector complex and subsequent unfolding of the effector for its insertion into the export gate (Akeda and Galán, 2005). Conversely, data also exist suggesting that the effector complexes bind directly to the export apparatus (Lara-Tejero *et al.*, 2011).

We detected an InvC-independent secretion of InvJ-HiBiT into the periplasm. InvJ as an early substrate of the T3SS does not have a cognate chaperone, conceivably simplifying its secretion through the export gate. However, we did not include a single *invC* deletion strain in the experiment. Nonetheless, the results could indicate that at the time point of early substrate secretion the cytoplasmic components such as the ATPase InvC are not required.

In conclusion, we could not investigate the role of SpaS in T3SS specificity switching, but our results indicate that this investigation is possible with the assay we developed. We did identify a needle deficient mutant that supports secretion of InvJ-HiBiT. The creation of a mutant harbouring the SpaS mutation for autonomous switching in combination with the $PrgI_{C\Delta10}$ mutation could help determine whether secretion of intermediate substrates can occur independently of needle length regulation.

6 Conclusion and outlook

By utilizing NLuc and its split variant, I was able to establish three robust, versatile, cheap, simple and quick assays to investigate different aspects of the T3SS such as secretion, injection and periplasmic localization of substrates. The different types of Nano-Glo detection Kits as well as the addition of DrkBiT facilitated the outcome of the assays. We proved that the NLuc assay is suitable for a HTP screening aimed at identifying T3SS inhibitors. Additionally, the assay enabled monitoring of secretion over time thus overcoming the limitations of previously developed assays. The periplasmic secretion assay was developed to investigate substrate specificity switching, but we ended up optimizing different technical aspects of the assay and addressing different challenges posed by the complex biological features of needle length control and substrate specificity switching.

Although we mainly focused on technical aspects, we have no doubt that the assays we developed will serve as powerful tools to address many different biological questions and advance our understanding of effector secretion hierarchy as well as effector topology and localization within host membranes and organelles. Moreover, we propose that these assays, because of their simplicity, could be used to investigate different secretion systems in other organisms.

7 Literature

Abby, S. S. and Rocha, E. P. C. (2012) 'The Non-Flagellar Type III Secretion System Evolved from the Bacterial Flagellum and Diversified into Host-Cell Adapted Systems', *PLoS Genetics*, 8(9). doi: 10.1371/journal.pgen.1002983.

Agrain, C. *et al.* (2005) 'Characterization of a Type III secretion substrate specificity switch (T3S4) domain in YscP from Yersinia enterocolitica', *Molecular Microbiology*, 56(1), pp. 54–67. doi: 10.1111/j.1365-2958.2005.04534.x.

Aizawa, S.-I. (2019) 'Flagellar Hook/Needle Length Control and Secretion Control in Type III Secretion Systems', in *Current Topics in Microbiology and Immunology*. Springer, Berlin, Heidelberg. doi: 10.1007/82_2019_169.

Akeda, Y. and Galán, J. E. (2005) 'Chaperone release and unfolding of substrates in type III secretion', *Nature*, 437(October). doi: 10.1038/nature03992.

Alakomi, H. L. *et al.* (2006) 'Weakening effect of cell permeabilizers on gram-negative bacteria causing biodeterioration', *Applied and Environmental Microbiology*, 72(7), pp. 4695–4703. doi: 10.1128/AEM.00142-06.

Amm, I., Sommer, T. and Wolf, D. H. (2013) 'Protein quality control and elimination of protein waste: The role of the ubiquitin-proteasome system', *Biochimica et Biophysica Acta - Molecular Cell Research*, 1843(1), pp. 182–96. doi: 10.1016/j.bbamcr.2013.06.031.

Antonoaea, R. *et al.* (2008) 'The periplasmic chaperone PpiD interacts with secretory proteins exiting from the SecYEG translocon', *Biochemistry*, 47(20), pp. 5649–5656. doi: 10.1021/bi800233w.

Armentrout, E. I. and Rietsch, A. (2016) 'The Type III Secretion Translocation Pore Senses Host Cell Contact', *PLoS Pathogens*, 12(3), pp. 1–20. doi: 10.1371/journal.ppat.1005530.

Arnold, R. *et al.* (2009) 'Sequence-Based Prediction of Type III Secreted Proteins', *PLoS Pathogens*, 5(4). doi: 10.1371/journal.ppat.1000376.

Auld, D. S. *et al.* (2008) 'Characterization of Chemical Libraries for Luciferase Inhibitory Activity', *Journal of Medicinal Chemistry*, 51(8), pp. 2372–2386. doi: 10.1021/jm701302v.

Auld, D. S. *et al.* (2009) 'A Basis for Reduced Chemical Library Inhibition of Firefly Luciferase Obtained from Directed Evolution', *Journal of Medicinal Chemistry*, 52(5), pp. 1450–1458. doi: 10.1021/jm8014525.

Baaden, M. and Sansom, M. S. P. (2004) 'OmpT: Molecular dynamics simulations of an outer membrane enzyme', *Biophysical Journal*. Elsevier, 87(5), pp. 2942–2953. doi: 10.1529/biophysj.104.046987.

Babic, A., Guérout, A. M. and Mazel, D. (2008) 'Construction of an improved RP4 (RK2)-based conjugative system', *Research in Microbiology*, 159, pp. 545–549. doi: 10.1016/j.resmic.2008.06.004.

Bahrani, F. K., Sansonetti, P. J. and Parsot, C. (1997) 'Secretion of Ipa proteins by Shigella flexneri: Inducer molecules and kinetics of activation', *Infection and Immunity*, 65(10), pp. 4005–4010. doi: 10.1128/iai.65.10.4005-4010.1997.

Baird, L. *et al.* (1991) 'Identification of the Escherichia coli sohB gene, a multicopy suppressor of the HtrA (DegP) null phenotype', *Journal of Bacteriology*, 173(18), pp. 5763–5770. doi: 10.1128/jb.173.18.5763-5770.1991.

Bakowski, M. A. *et al.* (2007) 'SopD acts cooperatively with SopB during Salmonella enterica serovar Typhimurium invasion', *Cellular Microbiology*, 9(12), pp. 2839–2855. doi: 10.1111/j.1462-5822.2007.01000.x.

Bange, G. *et al.* (2010) 'FlhA provides the adaptor for coordinated delivery of late flagella building blocks to the type III secretion system', *Proceedings of the National Academy of Sciences of the United States of America*, 107(25), pp. 11295–11300. doi: 10.1073/pnas.1001383107.

Beena, K., Udgaonkar, J. B. and Varadarajan, R. (2004) 'Effect of Signal Peptide on the Stability and Folding Kinetics of Maltose Binding Protein', *Biochemistry*, 43(12), pp. 3608–3619. doi: 10.1021/bi0360509.

Bergeron, J. R. C. *et al.* (2016) 'The Structure of a type 3 secretion system (T3SS) ruler protein suggests a molecular mechanism for needle length sensing', *Journal of Biological Chemistry*, 291(4), pp. 1676–1691. doi: 10.1074/jbc.M115.684423.

Bernal, I. *et al.* (2019) 'Molecular Organization of Soluble Type III Secretion System Sorting Platform Complexes', *Journal of Molecular Biology*. Elsevier Ltd, (xxxx). doi: 10.1016/j.jmb.2019.07.004.

Blaudeck, N. *et al.* (2003) 'Genetic analysis of pathway specificity during posttranslational protein translocation across the Escherichia coli plasma membrane', *Journal of Bacteriology*, 185(9), pp. 2811–2819. doi: 10.1128/JB.185.9.2811-2819.2003.

Boddicker, J. D. and Jones, B. D. (2004) 'Lon Protease Activity Causes Down-Regulation of Salmonella Pathogenicity Island 1 Invasion Gene Expression after Infection of Epithelial Cells', *Infection and Immunity*, 72(4), pp. 2002–2013. doi: 10.1128/IAI.72.4.2002-2013.2004.

Bodman, H. and Welker, N. E. (1969) 'Isolation of spheroplast membranes and stability of spheroplasts of Bacillus stearothermophilus.', *Journal of Bacteriology*, 97(2), pp. 924–935. doi: 10.1128/jb.97.2.924-935.1969.

Boyd, A. P., Lambermont, I. and Cornelis, G. R. (2000) 'Competition between the Yops of Yersinia enterocolitica for delivery into eukaryotic cells: Role of the SycE chaperone binding domain of YopE', *Journal of Bacteriology*, 182(17), pp. 4811–4821. doi: 10.1128/JB.182.17.4811-4821.2000.

Brawn, L. C., Hayward, R. D. and Koronakis, V. (2007) 'Salmonella SPI1 Effector SipA Persists after Entry and Cooperates with a SPI2 Effector to Regulate Phagosome Maturation and Intracellular Replication', *Cell Host and Microbe*. Elsevier Inc., 1(1), pp. 63–75. doi: 10.1016/j.chom.2007.02.001.

Briones, G., Hofreuter, D. and Galán, J. E. (2006) 'Cre reporter system to monitor the translocation of type III secreted proteins into host cells', *Infection and Immunity*, 74(2), pp. 1084–1090. doi: 10.1128/IAI.74.2.1084-1090.2006.

Broz, P. *et al.* (2007) 'Function and molecular architecture of the Yersinia injectisome tip complex', *Molecular Microbiology*, 65(5), pp. 1311–1320. doi: 10.1111/j.1365-2958.2007.05871.x.

Bula-Rudas, F. J., Rathore, M. H. and Maraqa, N. F. (2015) 'Salmonella Infections in Childhood', *Advances in Pediatrics*. Elsevier Inc, 62(1). doi: 10.1016/j.yapd.2015.04.005.

Burkinshaw, B. J. *et al.* (2015) 'Structural analysis of a specialized type III secretion system peptidoglycan-cleaving enzyme', *Journal of Biological Chemistry*, 290(16), pp. 10406–10417. doi: 10.1074/jbc.M115.639013.

Bustamante, V. H. *et al.* (2008) 'HilD-mediated transcriptional cross-talk between SPI-1 and SPI-2', *PNAS*, 105(38), pp. 14591–14596.

Castanheira, S. and García-del Portillo, F. (2017) 'Salmonella populations inside host cells', *Frontiers in Cellular and Infection Microbiology*, 7(OCT), pp. 1–12. doi: 10.3389/fcimb.2017.00432.

Chapman, S. *et al.* (2008) 'The photoreversible fluorescent protein iLOV outperforms GFP as a reporter of plant virus infection', *Proceedings of the National Academy of Sciences*, 105(50), pp. 20038–20043. doi: 10.1073/pnas.0807551105.

Charpentier, X. and Oswald, E. (2004) 'Identification of the Secretion and Translocation Domain of the Enteropathogenic and Enterohemorrhagic', *Journal of Bacteriology*, 186(16), pp. 5486–5495. doi: 10.1128/JB.186.16.5486.

Cherradi, Y. *et al.* (2013) 'Interplay between predicted inner-rod and gatekeeper in controlling substrate specificity of the type III secretion system', *Molecular Microbiology*, 87(6), pp. 1183–1199. doi: 10.1111/mmi.12158.

Christie, J. M. *et al.* (2012) 'Structural tuning of the fluorescent protein iLOV for improved photostability', *Journal of Biological Chemistry*, 287(26), pp. 22295–22304. doi: 10.1074/jbc.M111.318881.

Collazo, C. M. and Galán, J. E. (1997) 'The invasion-associated type III system of Salmonella typhimurium directs the translocation of Sip proteins into the host cell', *Molecular Microbiology*, 24(4), pp. 747–756. doi: 10.1046/j.1365-2958.1997.3781740.x.

Collier, D. N. *et al.* (1988) 'The antifolding activity of SecB promotes the export of the E. coli maltose-binding protein', *Cell*, 53(2), pp. 273–283. doi: 10.1016/0092-8674(88)90389-3.

Crane, J. M. and Randall, L. L. (2017) 'The Sec System: Protein Export in Escherichia coli', *EcoSal Plus*, 7(2), pp. 1–73. doi: 10.1128/ecosalplus.esp-0002-2017.

Dalbey, R. E., Wang, P. and van Dijl, J. M. (2012) 'Membrane Proteases in the Bacterial Protein Secretion and Quality Control Pathway', *Microbiology and Molecular Biology Reviews*, 76(2), pp. 311–330. doi: 10.1128/mmbr.05019-11.

Dean, P. (2011) 'Functional domains and motifs of bacterial type III effector proteins and their roles in infection', *FEMS Microbiology Reviews*, 35(6), pp. 1100–1125. doi: 10.1111/j.1574-6976.2011.00271.x.

Deane, J. E. *et al.* (2008) 'Crystal structure of Spa40, the specificity switch for the Shigella flexneri type III secretion system', *Molecular Microbiology*, 69(1), pp. 267–276. doi: 10.1111/j.1365-2958.2008.06293.x.

Deiwick, J. *et al.* (1998) 'Mutations in Salmonella pathogenicity island 2 (SPI2) genes affecting transcription of SPI1 genes and resistance to antimicrobial agents', *Journal of Bacteriology*, 180(18), pp. 4775–4780. doi: 10.1128/jb.180.18.4775-4780.1998.

Deng, W. *et al.* (2015) 'SepD/SepL-dependent secretion signals of the type III secretion system translocator proteins in enteropathogenic Escherichia coli', *Journal of Bacteriology*, 197(7), pp. 1263–1275. doi:

10.1128/JB.02401-14.

Denks, K. *et al.* (2014) 'The Sec translocon mediated protein transport in prokaryotes and eukaryotes', *Molecular Membrane Biology*. Informa Healthcare, pp. 58–84. doi: 10.3109/09687688.2014.907455.

Diepold, A. *et al.* (2010) 'Deciphering the assembly of the Yersinia type III secretion injectisome', *EMBO Journal*, 29(11), pp. 1928–1940. doi: 10.1038/emboj.2010.84.

Diepold, A. *et al.* (2012) 'Assembly of the Yersinia injectisome: The missing pieces', *Molecular Microbiology*, 85(5), pp. 878–892. doi: 10.1111/j.1365-2958.2012.08146.x.

Diepold, A. and Wagner, S. (2014) 'Assembly of the bacterial type III secretion machinery', *FEMS Microbiology Reviews*, 38(4), pp. 802–822. doi: 10.1111/1574-6976.12061.

Dietsche, T. *et al.* (2016) 'Structural and Functional Characterization of the Bacterial Type III Secretion Export Apparatus', *PLoS Pathogens*. Public Library of Science, 12(12). doi: 10.1371/journal.ppat.1006071.

Dill, K. A. *et al.* (2008) 'The Protein Folding Problem', *Annual Review of Biophys.*, 37(1), pp. 289–316. doi: 10.1038/jid.2014.371.

Dixon, A. S. *et al.* (2016) 'NanoLuc Complementation Reporter Optimized for Accurate Measurement of Protein Interactions in Cells', *ACS Chemical Biology*, 11(2), pp. 400–408. doi: 10.1021/acschembio.5b00753.

Driessen, A. J. M. and Nouwen, N. (2008) 'Protein Translocation Across the Bacterial Cytoplasmic Membrane', *Annual Review of Biochemistry*, 77(1), pp. 643–667. doi: 10.1146/annurev.biochem.77.061606.160747.

Duncan, M. C. *et al.* (2013) 'An NF-κB-based high-throughput screen identifies piericidins as inhibitors of the Yersinia pseudotuberculosis type III secretion system', *Antimicrobial Agents and Chemotherapy*, 58(2), pp. 1118–1126. doi: 10.1128/AAC.02025-13.

Edqvist, P. J. *et al.* (2003) 'YscP and YscU regulate substrate specificity of the Yersinia Type III Secretion System', *Journal of Bacteriology*, 185(7), pp. 2259–2266. doi: 10.1128/JB.185.7.2259.

Ehrbar, K. *et al.* (2004) 'InvB Is Required for Type III-Dependent Secretion of SopA in Salmonella enterica Serovar Typhimurium', *Journal of Bacteriology*, 186(4). doi: 10.1128/JB.186.4.1215-1219.2004.

Ehsani, S., Rodrigues, C. D. and Enninga, J. (2009) 'Turning on the spotlight - using light to monitor and characterize bacterial effector secretion and translocation', *Current Opinion in Microbiology*, 12(1), pp. 24–30. doi: 10.1016/j.mib.2008.11.007.

Van Engelenburg, S. B. and Palmer, A. E. (2010) 'Imaging type-III secretion reveals dynamics and spatial segregation of Salmonella effectors', *Nature Methods*, 7(4), pp. 325–330. doi: 10.1038/nmeth.1437.

England, C. G., Ehlerding, E. B. and Cai, W. (2016) 'NanoLuc: A Small Luciferase is Brightening up the Field of Bioluminescence', *Bioconjugate Chemistry*, 27(5), pp. 1175–1187. doi: 10.1021/acs.bioconjchem.6b00112.NanoLuc.

Enninga, J. *et al.* (2005) 'Secretion of type III effectors into host cells in real time', *Nature Methods*, 2(12), pp. 959–965. doi: 19.1038/NMETH804.

Epler, C. R. *et al.* (2012) 'Ultrastructural analysis of IpaD at the tip of the nascent MxiH type III secretion

apparatus of Shigella flexneri', *Journal of Molecular Biology*. Elsevier Ltd, 420(1–2), pp. 29–39. doi: 10.1016/j.jmb.2012.03.025.

Erhardt, M. *et al.* (2010) 'The role of the FliK molecular ruler in hook-length control in Salmonella enterica', *Molecular Microbiology*, 75(5), pp. 1272–1284. doi: 10.1111/j.1365-2958.2010.07050.x.

Erhardt, M. *et al.* (2011) 'An infrequent molecular ruler controls flagellar hook length in Salmonella enterica', *EMBO Journal*. Nature Publishing Group, 30(14), pp. 2948–2961. doi: 10.1038/emboj.2011.185.

Erhardt, M. *et al.* (2014) 'ATPase-Independent Type-III Protein Secretion in Salmonella enterica', *PLoS Genetics*. Public Library of Science, 10(11). doi: 10.1371/journal.pgen.1004800.

Fàbrega, A. and Vila, J. (2013) 'Salmonella enterica serovar Typhimurium skills to succeed in the host: Virulence and regulation', *Clinical Microbiology Reviews*, 26(2). doi: 10.1128/CMR.00066-12.

Fan, F. and Wood, K. V. (2007) 'Bioluminescent Assays for High-Throughput Screening', *ASSAY and Drug Development Technologies*, 5(1), pp. 127–136. doi: 10.1089/adt.2006.053.

Farrell, C. M., Grossman, A. D. and Sauer, R. T. (2005) 'Cytoplasmic degradation of ssrA-tagged proteins', *Molecular Microbiology*, 57(6), pp. 1750–1761. doi: 10.1111/j.1365-2958.2005.04798.x.

Fass, E. and Groisman, E. A. (2009) 'Control of Salmonella pathogenicity island-2 gene expression Ephraim', *Current Opinion in Microbiology*, 23(1), pp. 1–7. doi: 10.1038/jid.2014.371.

Fereja, T. H., Hymete, A. and Gunasekaran, T. (2013) 'A Recent Review on Chemiluminescence Reaction, Principle and Application on Pharmaceutical Analysis', *ISRN Spectroscopy*, pp. 1–12. doi: 10.1155/2013/230858.

Ferris, H. U. *et al.* (2005) 'FlhB regulates ordered export of flagellar components via autocleavage mechanism', *Journal of Biological Chemistry*, 280(50), pp. 41236–41242. doi: 10.1074/jbc.M509438200.

Ferris, H. U. and Minamino, T. (2006) 'Flipping the switch: bringing order to flagellar assembly', *Trends in Microbiology*, 14(12), pp. 519–526. doi: 10.1016/j.tim.2006.10.006.

Finch, P. W. *et al.* (1981) 'Complete nudeotide seqnence of the Escherichia coti ptr gene encoding Protease III', *Nucleic Acids Research*, 9(19), pp. 2589–2598.

Finn, C. E. *et al.* (2017) 'A second wave of Salmonella T3SS1 activity prolongs the lifespan of infected epithelial cells', *PLoS Pathogens*, 13(4), pp. 1–28. doi: 10.1371/journal.ppat.1006354.

Frees, D. *et al.* (2007) 'Clp ATPases and ClpP proteolytic complexes regulate vital biological processes in low GC, Gram-positive bacteria', *Molecular Microbiology*, 63(5), pp. 1285–1295. doi: 10.1111/j.1365-2958.2007.05598.x.

Freudl, R. (2018) 'Signal peptides for recombinant protein secretion in bacterial expression systems', *Microbial Cell Factories*. doi: 10.1186/s12934-018-0901-3.

Frost, S. *et al.* (2012) 'Autoproteolysis and Intramolecular Dissociation of Yersinia YscU Precedes Secretion of Its C-Terminal Polypeptide YscUCC', *PLoS ONE*, 7(11). doi: 10.1371/journal.pone.0049349.

Fu, Y. and Galán, J. E. (1999) 'A Salmonella protein antagonizes Rac-1 and Cdc42 to mediate host-cell recovery

after bacterial invasion', *Nature*, 401(6750), pp. 293–297. doi: 10.1038/45829.

Galán, J. E. (2001) 'Salmonella Interactions with Host Cells: Type III Secretion at Work', *Cell*, 17.

Galán, J. E. (2008) 'Energizing type III secretion machines : what is the fuel ?', 15(2), pp. 127–128.

Galán, J. E. *et al.* (2014) 'Bacterial Type III Secretion Systems : Specialized Nanomachines for Protein Delivery into Target Cells', *Annual Review of Microbiology*, (June), pp. 415–438. doi: 10.1146/annurev-micro-092412-155725.

Galán, J. E. and Waksman, G. (2018) 'Protein-Injection Machines in Bacteria', *Cell*, 172(6), pp. 1306–1318. doi: 10.1016/j.cell.2018.01.034.

Gao, X. *et al.* (2018) 'Structural insight into conformational changes induced by ATP binding in a type III secretion-associated ATPase from Shigella flexneri', *Frontiers in Microbiology*. Frontiers Media S.A., 9(1468). doi: 10.3389/fmicb.2018.01468.

García-Gómez, E. *et al.* (2011) 'The muramidase EtgA from enteropathogenic Escherichia coli is required for efficient type III secretion', *Microbiology*, 157(4), pp. 1145–1160. doi: 10.1099/mic.0.045617-0.

Gawthorne, J. A. *et al.* (2012) 'Express Your LOV: An Engineered Flavoprotein as a Reporter for Protein Expression and Purification', *PLoS ONE*, 7(12), pp. 1–6. doi: 10.1371/journal.pone.0052962.

Gawthorne, J. A. *et al.* (2016) 'Visualizing the Translocation and Localization of Bacterial Type III Effector Proteins by Using a Genetically Encoded Reporter System', *Applied and Environmental Microbiology*. American Society for Microbiology, 82(9), pp. 2700–2708. doi: 10.1128/aem.03418-15.

Gibson, D. G. *et al.* (2009) 'Enzymatic assembly of DNA molecules up to several hundred kilobases', *Nature Methods*, 6(5), pp. 343–345. doi: 10.1038/nmeth.1318.

Goodkind, M. J. and Harvey, E. N. (1952) 'Preliminary studies on oxygen consumption of luminous bacteria made with the oxygen electrode', *Journal of cellular and comparative physiology*, 39(1), pp. 45–56.

Gordon, M. A. (2008) 'Salmonella infections in immunocompromised adults', *Journal of Infection*, 56(6), pp. 413–422. doi: 10.1016/j.jinf.2008.03.012.

Green, A. A. and McElroy, W. D. (1956) 'Crystalline Firefly Luciferase', *Biochimica et Biophysica Acta*, 20(1), pp. 170–176. doi: 10.1016/0006-3002(56)90275-x.

Green, E. R. and Mecsas, J. (2016) 'Bacterial Secretion Systems: An Overview', *Microbiology Spectrum*, 4(1), pp. 1–19. doi: 10.1128/microbiolspec.vmbf-0012-2015.

Guo, R. *et al.* (2016) 'Steric trapping reveals a cooperativity network in the intramembrane protease GlpG', *Nature Chemical Biology*, 12(5), pp. 353–360. doi: 10.1038/nchembio.2048.

Hall, M. P. *et al.* (2012) 'Engineered luciferase reporter from a deep sea shrimp utilizing a novel imidazopyrazinone substrate', *ACS Chemical Biology*, 7(11), pp. 1848–1857. doi: 10.1021/cb3002478.

Haraga, A., Ohlson, M. B. and Miller, S. I. (2008) 'Salmonellae interplay with host cells', *Nature Reviews Microbiology*, 6(1). doi: 10.1038/nrmicro1788.

Hardt, W. D. *et al.* (1998) 'S. typhimurium Encodes an activator of Rho GTPases that induces membrane ruffling and nuclear responses in host cells', *Cell*, 93(5), pp. 815–826. doi: 10.1016/S0092-8674(00)81442-7.

Hardy, S. J. S. and Randall, L. L. (1991) 'A kinetic partitioning model of selective binding of nonnative proteins by the bacterial chaperone SecB', *Science*, 251(4992), pp. 439–443. doi: 10.1126/science.1989077.

Harmon, D. E. *et al.* (2010) 'Identification and characterization of small-molecule inhibitors of Yop translocation in Yersinia pseudotuberculosis', *Antimicrobial Agents and Chemotherapy*, 54(8), pp. 3241–3254. doi: 10.1128/AAC.00364-10.

Harms, N. *et al.* (2001) 'The Early Interaction of the Outer Membrane Protein PhoE with the Periplasmic Chaperone Skp Occurs at the Cytoplasmic Membrane', *Journal of Biological Chemistry*, 276(22), pp. 18804–18811. doi: 10.1074/jbc.M011194200.

Hayward, R. D. *et al.* (2005) 'Cholesterol binding by the bacterial type III translocon is essential for virulence effector delivery into mammalian cells', *Molecular Microbiology*, 56(3), pp. 590–603. doi: 10.1111/j.1365-2958.2005.04568.x.

Helaine, S. *et al.* (2014) 'Internalization of salmonella by macrophages induces formation of nonreplicating persisters', *Science*, 343(6167), pp. 204–208. doi: 10.1126/science.1244705.

Hessa, T. *et al.* (2007) 'Molecular code for transmembrane-helix recognition by the Sec61 translocon', *Nature*, 450(7172), pp. 1026–1030. doi: 10.1038/nature06387.

Hirano, T. *et al.* (1994) 'Roles of FliK and FlhB in determination of flagellar hook length in Salmonella typhimurium', *Journal of Bacteriology*, 176(17), pp. 5439–5449. doi: 10.1128/jb.176.17.5439-5449.1994.

Ho, O. *et al.* (2017) 'Characterization of the ruler protein interaction interface on the substrate specificity switch protein in the Yersinia type III secretion system', *Journal of Biological Chemistry*, 292(8), pp. 3299–3311. doi: 10.1074/jbc.M116.770255.

Ho, P. *et al.* (2013) 'Reporter Enzyme Inhibitor Study To Aid Assembly of Orthogonal Reporter Gene Assays', *ACS Chemical Biology*, 8(5), pp. 1009–1017. doi: 10.1021/cb3007264.

Hobbie, S. *et al.* (1997) 'lnvolvement of Mitogen-Activated Protein Kinase Pathways in the Nuclear Responses and Cytokine Production Induced by Salmonella typhimurium in Cultured Intestinal Epithelial Cells', 159. doi: 10.4049/jimmunol.1201393.

Hoiseth, S. K. and Stocker, B. A. D. (1981) 'Aromatic-dependent Salmonella typhimurium are non-virulent and effective as live vaccines', *Nature*, 291(May), pp. 238–239.

Horibe, T. *et al.* (2018) 'Evaluation of chemical chaperones based on the monitoring of Bip promoter activity and visualization of extracellular vesicles by real-time bioluminescence imaging', *Luminescence*, 33(1), pp. 249–255. doi: 10.1002/bio.3388.

Hu, B. *et al.* (2015) 'Visualization of the type III secretion sorting platform of Shigella flexneri', *Proceedings of the National Academy of Sciences of the United States of America*, 112(4), pp. 1047–1052. doi: 10.1073/pnas.1411610112.

Hu, J. *et al.* (2019) 'T3S injectisome needle complex structures in four distinct states reveal the basis of

membrane coupling and assembly', *Nature Microbiology*. Springer US. doi: 10.1038/s41564-019-0545-z.

Hu, J., Worrall, L. J. and Strynadka, N. C. (2020) 'Towards capture of dynamic assembly and action of the T3SS at near atomic resolution', *Current Opinion in Structural Biology*. Elsevier Ltd, 61, pp. 71–78. doi: 10.1016/j.sbi.2019.10.005.

Huber, D. *et al.* (2017) 'SecA Cotranslationally Interacts with Nascent Substrate Proteins In Vivo Damon', *Journal of Bacteriology*, 199(2), pp. 1–14.

Hueck, C. J. (1998) 'Type III protein secretion systems in bacterial pathogens of animals and plants.', *Microbiology and molecular biology reviews : MMBR*, 62(2), pp. 379–433. doi: 10.1111/j.1365-2958.2006.05301.x.

Ide, T. *et al.* (2003) 'Differential Modulation by Ca2+ of Type III Secretion of Diffusely Adhering Enteropathogenic Escherichia coli', *Infection and Immunity*, 71(4), pp. 1725–1732. doi: 10.1128/IAI.71.4.1725.

Ilyas, B., Tsai, C. N. and Coombes, B. K. (2017) 'Evolution of Salmonella-host cell interactions through a dynamic bacterial genome', *Frontiers in Cellular and Infection Microbiology*, 7(SEP). doi: 10.3389/fcimb.2017.00428.

Imada, K. *et al.* (2016) 'Insight into the flagella type III export revealed by the complex structure of the type III ATPase and its regulator', *Proceedings of the National Academy of Sciences of the United States of America*, 113(13), pp. 3633–3638. doi: 10.1073/pnas.1524025113.

Inouye, S. *et al.* (2000) 'Secretional luciferase of the luminous shrimp Oplophorus gracilirostris: cDNA cloning of a novel imidazopyrazinone luciferase', *FEBS Letters*, 481(April 1999), pp. 19–25.

Inouye, S. *et al.* (2013) 'C6-Deoxy coelenterazine analogues as an efficient substrate for glow luminescence reaction of nanoKAZ: The mutated catalytic 19kDa component of Oplophorus luciferase', *Biochemical and Biophysical Research Communications*. Elsevier Inc., 437(1), pp. 23–28. doi: 10.1016/j.bbrc.2013.06.026.

Ishikawa, S. *et al.* (1998) 'Regulation of a new cell wall hydrolase gene, cwlF, which affects cell separation in Bacillus subtilis', *Journal of Bacteriology*, 180(9), pp. 2549–2555. doi: 10.1128/jb.180.9.2549-2555.1998.

Iversen, P. W. *et al.* (2012) 'HTS Assay Validation', in Sittampalam, G. S. et al. (eds) *Assay Guidance Manual*. NCATS, pp. 1–31. Available at: http://www.ncbi.nlm.nih.gov/pubmed/22553862.

Iwanczyk, J. *et al.* (2007) 'Role of the PDZ domains in Escherichia coli DegP protein', *Journal of Bacteriology*, 189(8), pp. 3176–3186. doi: 10.1128/JB.01788-06.

Jaumouillé, V. *et al.* (2008) 'Cytoplasmic targeting of IpaC to the bacterial pole directs polar type III secretion in Shigella', *EMBO Journal*, 27(2), pp. 447–457. doi: 10.1038/sj.emboj.7601976.

Jentsch, S. (1996) 'When proteins receive deadly messages at birth', *Science*, 271(5251), pp. 955–956. doi: 10.1126/science.271.5251.955.

Journet, L. *et al.* (2003) 'The Needle Length of Bacterial Injectisomes Is Determined by a Molecular Ruler', *Science*, 302(5651), pp. 1757–1760. doi: 10.1126/science.1091422.

Kanemori, M., Yanagi, H. and Yura, T. (1999) 'The ATP-dependent HslVU/ClpQY protease participates in

turnover of cell division inhibitor SulA in Escherichia coli', *Journal of Bacteriology*, 181(12), pp. 3674–3680. doi: 10.1128/jb.181.12.3674-3680.1999.

Kaniga, K., Bossio, J. C. and Galán, J. E. (1994) 'The Salmonella typhimurium invasion genes invF and invG encode homologues of the AraC and PulD family of proteins', *Molecular Microbiology*, 13(4), pp. 555–568. doi: 10.1111/j.1365-2958.1994.tb00450.x.

Kaniga, K., Trollinger, D. and Galan, J. E. (1995) 'Identification of two targets of the type III protein secretion system encoded by the inv and spa loci of Salmonella typhimurium that have homology to the Shigella IpaD and IpaA proteins', *Journal of Bacteriology*, 177(24), pp. 7078–7085. doi: 10.1128/jb.177.24.7078-7085.1995.

Kato, J. *et al.* (2018) 'A protein secreted by the salmonella type iii secretion system controls needle filament assembly', *eLife*, 7, pp. 1–23. doi: 10.7554/eLife.35886.

Kato, J., Lefebre, M. and Galán, J. E. (2015) 'Structural Features Reminiscent of ATP-Driven Protein Translocases Are Essential for the Function of a Type III Secretion-Associated ATPase', *Journal of Bacteriology*. American Society for Microbiology, 197(18), pp. 3007–3014. doi: 10.1128/jb.00434-15.

Keiler, K. C., Waller, P. R. H. and Sauer, R. T. (1996) 'Role of a peptide tagging system in degradation of proteins synthesized from damaged messenger RNA', *Science*, 271(5251), pp. 990–993. doi: 10.1126/science.271.5251.990.

Kenjale, R. *et al.* (2005) 'The needle component of the type III secreton of Shigella regulates the activity of the secretion apparatus', *Journal of Biological Chemistry*, 280(52), pp. 42929–42937. doi: 10.1074/jbc.M508377200.

Kim, B. H. *et al.* (2007) 'Analysis of functional domains present in the N-terminus of the SipB protein', *Microbiology*, 153(9), pp. 2998–3008. doi: 10.1099/mic.0.2007/007872-0.

Kim, J. S. *et al.* (2013) 'Molecular characterization of the InvE regulator in the secretion of type III secretion translocases in Salmonella enterica serovar Typhimurium', *Microbiology (United Kingdom)*, 159(PART3), pp. 446–461. doi: 10.1099/mic.0.061689-0.

Kimbrough, T. G. and Miller, S. I. (2000) 'Contribution of Salmonella typhimurium type III secretion components to needle complex formation', *Proceedings of the National Academy of Sciences of the United States of America*, 97(20), pp. 11008–11013. doi: 10.1073/pnas.200209497.

Kinoshita, M. *et al.* (2013) 'Interactions of bacterial flagellar chaperone-substrate complexes with FlhA contribute to co-ordinating assembly of the flagellar filament', *Molecular Microbiology*, 90(6), pp. 1249–1261. doi: 10.1111/mmi.12430.

Kinoshita, M. *et al.* (2017) 'The role of intrinsically disordered C-terminal region of FliK in substrate specificity switching of the bacterial flagellar type III export apparatus', *Molecular Microbiology*, 105(4), pp. 572–588. doi: 10.1111/mmi.13718.

Kinoshita, M. *et al.* (2020) 'The flexible linker of the secreted FliK ruler is required for export switching of the flagellar protein export apparatus', *Scientific Reports*, 10(1), pp. 1–12. doi: 10.1038/s41598-020-57782-5.

Kovačić, F. *et al.* (2013) 'Structural and Functional Characterisation of TesA - A Novel Lysophospholipase A

from Pseudomonas aeruginosa', *PLoS ONE*, 8(7), pp. 1–12. doi: 10.1371/journal.pone.0069125.

Kramer, R. A., Dekker, N. and Egmond, M. R. (2000) 'Identification of active site serine and histidine residues in Escherichia coli outer membrane protease OmpT', *FEBS Letters*, 468(2–3), pp. 220–224. doi: 10.1016/S0014-5793(00)01231-X.

Krampen, L. *et al.* (2018) 'Revealing the mechanisms of membrane protein export by virulence-associated bacterial secretion systems', *Nature Communications*. Springer US, 9(1). doi: 10.1038/s41467-018-05969-w.

Kubori, T. *et al.* (2000) 'Molecular characterization and assembly of the needle complex of the Salmonella typhimurium type III protein secretion system', *Proceedings of the National Academy of Sciences of the United States of America*, 97(18), pp. 10225–10230. doi: 10.1073/pnas.170128997.

Kubori, T. and Galán, J. E. (2002) 'Salmonella type III secretion-associated protein InvE controls translocation of effector proteins into host cells.', *Journal of Bacteriology*, 184(17). doi: 10.1128/JB.184.17.4699.

Kuhlen, L. *et al.* (2018) 'Structure of the core of the type iii secretion system export apparatus', *Nature Structural and Molecular Biology*. Nature Publishing Group, 25(7). doi: 10.1038/s41594-018-0086-9.

Kuhlen, L. *et al.* (2020) 'The substrate specificity switch FlhB assembles onto the export gate to regulate type three secretion', *Nature Communications*. Springer US, 11(1), pp. 1–10. doi: 10.1038/s41467-020-15071-9.

Kuo, M. M.-C. *et al.* (2007) 'Patch Clamp and Phenotypic Analyses of a Prokaryotic Cyclic Nucleotide-gated K+ Channel Using Escherichia coli as a Host', *Journal of Biological Chemistry*, 282(33), pp. 24294–24301. doi: 10.1161/CIRCULATIONAHA.110.956839.

Kuroda, A. *et al.* (2001) 'Role of inorganic polyphosphate in promoting ribosomal protein degradation by the Lon protease in E. coli', *Science*, 293(5530), pp. 705–708. doi: 10.1126/science.1061315.

Kutsukake, K., Minamino, T. and Yokoseki, T. (1994) 'Isolation and characterization of FliK-independent flagellation mutants from Salmonella typhimurium', *Journal of Bacteriology*, 176(24), pp. 7625–7629. doi: 10.1128/jb.176.24.7625-7629.1994.

Lafont, F. *et al.* (2002) 'Initial steps of Shigella infection depend on the cholesterol / sphingolipid raft-mediated CD44 ± IpaB interaction', *EMBO Journal*, 21(17), pp. 4449–4457.

Lara-Tejero, M. *et al.* (2011) 'A sorting platform determines the order of protein secretion in Bacterial Type III Systems', *Science*, 331(6021). doi: 10.1126/science.1201476.A.

Lara-Tejero, M. and Galán, J. E. (2009) 'Salmonella enterica serovar Typhimurium pathogenicity island 1-encoded type III secretion system translocases mediate intimate attachment to nonphagocytic cells', *Infection and Immunity*, 77(7), pp. 2635–2642. doi: 10.1128/IAI.00077-09.

Lavander, M. *et al.* (2002) 'Proteolytic cleavage of the FlhB homologue YscU of Yersinia pseudotuberculosis is essential for bacterial survival but not for type III secretion', *Journal of Bacteriology*, 184(16), pp. 4500–4509. doi: 10.1128/JB.184.16.4500-4509.2002.

Leach, F. R. and Webster, J. J. (1986) 'Commercially Available Firefly Luciferase Reagents', in Marlene A. DeLuca, W. D. M. (ed.) *Methods in Enzymology*, pp. 51–70.

Lee, P.-C. P.-C. C. *et al.* (2014) 'Control of type III secretion activity and substrate specificity by the cytoplasmic regulator PcrG', *Proceedings of the National Academy of Sciences*. Proceedings of the National Academy of Sciences, 111(19), pp. E2027–E2036. doi: 10.1073/pnas.1402658111.

Lee, P.-C. and Rietsch, A. (2015) 'Fueling type III secretion', *Trends in Microbiology*. Elsevier Ltd, pp. 296–300. doi: 10.1016/j.tim.2015.01.012.

Lee, S. H. and Galán, J. E. (2004) 'Salmonella type III secretion-associated chaperones confer secretion-pathway specificity', *Molecular Microbiology*, 51(2), pp. 483–495. doi: 10.1046/j.1365-2958.2003.03840.x.

Lefebre, M. D. and Gálan, J. E. (2014) 'The inner rod protein controls substrate switching and needle length in a Salmonella type III secretion system', *Proceedings of the National Academy of Sciences of the United States of America*, 111(2), pp. 817–822. doi: 10.1073/pnas.1319698111.

Lloyd, S. A. *et al.* (2001) 'Yersinia YopE is targeted for type III secretion by N-terminal, not mRNA, signals', *Molecular Microbiology*, 39(2), pp. 520–531. doi: 10.1046/j.1365-2958.2001.02271.x.

Lombardi, C. *et al.* (2019) 'Structural and functional characterization of the type three secretion system (T3SS) needle of pseudomonas aeruginosa', *Frontiers in Microbiology*, 10(MAR). doi: 10.3389/fmicb.2019.00573.

Lorenz, W. W. *et al.* (1991) 'Isolation and expression of a cDNA encoding Renilla reniformis luciferase.', *Proceedings of the National Academy of Sciences*, 88(10), pp. 4438–4442. doi: 10.1073/pnas.88.10.4438.

Lou, L. *et al.* (2019) 'Salmonella Pathogenicity Island 1 (SPI-1) and Its Complex Regulatory Network', *Frontiers in Cellular and Infection Microbiology*, 9(July), pp. 1–12. doi: 10.3389/fcimb.2019.00270.

Lucas, R. L. *et al.* (2000) 'Multiple factors independently regulate hilA and invasion gene expression in Salmonella enterica serovar typhimurium', *Journal of Bacteriology*, 182(7), pp. 1872–1882. doi: 10.1128/JB.182.7.1872-1882.2000.

Lütticke, C. *et al.* (2012) 'E. coli LoiP (YggG), a metalloprotease hydrolyzing Phe-Phe bonds', *Molecular BioSystems*, 8(6), pp. 1775–1782. doi: 10.1039/c2mb05506f.

Maffei, B., Francetic, O. and Subtil, A. (2017) 'Tracking Proteins Secreted by Bacteria: What's in the Toolbox?', *Frontiers in Cellular and Infection Microbiology*, 7(May), pp. 1–17. doi: 10.3389/fcimb.2017.00221.

Majowicz, S. E. *et al.* (2010) 'The Global Burden of Nontyphoidal Salmonella Gastroenteritis', *Clinical Infectious Diseases*, 50(6), pp. 882–889. doi: 10.1086/650733.

Malet, H. *et al.* (2012) 'Newly folded substrates inside the molecular cage of the HtrA chaperone DegQ', *Nature Structural and Molecular Biology*, 19(2), pp. 152–157. doi: 10.1038/nsmb.2210.

Mallo, G. V. *et al.* (2008) 'SopB promotes phosphatidylinositol 3-phosphate formation on Salmonella vacuoles by recruiting Rab5 and Vps34', *Journal of Cell Biology*, 182(4), pp. 741–752. doi: 10.1083/jcb.200804131.

Marlovits, T. C. *et al.* (2006) 'Assembly of the inner rod determines needle length in the type III secretion injectisome', *Nature*, 441(6). doi: 10.1038/nature04822.

McElroy, W. D. and Ballentine, R. (1944) 'The Mechanism Of Bioluminescence', *PNAS*, 30(12), pp. 377–382. doi: 10.1210/endo-63-5-707.

McGhie, E. J., Hayward, R. D. and Koronakis, V. (2001) ‘Cooperation between actin-binding proteins of invasive Salmonella: SipA potentiates SipC nucleation and bundling of actin’, *EMBO Journal*, 20(9), pp. 2131–2139. doi: 10.1093/emboj/20.9.2131.

McGhie, E. J., Hayward, R. D. and Koronakis, V. (2004) ‘Control of actin turnover by a Salmonella invasion protein’, *Molecular Cell*. doi: 10.1016/S1097-2765(04)00053-X.

McIntosh, A. *et al.* (2017) ‘SipA Activation of Caspase-3 Is a Decisive Mediator of Host Cell Survival at Early Stages of Salmonella enterica Serovar Typhimurium Infection’, *Infection and Immunity*, 85(9), pp. 1–14. doi: 10.1128/iai.00393-17.

McShan, A. C. *et al.* (2017) ‘NMR identification of the binding surfaces involved in the Salmonella and Shigella Type III secretion tip-translocon protein–protein interactions’, *Proteins: Structure, Function and Bioinformatics*, 84(8), pp. 1097–1107. doi: 10.1002/prot.25055.

Merdanovic, M. *et al.* (2011) ‘Protein quality control in the bacterial periplasm’, *Microbial Cell Factories*, 65, pp. 149–68. doi: 10.1146/annurev-micro-090110-102925.

Michelini, E. *et al.* (2008) ‘Combining intracellular and secreted bioluminescent reporter proteins for multicolor cell-based assays’, *Photochemical and Photobiological Sciences*, 7(2), pp. 146–158. doi: 10.1039/b719181b.

Mills, E. *et al.* (2008) ‘Real-Time Analysis of Effector Translocation by the Type III Secretion System of Enteropathogenic Escherichia coli’, *Cell Host and Microbe*, 3(2), pp. 104–113. doi: 10.1016/j.chom.2007.11.007.

Minamino, T. *et al.* (2004) ‘Domain organization and function of Salmonella FliK, a flagellar hook-length control protein’, *Journal of Molecular Biology*, 341(2), pp. 491–502. doi: 10.1016/j.jmb.2004.06.012.

Minamino, T. *et al.* (2012) ‘Interaction between FliI ATPase and a flagellar chaperone FliT during bacterial flagellar protein export’, *Molecular Microbiology*, 83(1), pp. 168–178. doi: 10.1111/j.1365-2958.2011.07924.x.

Minamino, T. *et al.* (2014) ‘The bacterial flagellar protein export apparatus processively transports flagellar proteins even with extremely infrequent ATP hydrolysis’, *Scientific Reports*. Nature Publishing Group, 4. doi: 10.1038/srep07579.

Minamino, T. *et al.* (2016) ‘The Bacterial Flagellar Type III Export Gate Complex Is a Dual Fuel Engine That Can Use Both H+ and Na+ for Flagellar Protein Export’, *PLoS Pathogens*. Public Library of Science, 12(3). doi: 10.1371/journal.ppat.1005495.

Minamino, T. and Macnab, R. M. (2000) ‘Domain Structure of Salmonella FlhB, a Flagellar Export Component Responsible for Substrate Specificity Switching’, *JOURNAL OF BACTERIOLOGY*, 182(17), pp. 4906–4914. Available at: http://jb.asm.org/.

Minamino, T. and Namba, K. (2008) ‘Distinct roles of the FliI ATPase and proton motive force in bacterial flagellar protein export’, *Nature*. Nature Publishing Group, 451(7177), pp. 485–488. doi: 10.1038/nature06449.

Miot, M. and Betton, J.-M. (2004) ‘Protein quality control in the bacterial periplasm’, *Microbial Cell Factories*, 3(4), pp. 121–134. doi: 10.1186/1475-2859-3-4.

Monjarás Feria, J. V. *et al.* (2015) ‘Role of Autocleavage in the Function of a Type III Secretion Specificity

Switch Protein in Salmonella enterica Serovar Typhimurium', *mBio*, 6(5), pp. 1–8. doi: 10.1128/mbio.01459-15.

Mueller, C. A. *et al.* (2005) 'The V-antigen of Yersinia forms a distinct structure at the tip of injectisome needles', *Science*, 310(5748), pp. 674–676. doi: 10.1126/science.1118476.

Nakajima, Y. *et al.* (2004) 'cDNA Cloning and Characterization of a Secreted Luciferase from the Luminous Japanese Ostracod , Cypridina noctiluca', *Bioscience, Biotechnology, and Biochemistry*, 68(3), pp. 565–570.

Natale, P., Brüser, T. and Driessen, A. J. M. (2008) 'Sec- and Tat-mediated protein secretion across the bacterial cytoplasmic membrane-Distinct translocases and mechanisms', *Biochimica et Biophysica Acta - Biomembranes*, 1778(9), pp. 1735–1756. doi: 10.1016/j.bbamem.2007.07.015.

Natarajan, J. *et al.* (2020) 'Yeast can express and assemble bacterial secretins in the mitochondrial outer membrane', *Microbial Cell*, 7(1), pp. 15–27. doi: 10.15698/mic2020.01.703.

De Nisco, N. J., Rivera-Cancel, G. and Orth, K. (2018) 'The Biochemistry of Sensing: Enteric Pathogens Regulate Type III Secretion in Response to Environmental and Host Cues', *mBio*, 9(1), pp. 1–15. doi: 10.1128/mbio.02122-17.

Notti, R. Q. and Stebbins, C. . E. (2016) 'The Structure and Function of Type III Secretion Systems', *Microbiology Spectrum*, 4(1). doi: 10.1128/microbiolspec.VMBF-0004-2015.

Olivares, A. O., Baker, T. A. and Sauer, R. T. (2016) 'Mechanistic insights into bacterial AAA+ proteases and protein- remodelling machines', *Nature Reviews Microbiology*, 14(1), pp. 33–44. doi: 10.1038/nrmicro.2015.4.

Olivares, A. O., Baker, T. A. and Sauer, R. T. (2018) 'Mechanical Protein Unfolding and Degradation', *Annual Review of Physiology*, 80(1), pp. 413–429. doi: 10.1146/annurev-physiol-021317-121303.

Palmer, A. D., Kim, K. and Slauch, J. M. (2019) 'PhoP-Mediated Repression of the SPI1 Type 3 Secretion System in Salmonella enterica Serovar Typhimurium', *Journal of Bacteriology*, 201(16), pp. 1–15.

Park, S. *et al.* (1988) 'Modulation of folding pathways of exported proteins by the leader sequence', *Science*, 239(4843), pp. 1033–1035. doi: 10.1126/science.3278378.

Paul, K. *et al.* (2008) 'Energy source of flagellar type III secretion', *Nature*. Nature Publishing Group, 451(7177), pp. 489–492. doi: 10.1038/nature06497.

Piscatelli, H. L., Li, M. and Zhou, D. (2016) 'Dual 4- and 5-phosphatase activities regulate SopB-dependent phosphoinositide dynamics to promote bacterial entry', *Cellular Microbiology*, 18(5), pp. 705–719. doi: 10.1111/cmi.12542.

Portaliou, A. G. *et al.* (2017) ' Hierarchical protein targeting and secretion is controlled by an affinity switch in the type III secretion system of enteropathogenic Escherichia coli ', *The EMBO Journal*, 36(23), pp. 3517–3531. doi: 10.15252/embj.201797515.

Que, F., Wu, S. and Huang, R. (2013) 'Salmonella pathogenicity Island 1(SPI-1) at work', *Current Microbiology*, 66(6), pp. 582–587. doi: 10.1007/s00284-013-0307-8.

Radics, J., Königsmaier, L. and Marlovits, T. C. (2014) 'Structure of a pathogenic type 3 secretion system in action', *Nature Structural and Molecular Biology*, 21(1), pp. 82–87. doi: 10.1038/nsmb.2722.

Raffatellu, M. *et al.* (2004) 'SipA, SopA, SopB, SopD, and SopE2 Contribute to Salmonella enterica Serotype Typhimurium Invasion of Epithelial Cells', *Infection and Immunity*, 73(1), pp. 146–154. doi: 10.1128/iai.73.1.146-154.2005.

Ramachandran, R. *et al.* (2002) 'Functional interactions of HslV (ClpQ) with the atpase HslU (ClpY)', *Proceedings of the National Academy of Sciences of the United States of America*, 99(11), pp. 7396–7401. doi: 10.1073/pnas.102188799.

Ramamurthi, K. S. and Schneewind, O. (2003) 'Substrate recognition by the Yersinia type III protein secretion machinery', *Molecular Microbiology*, 50(4), pp. 1095–1102. doi: 10.1046/j.1365-2958.2003.03777.x.

Ramos-Morales, F. (2012) 'Impact of Salmonella enterica Type III Secretion System Effectors on the Eukaryotic Host Cell', *ISRN Cell Biology*, 2012, pp. 1–36. doi: 10.5402/2012/787934.

Riordan, K. E. and Schneewind, O. (2008) 'YscU cleavage and the assembly of Yersinia type III secretion machine complexes', *Molecular Microbiology*, 68(6), pp. 1485–1501. doi: 10.1111/j.1365-2958.2008.06247.x.

Rüter, C. and Schmidt, M. A. (2016) 'Cell-Penetrating Bacterial Effector Proteins: Better Tools than Targets', *Trends in Biotechnology*. Elsevier Ltd, 35(2), pp. 109–120. doi: 10.1016/j.tibtech.2016.08.002.

Sachelaru, I. *et al.* (2014) 'Dynamic interaction of the Sec translocon with the chaperone PpiD', *Journal of Biological Chemistry*, 289(31), pp. 21706–21715. doi: 10.1074/jbc.M114.577916.

Sakoh, M., Ito, K. and Akiyama, Y. (2005) 'Proteolytic activity of HtpX, a membrane-bound and stress-controlled protease from Escherichia coli', *Journal of Biological Chemistry*, 280(39), pp. 33305–33310. doi: 10.1074/jbc.M506180200.

Salcedo, S. P. and Holden, D. W. (2003) 'SseG, a virulence protein that targets Salmonella to the Golgi network', *EMBO Journal*, 22(19), pp. 5003–5014. doi: 10.1093/emboj/cdg517.

Sansonetti, P. (2002) 'Host-pathogen interactions: the seduction of molecular cross talk', *Gut*, 50. doi: 10.1136/gut.50.suppl_3.iii2.

Sapsford, K. E., Berti, L. and Medintz, I. L. (2006) 'Materials for Fluorescence Resonance Energy Transfer Analysis : Beyond Traditional Donor – Acceptor Combinations', *Angew Chem Int Ed Engl.*, 45(28), pp. 4562–4588. doi: 10.1002/anie.200503873.

Schibich, D. *et al.* (2016) 'Global profiling of SRP interaction with nascent polypeptides', *Nature*. Nature Publishing Group, 536(7615), pp. 219–223. doi: 10.1038/nature19070.

Schlumberger, M. C. *et al.* (2005) 'Real-time imaging of type III secretion: Salmonella SipA injection into host cells', *Proceedings of the National Academy of Sciences of the United States of America*, 102(35), pp. 12548–12553. doi: 10.1073/pnas.0503407102.

Schlumberger, M. C. *et al.* (2007) 'Two newly identified SipA domains (F1, F2) steer effector protein localization and contribute to Salmonella host cell manipulation', *Molecular microbiology*, 65(3), pp. 741–760. doi: 10.1111/j.1365-2958.2007.05823.x.

Schraidt, O. *et al.* (2010) 'Topology and organization of the Salmonella typhimurium type III secretion needle complex components', *PLoS Pathogens*. Public Library of Science, 6(4), pp. 1–12. doi:

10.1371/journal.ppat.1000824.

Schulein, R. *et al.* (2005) 'A bipartite signal mediates the transfer of type IV secretion substrates of Bartonella henselae into human cells', *Proceedings of the National Academy of Sciences*, 102(3), pp. 856–861. doi: 10.1073/pnas.0406796102.

Schwinn, M. K. *et al.* (2018) 'CRISPR-Mediated Tagging of Endogenous Proteins with a Luminescent Peptide', *ACS Chemical Biology*, 13(2), pp. 467–474. doi: 10.1021/acschembio.7b00549.

Shahrizal, M. *et al.* (2019) 'Structural Basis for the Function of the β-Barrel Assembly-Enhancing Protease BepA', *Journal of Molecular Biology*. Elsevier Ltd, 431(3), pp. 625–635. doi: 10.1016/j.jmb.2018.11.024.

Shen, D. K. and Blocker, A. J. (2016) 'MxiA, MxiC and IpaD regulate substrate selection and secretion mode in the T3SS of Shigella flexneri', *PLoS ONE*, 11(5), pp. 1–19. doi: 10.1371/journal.pone.0155141.

Shimomura, O. *et al.* (1978) 'Properties and Reaction Mechanism of the Bioluminescence System of the Deep-Sea Shrimp Oplophorus gracilorostris', *Biochemistry*, 17(6), pp. 994–998. doi: 10.1021/bi00599a008.

Shimomura, O. and Johnson, F. H. (1970) 'MECHANISMS IN THE QUANTUM YIELD OF CYPRIDINA BIOLUMINESCENCE', *Photochemistry and Photobiology*, 12(4), pp. 291–295. doi: 10.1111/j.1751-1097.1970.tb06061.x.

Silber, K. R., Keiler, K. C. and Sauer, R. T. (1992) 'Tsp: A tail-specific protease that selectively degrades proteins with nonpolar C termini', *Proceedings of the National Academy of Sciences of the United States of America*, 89(1), pp. 295–299. doi: 10.1073/pnas.89.1.295.

Singh, S. K. *et al.* (2012) 'Three redundant murein endopeptidases catalyse an essential cleavage step in peptidoglycan synthesis of Escherichia coli K12', *Molecular Microbiology*, 86(5), pp. 1036–1051. doi: 10.1111/mmi.12058.

Soltes, G. R. *et al.* (2017) 'Distinctive roles for periplasmic proteases in the maintenance of essential outer membrane protein assembly', *Journal of Bacteriology*, 199(20). doi: 10.1128/JB.00418-17.

Sorg, I. *et al.* (2007) 'YscU recognizes translocators as export substrates of the Yersinia injectisome', *EMBO Journal*, 26(12), pp. 3015–3024. doi: 10.1038/sj.emboj.7601731.

Sory, M. P. *et al.* (1995) 'Identification of the YopE and YopH domains required for secretion and internalization into the cytosol of macrophages, using the cyaA gene fusion approach', *Proceedings of the National Academy of Sciences of the United States of America*. Proceedings of the National Academy of Sciences, 92(26), pp. 11998–12002. doi: 10.1073/pnas.92.26.11998.

Spiers, A. *et al.* (2002) 'PDZ domains facilitate binding of high temperature requirement protease A (HtrA) and tail-specific protease (Tsp) to heterologous substrates through recognition of the small stable RNA A (ssrA)-encoded peptide', *Journal of Biological Chemistry*, 277(42), pp. 39443–39449. doi: 10.1074/jbc.M202790200.

Spiess, C., Beil, A. and Ehrmann, M. (1999) 'A temperature-dependent switch from chaperone to protease in a widely conserved heat shock protein', *Cell*, 97(3), pp. 339–347. doi: 10.1016/S0092-8674(00)80743-6.

Spreter, T. *et al.* (2009) 'A conserved structural motif mediates formation of the periplasmic rings in the type III secretion system', *Nature Structural and Molecular Biology*, 16(5), pp. 468–476. doi: 10.1038/nsmb.1603.

Srikanth, C. V. *et al.* (2010) 'Salmonella pathogenesis and processing of secreted effectors by caspase-3', *Science*, 330(6002), pp. 390–393. doi: 10.1126/science.1194598.

Stapels, D. A. C. *et al.* (2018) 'Salmonella persisters undermine host immune defenses during antibiotic treatment', *Science*, 362(6419), pp. 1156–1160. doi: 10.1126/science.aat7148.

Stecher, B. *et al.* (2007) 'Salmonella enterica serovar typhimurium exploits inflammation to compete with the intestinal microbiota', *PLoS Biology*, 5(10), pp. 2177–2189. doi: 10.1371/journal.pbio.0050244.

Steele-Mortimer, O. (2008) 'The Salmonella-containing Vacuole – Moving with the Times', *Current Opinion in Microbiology*, 23(1), pp. 1–7. doi: 10.1038/jid.2014.371.

Steinberg, R. *et al.* (2018) 'Co-translational protein targeting in bacteria', *FEMS Microbiology Letters*, 365(11), pp. 1–15. doi: 10.1093/femsle/fny095.

Stender, S. *et al.* (2000) 'Identification of SopE2 from Salmonella typhimurium, a conserved guanine nucleotide exchange factor for Cdc42 of the host cell', *Molecular Microbiology*, 36(6), pp. 1206–1221. doi: 10.1046/j.1365-2958.2000.01933.x.

Stensrud, K. F. *et al.* (2008) 'Deoxycholate interacts with IpaD of Shigella flexneri in inducing the recruitment of IpaB to the type III secretion apparatus needle tip', *Journal of Biological Chemistry*, 283(27), pp. 18646–18654. doi: 10.1074/jbc.M802799200.

Straley, S. C. *et al.* (1993) 'Regulation by Ca2+ in the Yersinia low-Ca2+ response', *Molecular Microbiology*, 8(6), pp. 1005–1010.

Su, M. Y. *et al.* (2017) 'Structural basis of adaptor-mediated protein degradation by the tail-specific PDZ-protease Prc', *Nature Communications*. Springer US, 8(1), pp. 1–13. doi: 10.1038/s41467-017-01697-9.

Sudhakar, P. *et al.* (2019) 'Targeted interplay between bacterial pathogens and host autophagy', *Autophagy*. Taylor & Francis, 15(9), pp. 1620–1633. doi: 10.1080/15548627.2019.1590519.

Sukhan, A. *et al.* (2001) 'Genetic analysis of assembly of the Salmonella enterica serovar Typhimurium type III secretion-associated needle complex', *Journal of Bacteriology*, 183(4), pp. 1159–1167. doi: 10.1128/JB.183.4.1159-1167.2001.

Suzuki, T. *et al.* (1987) 'Characterization of the sppA gene coding for protease IV, a signal peptide peptidase of Escherichia coli', *Journal of Bacteriology*, 169(6), pp. 2523–2528. doi: 10.1128/jb.169.6.2523-2528.1987.

Tannous, B. A. *et al.* (2004) 'Codon-optimized gaussia luciferase cDNA for mammalian gene expression in culture and in vivo', *Molecular Therapy*. The American Society of Gene Therapy, 11(3), pp. 435–443. doi: 10.1016/j.ymthe.2004.10.016.

Terashima, H. *et al.* (2018) ' In Vitro Reconstitution of Functional Type III Protein Export and Insights into Flagellar Assembly ', *mBio*. American Society for Microbiology, 9(3). doi: 10.1128/mbio.00988-18.

Terebiznik, M. R. *et al.* (2002) 'Elimination of host cell Ptdlns(4, 5)P2 by bacterial SigD promotes membrane fission during invasion by Salmonella', *Nature Cell Biology*, 4(10), pp. 766–773. doi: 10.1038/ncb854.

Tipping, M. J. *et al.* (2013) 'Load-dependent assembly of the bacterial flagellar motor', *mBio*, 4(4), pp. 1–6. doi:

10.1128/mBio.00551-13.

Tomabechi, Y. *et al.* (2016) 'Crystal structure of nanoKAZ: The mutated 19 kDa component of Oplophorus luciferase catalyzing the bioluminescent reaction with coelenterazine', *Biochemical and Biophysical Research Communications*. Elsevier Ltd, 470(1), pp. 88–93. doi: 10.1016/j.bbrc.2015.12.123.

Torres-Vargas, C. E. *et al.* (2019) 'The inner rod of virulence-associated type III secretion systems constitutes a needle adapter of one helical turn that is deeply integrated into the system's export apparatus', *Molecular Microbiology*, 112(3), pp. 1–14. doi: 10.1111/mmi.14327.

Truscott, K. N., Bezawork-Geleta, A. and Dougan, D. A. (2011) 'Unfolded protein responses in bacteria and mitochondria: A central role for the ClpXP machine', *IUBMB Life*, 63(11), pp. 955–963. doi: 10.1002/iub.526.

Tsilibaris, V., Maenhaut-Michel, G. and Van Melderen, L. (2006) 'Biological roles of the Lon ATP-dependent protease', *Research in Microbiology*, 157(8), pp. 701–713. doi: 10.1016/j.resmic.2006.05.004.

Tsirigotaki, A. *et al.* (2017) 'Protein export through the bacterial Sec pathway', *Nature Reviews Microbiology*. Nature Publishing Group, 15(1), pp. 21–36. doi: 10.1038/nrmicro.2016.161.

Tsou, L. K. *et al.* (2016) 'Antibacterial Flavonoids from Medicinal Plants Covalently Inactivate Type III Protein Secretion Substrates.', *Journal of the American Chemical Society*, 138(7), pp. 2209–18. doi: 10.1021/jacs.5b11575.

Uchiya, K. I. *et al.* (1999) 'A Salmonella virulence protein that inhibits cellular trafficking', *EMBO Journal*, 18(14), pp. 3924–3933. doi: 10.1093/emboj/18.14.3924.

Valent, Q. A. *et al.* (1995) 'Early events in preprotein recognition in E. coli: interaction of SRP and trigger factor with nascent polypeptides.', *The EMBO Journal*, 14(22), pp. 5494–5505. doi: 10.1002/j.1460-2075.1995.tb00236.x.

VanEngelenburg, S. B. and Palmer, A. E. (2008) 'Quantification of Real-Time Salmonella Effector Type III Secretion Kinetics Reveals Differential Secretion Rates for SopE2 and SptP Schuyler', *Cell*, 15(6), pp. 619–628. doi: DOI 10.1016/j.chembiol.2008.04.014.

Vazquez-Torres, A. *et al.* (1999) 'Extraintestinal dissemination CD18-expressing phagocytes', *Nature*, 401(October), pp. 623–626.

Voos, W. and Pollecker, K. (2020) 'The mitochondrial lon protease: Novel functions off the beaten track?', *Biomolecules*, 10(2). doi: 10.3390/biom10020253.

Wagner, S. *et al.* (2010) 'Organization and coordinated assembly of the type III secretion export apparatus', *Proceedings of the National Academy of Sciences*. Proceedings of the National Academy of Sciences, 107(41), pp. 17745–17750. doi: 10.1073/pnas.1008053107.

Wagner, S. *et al.* (2018) 'Bacterial type III secretion systems: A complex device for the delivery of bacterial effector proteins into eukaryotic host cells', *FEMS Microbiology Letters*, 365(19), pp. 1–13. doi: 10.1093/femsle/fny201.

Wang, P. *et al.* (2008) 'Escherichia coli signal peptide peptidase A is a serine-lysine protease with a lysine recruited to the nonconserved amino-terminal domain in the S49 protease family', *Biochemistry*, 47(24), pp.

6361–6369. doi: 10.1021/bi800657p.

Waudby, C. A., Dobson, C. M. and Christodoulou, J. (2019) 'Nature and Regulation of Protein Folding on the Ribosome', *Trends in Biochemical Sciences*. Elsevier Inc., 44(11), pp. 914–926. doi: 10.1016/j.tibs.2019.06.008.

Wee, D. H. and Hughes, K. T. (2015) 'Molecular ruler determines needle length for the Salmonella Spi-1 injectisome', *Proceedings of the National Academy of Sciences of the United States of America*, 112(13), pp. 4098–4103. doi: 10.1073/pnas.1423492112.

Weski, J. and Ehrmann, M. (2012) 'Genetic analysis of 15 protein folding factors and proteases of the Escherichia coli cell envelope', *Journal of Bacteriology*, 194(12), pp. 3225–3233. doi: 10.1128/JB.00221-12.

Westerhausen, S. *et al.* (2020) 'A NanoLuc luciferase-based assay enabling the real-time analysis of protein secretion and injection by bacterial type III secretion systems', *Molecular Microbiology*, 113(6), pp. 1240– 1254. doi: https://doi.org/10.1111/mmi.14490.

de Wet, J. R. *et al.* (1987) 'Firefly luciferase gene: structure and expression in mammalian cells.', *Molecular and Cellular Biology*, 7(2), pp. 725–737. doi: 10.1128/mcb.7.2.725.

Wiesand, U. *et al.* (2009) 'Structure of the Type III Secretion Recognition Protein YscU from Yersinia enterocolitica', *Journal of Molecular Biology*. Elsevier Ltd, 385(3), pp. 854–866. doi: 10.1016/j.jmb.2008.10.034.

Winnen, B. *et al.* (2008) 'Hierarchical effector protein transport by the Salmonella typhimurium SPI-1 Type III secretion system', *PLoS ONE*, 3(5), pp. 1–8. doi: 10.1371/journal.pone.0002178.

Worrall, L. J. *et al.* (2016) 'Near-atomic-resolution cryo-EM analysis of the Salmonella T3S injectisome basal body', *Nature*, 540(7634), pp. 597–601. doi: 10.1038/nature20576.

Worrall, L. J., Vuckovic, M. and Strynadka, N. C. J. (2010) 'Crystal structure of the C-terminal domain of the Salmonella type III secretion system export apparatus protein InvA.', *Protein science : a publication of the Protein Society*, 19(5), pp. 1091–1096. doi: 10.1002/pro.382.

Wu, C. *et al.* (2009) 'In vivo far-red luminescence imaging of a biomarker based on BRET from Cypridina bioluminescence to an organic dye', *Proceedings of the National Academy of Sciences*, 106(37), pp. 15599–15603. doi: 10.1073/pnas.0908594106.

Xing, Q. *et al.* (2018) 'Structures of chaperone-substrate complexes docked onto the export gate in a type III secretion system', *Nature Communications*. Nature Publishing Group, 9(1). doi: 10.1038/s41467-018-04137-4.

Yamaguchi, I. (1975) 'Oplophorus oxyluciferin and a model luciferin compound biologically active with Oplophorus luciferase', *Biochemical Journal*, 151(1), pp. 9–15. doi: 10.1042/bj1510009.

Yamamoto, M. *et al.* (2019) 'Cell cell and virus cell fusion assay based analyses of alanine insertion mutants in the distal 9 portion of the JRFL gp41 subunit from HIV-1', *Journal of Biological Chemistry*, 294(14), pp. 5677–5687. doi: 10.1074/jbc.RA118.004579.

Young, B. M. and Young, G. M. (2002) 'Yp1A is exported by the Ysc, Ysa, and flagellar type III secretion systems of Yersinia enterocolitica', *Journal of Bacteriology*. American Society for Microbiology, 184(5), pp. 1324–1334. doi: 10.1128/JB.184.5.1324-1334.2002.

Yount, J. S. *et al.* (2010) 'Visible fluorescence detection of type III protein secretion from bacterial pathogens', *Journal of the American Chemical Society*, 132(24), pp. 8244–8245. doi: 10.1021/ja102257v.

Zarivach, R. *et al.* (2008) 'Structural analysis of the essential self-cleaving type III secretion proteins EscU and SpaS', *Nature*. Nature Publishing Group, 453(7191), pp. 124–127. doi: 10.1038/nature06832.

Zhang, J. H., Chung, T. D. Y. and Oldenburg, K. R. (1999) 'A simple statistical parameter for use in evaluation and validation of high throughput screening assays', *Journal of Biomolecular Screening*, 4(2), pp. 67–73. doi: 10.1177/108705719900400206.

Zhang, X. *et al.* (2010) 'Sequential checkpoints govern substrate selection during cotranslational protein targeting', *Science*, 328(5979), pp. 757–760. doi: 10.1126/science.1186743.

Zhang, Y. *et al.* (2017) 'Visualization and characterization of individual type III protein secretion machines in live bacteria.', *Proceedings of the National Academy of Sciences of the United States of America*. National Academy of Sciences, 114(23), pp. 6098–6103. doi: 10.1073/pnas.1705823114.

Zhao, J. *et al.* (2016) 'Self-Assembling NanoLuc Luciferase Fragments as Probes for Protein Aggregation in Living Cells', *ACS Chemical Biology*, 11(1), pp. 132–138. doi: 10.1021/acschembio.5b00758.

Zhou, D., Mooseker, M. S. and Galán, J. E. (1999) 'Role of the S. typhimurium Actin-Binding Protein SipA in Bacterial Internalization', *Science*, 283(5410). doi: 10.1126/science.283.5410.2092.

8 Appendix

8.1 Additional data

8.1.1 Luminescence measurement results of MBP-NLuc in different *E.coli* mutant strains

Low copy plasmid (p15A ori, pT2) harbouring $MBP_{R8L\_S13L\_T16L}$-$NLuc^{ssrA}$ (indicated as +) and $MBP_{-sigseq}$-$NLuc^{ssrA}$ (indicated as -) were transformed into the different *E. coli* strains. Therefore, bacteria were grown for 5 hrs at 37°C, afterwards 0.5 ODU were collected and treated with EDTA to permeabilize the outer membrane. Samples were transferred to a 384-well plate and the corresponding luciferase reagents were supplemented for the detection of luminescence activity.

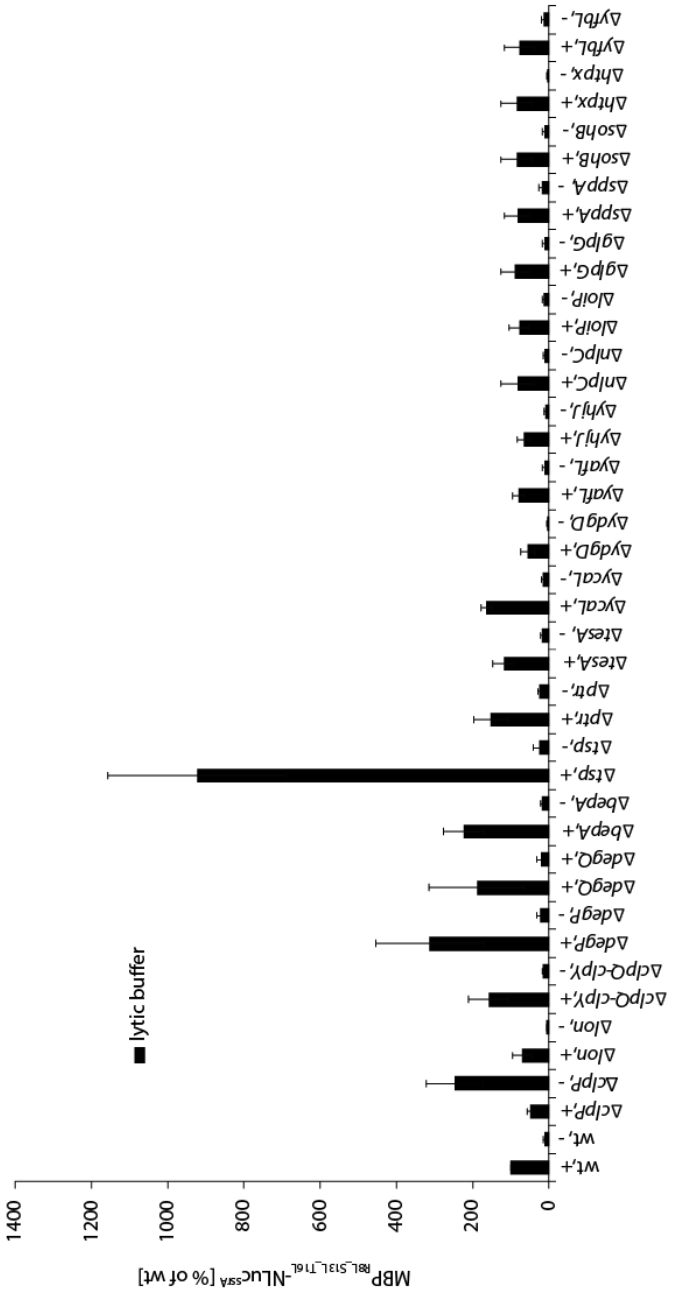

8.1.2 Luminescence measurement of MBP-LgBiT in different E.*coli* mutant strains

Low copy plasmid (p15A ori, pT2) harbouring $MBP_{R8L\_S13L\_T16L}$-$LgBiT^{ssrA}$ (indicated as +) and $MBP_{-sigseq}$-$LgBiT^{ssrA}$ (indicated as -) were transformed into the different *E. coli* strains. Therefore, bacteria were grown for 5 hrs at 37°C, afterwards 0.5 ODU were collected and treated with EDTA to permeabilize the outer membrane. Samples were transferred to a 384-well plate and the corresponding luciferase reagents were supplemented for the detection of luminescence activity.

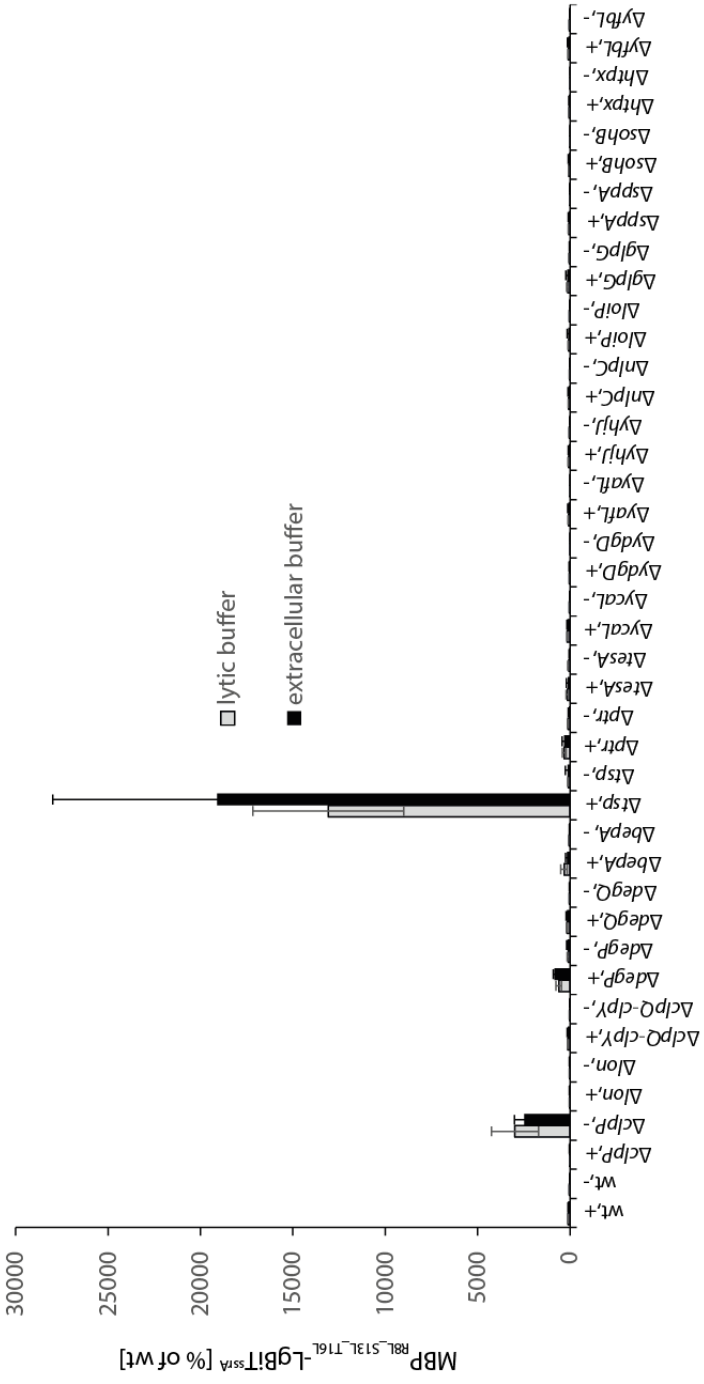

8.1.3 Western-blot results of MBP-NLuc and MBP-LgBiT in different E.*coli* mutant strains

Low copy plasmid (p15A ori, pT2) harbouring $MBP_{R8L\_S13L\_T16L}$-$LgBiT^{ssrA}$ and $MBP_{R8L\_S13L\_T16L}$-$NLuc^{ssrA}$ as well as the corresponding MBP without signal sequence constructs were transformed into the different *E. coli* strains. Bacteria were grown at 37°C for 5 hrs, afterwards 0.5 ODU were collected and treated with sucrose, EDTA and lysozyme to separate the periplasm and outer membrane from the cytoplasm. Samples were run on SDS PAGE followed by Western blotting and immunodetection of the MBP-tag was carried out. RpoB was used as loading control in spheroplast fraction and as control for cell lysis in the periplasmic and outer fraction.

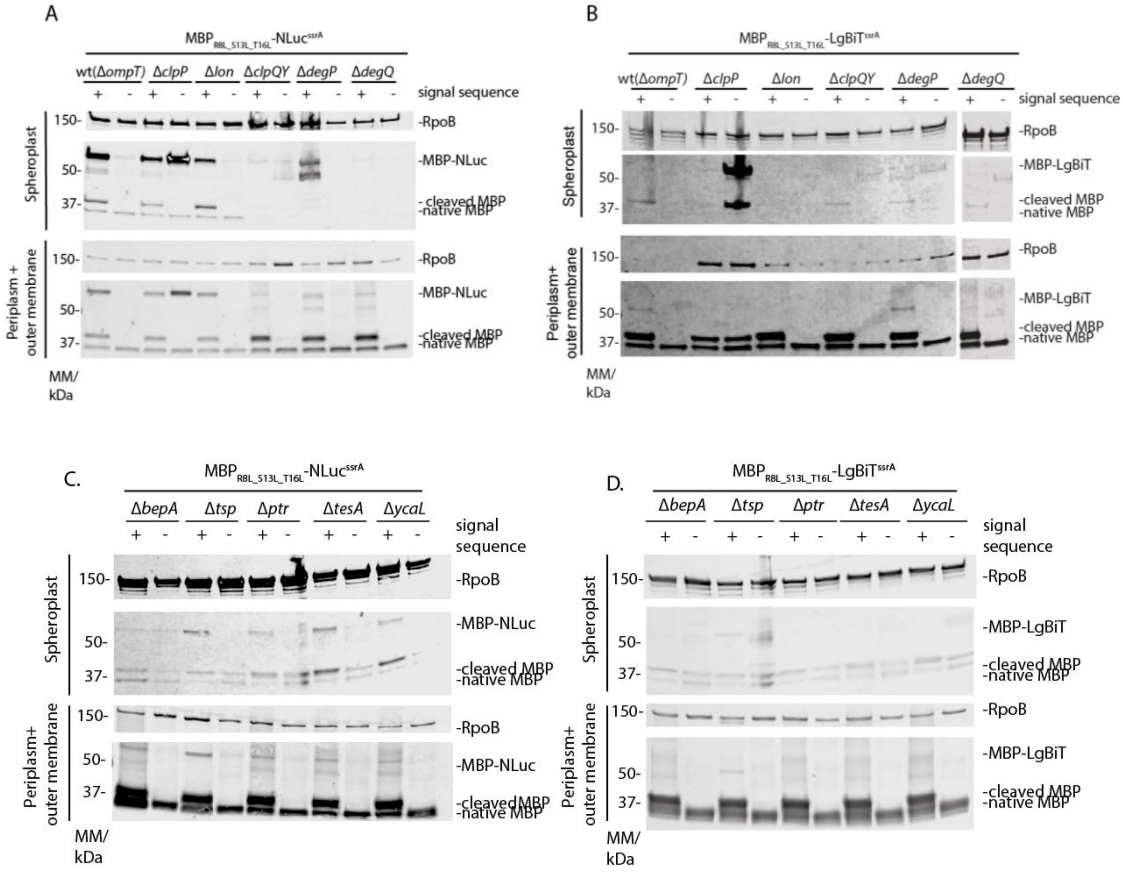

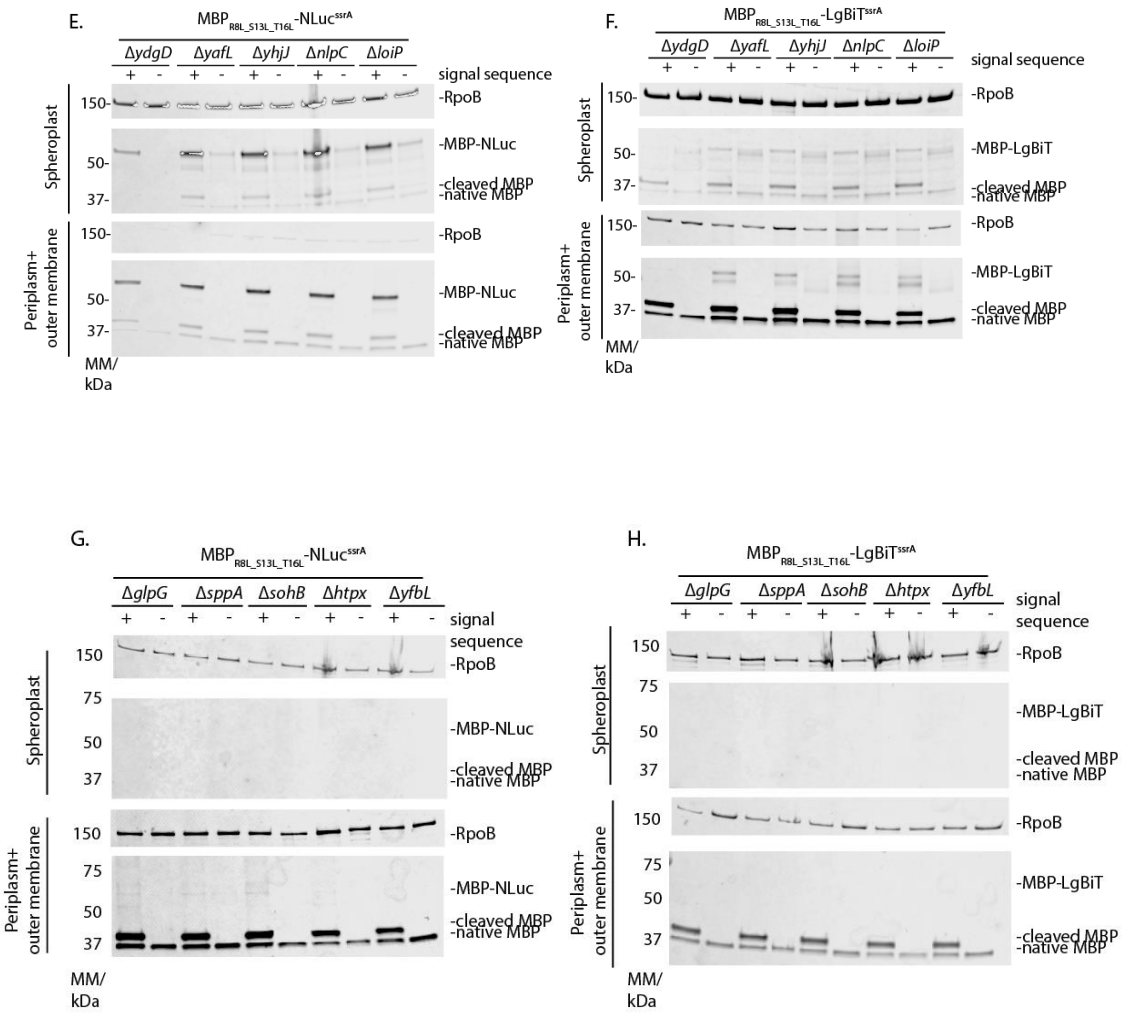
E.
MBP R8L_S13L_T16L-NLuc ssrA
ΔydgD
ΔyafL
ΔyhjJ
ΔnlpC
ΔloiP
signal sequence
Spheroplast
Periplasm+ outer membrane
150-
50-
37-
-RpoB
-MBP-NLuc
-cleaved MBP
-native MBP
MM/ kDa
F.
MBP R8L_S13L_T16L-LgBiT ssrA
ΔydgD
ΔyafL
ΔyhjJ
ΔnlpC
ΔloiP
signal sequence
Spheroplast
Periplasm+ outer membrane
150-
50-
37-
-RpoB
-MBP-LgBiT
-cleaved MBP
-native MBP
MM/ kDa
G.
MBP R8L_S13L_T16L-NLuc ssrA
ΔglpG
ΔsppA
ΔsohB
Δhtpx
ΔyfbL
signal sequence
Spheroplast
Periplasm+ outer membrane
150
75
50
37
-RpoB
-MBP-NLuc
-cleaved MBP
-native MBP
MM/ kDa
H.
MBP R8L_S13L_T16L-LgBiT ssrA
ΔglpG
ΔsppA
ΔsohB
Δhtpx
ΔyfbL
signal sequence
Spheroplast
Periplasm+ outer membrane
150
75
50
37
-RpoB
-MBP-LgBiT
-cleaved MBP
-native MBP
MM/ kDa

8.2 List of publication and personal contribution

8.2.1 Publication included in this thesis

1. Sibel Westerhausen, Melanie Nowak, Claudia Edith Torres-Vargas, Ursula Bilitewski, Erwin Bohn, Iwan Grin and Samuel Wagner. 2020. A NanoLuc luciferase-based assay enabling the real-time analysis of protein secretion and injection by bacterial type III secretion systems. *Mol Microbiol*. 2020; 113: 1240– 1254. https://doi.org/10.1111/mmi.14490

I performed most of the experiments with exception of experiments shown in Figure 3 and Figure S1. I analysed the data for the majority of the figures except for Figure S1 and contributed to the analysis of Figure 3. I designed the conceptual figure 6. I participitated in writing the manuscript. Furthermore, I contributed to the development of the study.

8.2.2 Additional publications

2. Steenhuis, M., Abdallah, A.M., de Munnik, S.M., Kuhne, S., Sterk, G.-J., van den Berg van Saparoea, B., Westerhausen, S., Wagner, S., van der Wel, N.N., Wijtmans, M., van Ulsen, P., Jong, W.S.P. and Luirink, J. (2019), Inhibition of autotransporter biogenesis by small molecules. Mol Microbiol, 112: 81-98. doi:10.1111/mmi.14255

3. Samuel Wagner, Iwan Grin, Silke Malmsheimer, Nidhi Singh, Claudia E Torres-Vargas, Sibel Westerhausen, Bacterial type III secretion systems: a complex device for the delivery of bacterial effector proteins into eukaryotic host cells, *FEMS Microbiology Letters*, Volume 365, Issue 19, October 2018, fny201, https://doi.org/10.1093/femsle/fny201

Danksagung / Acknowledgment

Zunächst möchte ich mich bei meinem Doktorvater Prof. Ph.D. Samuel Wagner bedanken, der mir diese Arbeit ermöglicht hat. Ich danke dir für all die Freiheiten und das entgegengebrachte Vetrauen. Ich konnte meine eigenen Fehler machen, bei denen du mir den zündenden Funken in die richtige Richtung gegeben hast. Vielen Dank für die Geduld und das offene Ohr für all meine Probleme sowie die großartige Betreuung. Ich habe in den letzten Jahren sehr viel in deiner Arbeitsgruppe gelernt.

Ich möchte zudem Prof. Dr. Ana Garcia-Sáez für ihre Betreuung und Interesse an dieser Arbeit danken. Ich danke auch Prof. Dr. Doron Rapaport. und Prof. Dr. Gabriele Dodt sowie Dr. Erwin Bohn für ihre Bereitschaft Prüfer in meiner Verteidigung zu werden.

Ich möchte Erwin zusätzlich auch für seine wertvolle Unterstützung und Beitrag zu dieser Arbeit danken.

In addition, I would like to thank Libera for her proofreading and all her suggestions contributing to this thesis! Thanks a lot, it helped me so much!

Einen großen Dank geht auch an alle Mitarbeiter der Wagner Gruppe. Dabei möchte ich insbesondere unseren beiden technischen Assistentinnen Andrea und Melanie danken. Ihr seid großartig!

I would also like to thank Nidhi. You were such a great labmate and friend. I always enjoyed our scientific and non-scientific discussions. And thanks a lot for your proofreading!

Dr. Julia and Claudia, it was always so much fun to spend our incubation times together.

Auch danke ich unserem Postdoc und Labmanager Iwan sehr. Danke dass du uns sehr vieles gelehrt hast.

Zudem geht ein besonderer Dank natürlich an alle (ehemaligen) Hiwis und Studenten der AG Wagner: Jialin, Sandra, Sofie, Felix, Marcus, Marina und Andi, ihr habt soviel zu einer angenehmen Atmosphäre beigetragen und es gab immer etwas zu lachen.

Desweiteren danke ich meiner Mama, meinen Schwestern und meinem Bruder für all ihre Unterstützung und Liebe in dieser Zeit.

Mein besonderer Dank gilt auch meiner Freundin Christina, die mich immer aufgemuntert und in schwierigen Zeiten mir mit vielen Ratschlägen beigestanden hat.

Ganz besonders danke ich meinem Mann Markus. Du hast immer an mich geglaubt und mich nie aufgeben lassen egal wie ausweglos die Situation für mich auch erschien. Ohne dich hätte ich das nie geschafft. Danke für alles.